New insights on the Regulator of G protein Signaling 2 (RGS2) in platelets, the metabolic syndrome and type 2 diabetes mellitus

Table of contents

Abbreviations

AA	amino acid
AC	adenylyl cyclase
ACN	acetonitrile
ADP	adenosine diphosphate
AHO	Albright hereditary osteodystrophy
Ang II	Angiotensin II
ATP	adenosine triphosphate
βcat	β catenin
BFU-MK	burst-forming unit-megakaryocyte
BVA	biological variation analysis
cAMP	cyclic adenosine monophosphate
cDNA	complementary DNA
cGMP	cyclic guanosine monophosphate
CFU-MK	colony-forming unit-megakaryocyte
CNS	central nervous system
C-terminus	carboxyl-terminus
CYP	cytochrome P450
D	dishevelled
DAG	diacylglycerol
DEP domain	dishevelled/EGL-10/PLeckstrin domain
DH domain	DBL-homology domain
DIGE	differential gel electrophoresis
DMEM	Dulbecco's modified Eagle's medium
DMR	differentially methylated region
DMS	demarcation membrane system
DNA	desoxyribonucleic acid
Dpf	days post fertilization

DTS	dense tubular system
DTT	dithiothreitol
Dys	dystrophine
ECL	enhanced chemiluminescence
EDTA	ethylenediaminetetraacetic acid
eIF2Bε	eukaryotic initiation factor 2Bε
EP receptor	receptor for E series of prostaglandins
FACS	fluorescence-activated cell sorting
FSC	forward scatter
GoS8	G_0/G_1 switch regulatory gene 8
GAP	guanosine triphosphate activating protein
GDP	guanosine diphosphate
GEF	guanine nucleotide exchange factor
GFP	green fluorescent protein
GGL domain	G protein γ subunit like domain
GNAS	gene encoding the stimulatory G protein α subunit
GPCR	G protein-coupled receptor
G protein	GTP-binding protein
GSK	glycogen synthase kinase
GTP	guanosine triphosphate
HRP	horseradish peroxidase
HSC	hemotopoietic stem cell
IL-2	interleukin-2
IP receptor	prostaglandin I_2 receptor
IP_3	inositol 1,4,5-triphosphate
IQ	intelligence quotient
kb	kilobases
kDa	kilo Dalton
MALDI-TOF	matrix-assisted laser desorption/ionization-time of flight

MEP	megakaryocyte-erythroid progenitor
MK	megakaryocyte
M-MLV	Moloney murine leukemia virus
MOWSE	molecular weight search
mRNA	messenger RNA
MS	mass spectrometry
NCBI	national center for biotechnology information
NESP55	neuroendocrine secretory protein (55 kDa)
NLS	nuclear localization signal
NO	nitric oxide
N-terminus	amino-terminus
P2Y receptor	purinergic receptor
PACAP	pituitary adenylate cyclase activating peptide
PAGE	polyacrylamide gel electrophoresis
PBS	phosphate-buffered saline
PCR	polymerase chain reaction
PDE	phosphodiesterase
PDZ domain	PSD-95/Disk-Large/ZO-1 domain
PGI_2	prostaglandin I_2, prostacyclin
PH domain	pleckstrin-homology domain
PHPIa	pseudohypoparathyroidism type Ia
PI3P	phosphatidylinositol 3-phosphate
PIP_2	phosphatidylinositol bisphosphate
PKA	protein kinase A
PKC	protein kinase C
PKGI-α	protein kinase GI-α
PLC	phospholipase C
PMSF	phenylmethylsulfonyl fluoride
PP2A	protein phosphatase 2A

PPARγ	peroxisome proliferator-activated receptor γ
PPHP	pseudopseudohypoparathyroidism
PRP	platelet-rich plasma
PTB domain	phosphotyrosine binding domain
PX domain	phox-homology domain
RBD	Ras binding domain
RGS protein	regulator of G protein signaling protein
RIPA buffer	radioimmunoprecipitation assay buffer
RNA	ribonucleic acid
RPMI	Roswell park memorial institute
SD	standard deviation
SDS	sodium dodecyl sulphate
Ser	serine
SNP	single nucleotide polymorphism
SSC	side scatter
T2DM	type 2 diabetes mellitus
TBS	tris-buffered saline
TCA	trichloroacetic acid
TFA	trifluoroacetic acid
TRPV6	transient receptor potential vanilloid type 6
TXA_2	thromboxane A_2
UTR	untranslated region
VASP	vasodilator-stimulated phosphoprotein
VIP	vasoactive intestinal peptide
VPAC1 receptor	vasoactive intestinal peptide/pituitary adenylate cyclase activating peptide receptor 1
WISC-R	Wechsler intelligence scale for children
Wt	wild type
Wt:vol	weight/volume

XLαs	extra-large stimulatory GTP-binding protein α subunit

Chapter I
General introduction

I. Platelets

Platelets are enucleated cells, shed from large precursor cells in the bone marrow, the megakaryocytes [1]. They are essential players in the process of primary hemostasis. A platelet count that is too low can result in bleeding problems, too many platelets can cause thrombus formation [2]. This infers that the processes of megakaryocyte differentiation (megakaryopoiesis) and platelet production (thrombopoiesis) need to be tightly regulated.

1 MEGAKARYOPOIESIS

Megakaryocytes differentiate from hematopoietic stem cells (HSCs) in the bone marrow. These stem cells have the ability to self renew and differentiate to all types of blood cells via the process of hematopoiesis. Cells are committed to a certain blood cell lineage by a specific gene expression pattern, regulated by cell specific transcription factors [3]. In addition, specific growth factors can direct the proliferation and differentiation into one specific blood cell type.

At the beginning of megakaryopoiesis, a HSC differentiates into a bipotent megakaryocyte-erythroid progenitor cell (MEP). After commitment to the megakaryocytic lineage, it passes through 2 phases: the proliferation phase and the maturation phase (Fig.1) [4, 5]. The proliferation phase starts with the least committed precursor, the burst-forming unit-megakaryocyte (BFU-MK). This cell gives rise to large colonies, containing up to several hundred cells [6, 7]. The next colony morphology is the colony-forming unit-megakaryocyte (CFU-MK), which develops in a simple colony that contains 3 – 50 megakaryocytes. BFU-MK is thought to represent the primitive progenitor, CFU-MK the mature progenitor [6]. The latter has a limited proliferative capacity and starts the process of endomitosis, a prematurely ended mitosis during which the cell replicates its DNA in the absence of karyokinesis and cytokinesis [8]. Mononuclear progenitor cells undergo multiple rounds of endomitosis and thus become polyploid. These cells start the

maturation phase, which consists of 3 stages and lasts 4 to 5 days. The first stage is the megakaryoblast, which undergoes further differentiation and endomitosis to become the promegakaryocyte. This cell type has a large polyploid nucleus, with a DNA content usually ranging from 8N to 64N, but possible up to 128N [9]. This polyploidy ensures an increased transcription, which is necessary to deliver sufficient mRNA to provide hundreds of platelets with proteins. Next, the cells are enriched in platelet-specific cytoplasmatic organelles and membrane constituents. The cell has then reached the stage of the mature, proplatelet-producing megakaryocyt [4].

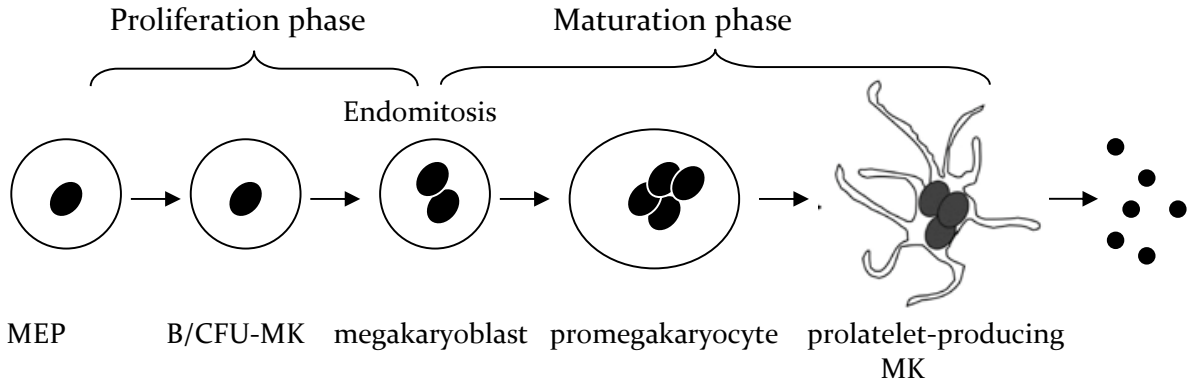

Figure 1: The process of megakaryopoiesis.

The megakaryocyte-erythroid progenitor cell (MEP) is committed to the megakaryocytic cell lineage and differentiates to the burst- and colony-forming unit-megakaryocyte (B/CFU-MK), the latter being more mature and with a limited proliferative capacity. This cell type starts the process of endomitosis, resulting in the megakaryoblast stage. After further polyploidization the promegakaryocyte cell type arises, which is the direct progenitor of the proplatelet-producing megakaryocyte (MK).

2 THROMBOPOIESIS

Mature megakaryocytes contain platelet specific proteins and organelles, and the demarcation membrane system (DMS), which is incorporated in the plasma

membrane of the platelets [10]. The megakaryocytes form long cytoplasmic projections, the proplatelets, which are fragmented to form platelets [11]. Proplatelet formation starts with the extension of thick pseudopodia. They elongate and after repetitive cycles of extension, retraction, bending and branching they form thin proplatelet processes (2-4 μm). Eventually, the nucleus is surrounded by a branched network of thin proplatelets containing almost all cytoplasmic constituents. During the process of platelet production, proplatelets branch to form more termini. These ends are the only sites where the microtubular organization is similar to that in platelets, demonstrating that platelet production is completed at the termini of the proplatelets [12]. Thus, the branching of the proplatelets provides an elegant mechanism to increase the number of ends and to enable each megakaryocyte to give rise to about 1000 to 3000 platelets [13]. Platelets are released in the circulation at the bone marrow sinusoids. Mature megakaryocytes reside less than 1 μm from a marrow sinus wall, and naked nuclei can be seen in the marrow implying that release of megakaryocyte cytoplasm occurs in the marrow sinusoids [14, 15]. Several researchers have suggested that a portion of the platelet production takes place in the lungs, and proplatelet producing megakaryocytes have been reported in the pulmonary circulation of the rat [16] and the mouse [17].

The formation of proplatelets and subsequent platelet production involves massive reorganization of megakaryocyte membranes and cytoskeletal components, including actin and tubulin. Actin is involved in the branching of proplatelets, as it is enriched at sites of bifurcation [12], and tubulin is involved in the reorganization of the microtubule cytoskeleton. The linear arrays of microtubules present throughout proplatelet processes probably serve as tracks for the transport of membranes, organelles and granules into developing platelets [18].

3 PLATELET MORPHOLOGY

The platelet membrane contains several receptors, responsible for adhesion to damaged vessel walls or other platelets, and for their activation or inhibition.

The platelet surface shows multiple invaginations, mostly referred to as the open canalicular system. This system creates a connection between the intracellular cytoplasm and the surface, allowing the entrance of plasma components and the release of platelet contents [19].

Intracellularly, platelets contain the dense tubular system (DTS), derived from the smooth endoplasmatic reticulum of the megakaryocyte. It functions as a calcium sequestrating organelle and acts to maintain the resting free calcium concentration at a fixed level [20]. In addition, it is the major site for prostanoid biosynthesis [21].

Three types of secretory granules can be found within platelets, whose contents are released upon platelet activation [22]

- Alpha granules are most numerous and contain large adhesive and healing proteins, growth factors, cytokines, coagulation proteins, adhesion proteins and protease inhibitors;
- dense granules store small non-protein molecules that are secreted to recruit other platelets: ADP, ATP, serotonine, pyrophosphate and calcium;
- lysosomes contain hydrolytic enzymes to eliminate circulating platelet aggregates.

Finally, platelets hold a system of contractile proteins, responsible for the shape change, the first step in the activation of platelets. This mainly consists of actin filaments and microtubuli [23].

4 PLATELET FUNCTION

Platelets are indispensable during the process of primary hemostasis. Exposure of subendothelial substances from the damaged blood vessel wall leads to the adherence of platelets to the site of injury. In response to the thrombogenic surface or locally produced agonists, like collagen and ADP, platelets become

activated. They first undergo shape change, leading to the secretion of platelet granules. The calcium required for granule movements is provided by the DTS. Mitochondria together with glycogen fulfill the energy requirements for the secretory function. Secreted granular products are important in the recruitment of additional platelets.

Platelet activation and subsequent recruitment of additional platelets is strongly dependent on different intracellular signaling pathways mediated in part by heterotrimeric G proteins.

II. G protein-mediated signaling

1 HETEROTRIMERIC G PROTEINS

1.1 General features

Heterotrimeric G proteins are involved in numerous metabolic, endocrinologic and developmental processes [24]. They are composed of 3 subunits: a GDP-binding α subunit, a β subunit and a γ subunit. In the inactive state this complex is bound to a G protein-coupled receptor (GPCR). These receptors have a characteristic 7-transmembrane-spanning conformation. When their extracellular ligand binds, they induce the exchange of the GDP bound to the G protein α subunit for the activating nucleotide GTP. This leads to a conformational change, separating the α subunit from the βγ dimer. Both complexes can now activate specific effector proteins, and thus initiate intracellular changes. Several subtypes of G proteins exist, depending on the type of the α subunit. The 3 most important α subunits are Gsα, Giα and Gqα. Gsα activates adenylyl cyclase (AC), leading to the production of cyclic adenosine monophosphate (cAMP), Giα inhibits cAMP production and Gqα stimulates phospholipase Cβ (PLCβ) activity, inducing calcium release and activation of protein kinase C (PKC) (Fig. 2).

Signaling ends when the intrinsic GTPase activity of the α subunit converts the GTP back to GDP, which leads to the reassociation with the βγ dimer to form the inactive heterotrimeric complex [25].

A

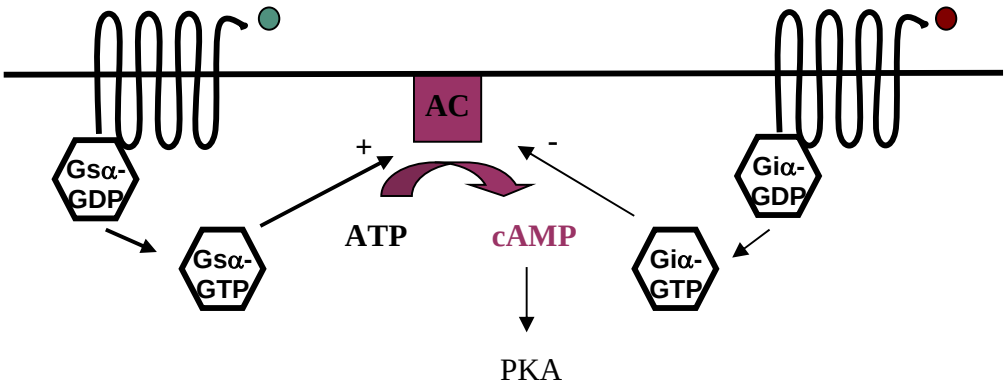

B

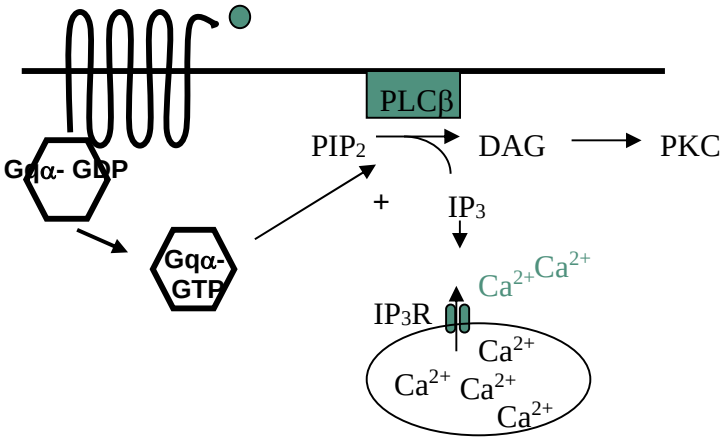

Figure 2: G protein-mediated signaling: Gsα, Giα and Gqα

A. Activation of Gsα and Giα leads to stimulation and inhibition of adenylyl cyclase (AC) activity, respectively. AC mediates the conversion of ATP to cyclic AMP (cAMP), which activates protein kinase A (PKA). Gsα activity thus leads to an increase in cAMP, whereas Giα activity reduces cAMP production.

B. Gqα activation stimulates phospholipase Cβ (PLCβ) activity. This leads to an enhanced production of diacylglycerol (DAG) and inositol trisphosphate (IP_3). DAG leads to activation of protein kinase C (PKC) and IP_3 mediates intracellular calcium release.

1.2 Focus on Gsα

1.2.1 Gene structure

The gene encoding Gsα (*GNAS*) is located on chromosome 20q13 and is part of the most complex imprinted gene cluster described up to now. It gives rise to maternally, paternally and biallelically expressed transcripts that share a common set of downstream exons [26]. The cluster comprises 4 alternative first exons and promoters that splice onto exon 2 of the classical GNAS gene, and that are all located in three differentially methylated regions (DMRs) [27-29] (Fig.3). The first upstream one is NESP and gives rise to a maternally derived NESP55 (neuroendocrine-specific protein) transcript [26, 30]. A paternally derived transcript, named XL, is generated starting from the second alternative promoter and first exon XL. This transcript gives rise to an extra large variant of the stimulatory G protein, XLαs. The exon A/B promoter gives rise to a paternal non-coding transcript [27]. Finally, the classical transcript for Gsα comprises 13 exons and is biallelically expressed in most tissues. It is imprinted from the paternal allele in specific tissues, including pituitary and thyroid tissues [31], the renal proximal tubules, gonads [32] and the paraventricular nucleus of the hypothalamus [33].

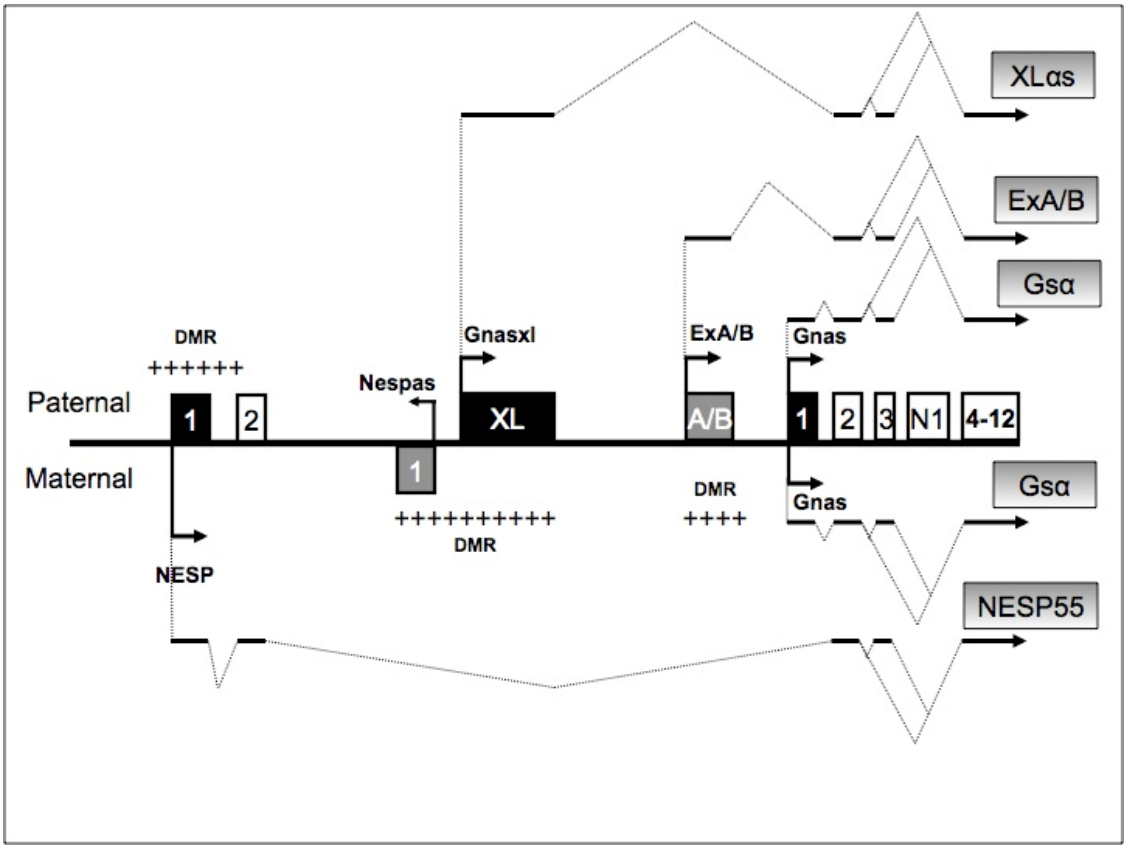

Figure 3: Schematic representation of the *GNAS* cluster.

Exons are depicted as boxes. First exons are black when leading to a coding transcript, and gray when transcripts are non-coding. Arrows indicate the direction of the different transcripts. Differential splicing is indicated by the dotted lines. DMR: differentially methylated region. The first upstream exon (NESP) gives rise to a maternally derived transcript, NESP55. The XL exon leads to a paternal transcript, XLαs. A non-coding paternal transcript, ExA/B, is transcribed from exon A/B. Finally Gsα is transcribed from both alleles in most tissues, starting from the Gnas exon.

1.2.2 Gsα and human pathology

Heterozygous inactivating mutations, resulting in Gsα haploinsufficiency, result in a characteristic syndrome: Albright Hereditary Osteodystrophy (AHO). Patients with AHO show a short stature, shortening of the various long bones in

the hands and feet (brachydactyly), subcutaneous ossifications, rounded face and neurobehavioral deficits. The severity of these manifestations varies greatly and some patients with mutations have only minimal clinical features [34]. When AHO is caused by mutations in the maternal *GNAS* allele, patients also develop multiple hormone resistance (to parathyroid hormone, thyroid stimulating hormone, growth hormone-releasing hormone and gonadotropins). This condition is referred to as pseudoparahypothyroidism type 1A (PHP1A). When the mutation is present on the paternal *GNAS* allele, this hormone resistance is not present and the condition is known as pseudopseudohypoparathyroidism (PPHP) [35]. This difference in clinical phenotype is due to the fact that Gsα is primarily expressed from the maternal allele in the target tissues of these respective hormones [31]. The short stature in the patients is probably the result of a primary skeletal growth plate defect rather than growth hormone deficiency. One study shows lower metabolic rates in patients with PHP1A, suggesting a defect in the central nervous system (CNS) regulation [36]. This was also observed in mice with a CNS-specific disruption of the maternal *GNAS* allele. They show an obese phenotype, resulting from a lower sympathetic nervous system activity, lower energy expenditure rates, and reduced activity levels. The mice also developed hyperglycemia, glucose intolerance and insulin resistance, independent of the obesity. In contrast, disruption of the paternal allele did not affect the metabolic phenotype [33].

Activating mutations of Gsα are also involved in human pathology. Activating somatic Gsα mutations, leading to cell proliferation, have been identified in endocrine tumors, like pituitary adenomas [37] and thyroid adenomas [38]. When these mutations occur during embryogenesis they cause McCune-Albright syndrome. This is a sporadic disorder characterized by polyostotic fibrous displasia, café-au-lait skin hyperpigmentation and autonomous hyperfunction of several endocrine glands [39].

Several mouse models have suggested a role for Gsα signaling in glucose metabolism. The different mouse models and their characteristics are summarized

in table 1. In general, loss of Gsα signaling in tissues involved in glucose metabolism seems to lead to glucose intolerance and reduced insulin sensitivity.

Table 1: Tissue-specific Gsα disruption in mice

Gsα deficient tissue	Phenotype
General disruption of the maternal allele	Obesity, hypertriglyceridemia and insulin resistance [40]
Pancreatic β cells	Hypoglycemia and glucose intolerance with severe hypoinsulinemia. Reduced islet content and insulin release [41]
Central nervous system	Obesity, peripheral insulin resistance and diabetes [33]
Muscle	Reduced muscle mass and glucose intolerance without insulin resistance [42]

In conclusion, Gs protein activity is important in normal physiological processes, and needs to be regulated in order to prevent insufficient or excess stimulation of its effector, which could lead to pathological conditions. An important group of regulators of G protein activity in general are the regulator of G protein signaling (RGS) proteins.

2 REGULATOR OF G PROTEIN SIGNALING PROTEINS

2.1 RGS protein family

RGS proteins negatively regulate G protein-mediated signaling. They were first identified to act by enhancing the intrinsic GTPase activity of the α subunit of heterotrimeric G proteins [43]. Now it is clear that they can also regulate G protein-effector interactions directly [44].

2.1.1 Classification

All RGS proteins contain a characteristic RGS domain, necessary for their GTPase activating protein (GAP) activity. So far more than 20 different RGS proteins have been identified, which are subdivided in 9 subfamilies, based on their additional domains (Table 2). Two different nomenclatures have been proposed for the different subfamilies, one arbitrary name (A-I) [45], and one based on the representative member [46].

Table 2 summarizes the different subfamilies and their characteristic domains, which provide additional functions to the proteins, apart from the GAP activity of the RGS domain [47, 48].

2.1.2 Mechanism of action

The characteristic RGS domain is necessary for binding Gα subunits and accelerating hydrolysis of the active GTP-bound α subunit back to the inactive GDP-bound state (Fig.4) [49]. The RGS domain folds as a bundle of 9 α-helices. Three interhelix loops make contact with 3 of the switch regions in the GTP-binding domain of Gα [50]. Hydrolysis of GTP bound to the G protein α subunit proceeds through a bipyramidal transition state intermediate. RGS proteins act by decreasing the activation energy for hydrolysis by energetically stabilizing the transition state complex [51] and can accelerate hydrolysis > 2000 fold.

The physiological actions of RGS proteins take place at the plasma membrane. However, RGS proteins are not strongly attached to the plasma membrane by a common targeting motif. Therefore they need to be translocated to the plasma membrane upon activation of a GPCR or the associated G protein. Their characteristic domains provide mechanisms to associate with the receptor and the plasma membrane, and often RGS proteins are able to interact with accessory proteins to alter their subcellular localization and stability.

GPCRs often exist as dimers or larger oligomers, and multiple G protein units might also be present. It is becoming more accepted that RGS proteins interact in a complex manner with multiple G proteins contained within heterotrimeric signaling complexes, together with the GPCRs and the G proteins [52].

Table 2: The RGS protein subfamilies

Subfamily	Structure	Members	Characteristic domains
A/RZ		GAIP/RGS19, RGSZ1/RGS20, RGSZ2/RGS17, Ret-RGS1	**Cysteine string motif**: site for palmitoylation; important for membrane-anchoring and protein-protein interactions
B/R4		RGS1-5, RGS8, RGS13, RGS16, RGS18, RGS21	**Amphipathic α-helix**: binding of vesicles containing acidic phospholipids, targeting plasma membrane, several palmitoylation sites, contains a nuclear localization signal (NLS)
C/R7		RGS6, RGS7, RGS9, RGS11	**GGL domain** (G protein γ subunit-like): binds the β subunit Gβ5, preferentially expressed in neural tissues **DEP** (Disheveled/EGL-10/Pleckstrin) **domain**: interacts specifically with a selective set of GPCRs and RGS-binding proteins, membrane-anchoring and subcellular targeting
D/R12		RGS10, RGS12, RGS14	**GoLoco domain**: G-protein regulatory motif; binds GDP-bound Gα subunits and inhibit exchange of GDP for GTP **PDZ** (PSD-95/Disk-Large/ZO-1) **domain**: interaction with C-terminus of GPCRs **PTB domain**: phosphotyrosine binding domain
E/RA		Axin, Conductin	Do not act as GAPs **D** (Dishevelled); **PP2A** (protein phosphatase 2A); **GSK** (glycogen synthase kinase) and **βcat** (β catenin) **binding domains**: key regulators of Wnt - β-Catenin signaling
F/GEF		P115-RhoGEF, PDZ-RhoGEF, LARG	RhoGEFs (Ras homology-specific Guanine nucleotide Exchange Factors) **DH** (Dbl-homology) **domain**: regulation of GEF activity **PH** (pleckstrin-homology) **domain**: subcellular localization
G/GRK		GRK1-7	**Kinase domain**: serine/threonine kinase activity **PH domain**: subcellular localization
H/SNX	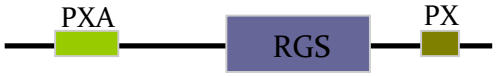	RGS-PX1 (SNX13), SNX14, SNX25	**PX** (phox-homology) **domain**: targeting to PI3P-enriched membranes, such as endosomes, to exert their function in intracellular trafficking
I/D-AKAP2		D-AKAP2	Multiple **RGS domains**

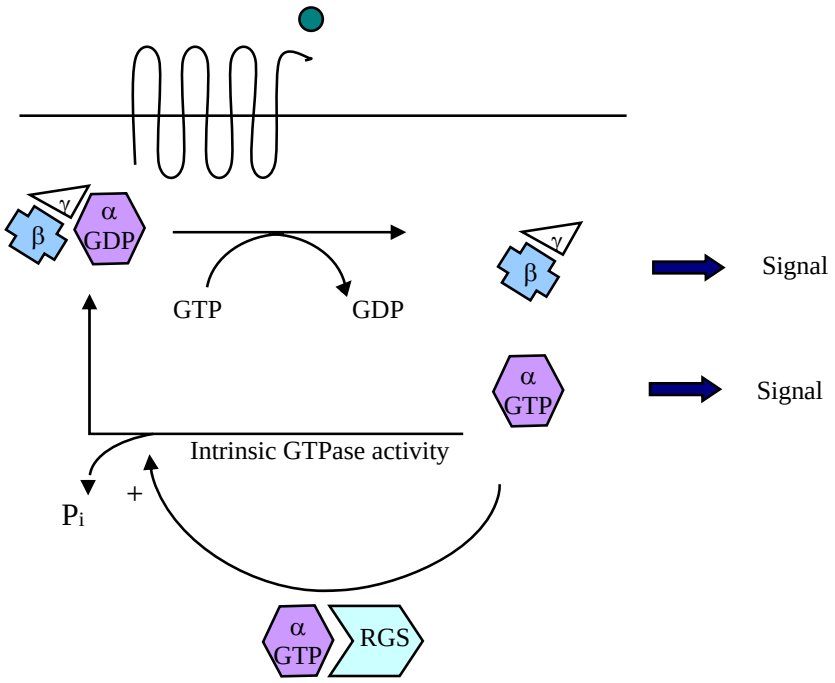

Figure 4: RGS proteins negatively regulate G protein-mediated signaling.
Upon activation of the GPCR, the coupled G protein exchanges GDP for GTP at its α subunit. The α subunit dissociates from the βγ subunit, and both complexes induce intracellular signals. Signaling is ended by the intrinsic GTPase activity of the α subunit, which is accelerated by the binding of a RGS protein. GTP is hydrolyzed back to GDP, leading to the reassociation of the heterotrimeric G protein.

2.1.3 Selectivity and specificity

Over 20 RGS proteins have been identified, all of them regulating preferred G protein α subunits and GPCRs. This specificity is mediated by several mechanisms (Table 3).

Table 3: Mechanisms for selectivity of RGS proteins

Spatiotemporal-specific expression	Co-expression with the target proteins at the right time and in the right location
RGS domain	Selective interaction with particular Gα subunits, determined by specific sequences within the RGS domains and the Gα subunits [50, 53].
Characteristic N-terminal domains	Involved in plasma membrane targeting and subcellular localization, direct contact with and specific recognition of GPCRs, effector proteins and ion channels. region of the GPCR.
Specific adaptor or scaffold proteins	Bridges between the N-terminal, C-terminal or other special regions of RGS proteins with GPCRs, G proteins or effectors.
Alternative splicing variants	Alternatively spliced variants that display distinct selectivity and functions.
Posttranslational modifications	Phosphorylation, glycosylation and palmitoylation. They have no consistent effects. Phosphorylation is able to enhance or reduce GAP activity, alter their subcellular location and influence protein stability.
GPCR C-terminus and third intracellular loop	Specific sites for interaction with the RGS protein

2.2 Focus on Regulator of G protein signaling 2

Regulator of G protein Signaling 2 (RGS2) is a member of the B/R4 subfamily of RGS proteins. It was first described by Siderovski *et al.* as GoS8, a helix-loop-helix phosphoprotein resembling a set of G_o/G_1 switch regulatory genes [54]. The gene is composed of 5 exons that are distributed over 1.3 kb on chromosome 1 q31 [55]. The first exon contains 4 in-frame start codons and 4 different RGS2 protein isoforms have been identified [56]. These proteins initiate at start codons at position 1, 5, 16 and 33 of the full length protein. The largest open reading frame encodes a hydrophilic, basic protein of 211 amino acids (Fig.5).

2.2.1 RGS2 expression

RGS2 is expressed widely in both mouse and human tissues [57]. It regulates G protein-mediated responses in the immune system, brain, heart, lung, bone, and olfactory epithelium.

RGS2 expression is rapidly and selectively upregulated in response to several stimuli, such as angiotensin II (Ang II) [58, 59], and increased cAMP and phosphoinositide production [60], thereby acting as a negative feedback regulatory system and cross regulating Gs and Gq signaling pathways, respectively.

2.2.2 Functional domains

RGS2 contains a RGS domain flanked by short N- and C-terminal sequences. The N-terminus is involved in the interaction with several proteins, providing additional activities to RGS2 (Fig.5).

2.2.2.1 The RGS domain

The RGS domain of RGS2 ranges from amino acids (AA) 79 to 205 [61]. It is able to bind the α subunits of Gi and Gq, and to stimulate their intrinsic GTPase activity. RGS2 does not act as a GAP for Gsα, but it has been shown to bind this α subunit and inhibit its activity, probably via steric hindrance.

Another function of the RGS domain of RGS2 is controlling protein synthesis. It binds to eukaryotic initiation factor 2B ε subunit (eIF2Bε) and inhibits the translation of mRNA into new protein. This function maps to a stretch of 37 AA residues within the RGS domain (AA 79-116) [62].

2.2.2.2 The N-terminal domain

- Binding site of scaffold proteins

Spinophilin is a scaffolding protein with several protein binding modules. It binds the N-terminal domain of RGS2 and the third intracellular loop of the GPCR, and thus actively regulates signaling by recruiting the RGS protein to the GPCR complex. For example, spinophilin enhances the inhibitory effect of RGS2 on α adrenergic-mediated calcium production [63].

Neurabin is structurally similar to spinophilin, but enhances calcium signaling by GPCRs. It also binds the N-terminal domain of RGS2, but does not interact with the third intracellular loop of the GPCR, so it removes the RGS protein from the GPCR-G protein complex to enhance GPCR signaling intensity [64].

Tubulin directly interacts with RGS2 via a short region at the RGS2 N-terminus: AA 41-60 [65]. *In vitro* studies show that RGS2 promotes the outgrowth of neurites in neuronal PC12 cells by stimulating microtubule polymerization.

The ***TRPV6 calcium channel*** interacts with the N-terminal domain of RGS2, which affects the gating properties of the channel. The TRPV6 channel displays characteristic inward currents carried by calcium or monovalent cations as natrium and plays a major role in calcium transport. RGS2 inhibits both Na^{+} as Ca^{2+} currents through TRPV6, without the involvement of GPCR signaling [66].

- Interaction with effector proteins

RGS2 binds some ***AC subtypes*** to attenuate the ability of the activated Gs protein to modulate AC, thereby decreasing cAMP production [67]. This inhibition seems to be independent of any change in G protein GTPase activity, and thus may be steric or conformational in nature. The inhibition of AC type V was mediated by the first 19 amino acids of RGS2 and 3 residues are specifically required to inhibit AC function: Val9, Gln10 and His11 [68]. The RGS2 protein isoforms initiated at the start codons at positions 16 and 33 show an impaired inhibitory activity toward AC V, resulting from the absence of this AC interaction domain [56].

RGS2 can effectively diminish Gq-mediated ***PLCβ*** activation in the absence of GTPase activity [69].

- Regulation of subcellular localization

RGS2 is localized primarily in the nucleus. The N-terminal domain functions as a ***nuclear retention signal***. RGS2 enters the nucleus by passive diffusion where it is retained until it is recruited to the plasma membrane in response to activated G

proteins. RGS protein association with other factors in the cytoplasm, nucleus and Golgi helps to maintain an inactive pool of RGS proteins that can be recruited to the plasma membrane in response to specific signals [70]. The ***amphipathic α-helix*** between AA residues 32 and 54 is responsible for the interaction with the plasma membrane [61].

- Interaction with GPCRs

The short segment N-terminal to the α-helix, as well as the loop between the helix and the RGS domain play a role in selective recognition of GPCRs. RGS2 binds the third intracellular loop of specific G protein-coupled receptors and forms a stable heterotrimeric complex with the activated Gα subunit (through the RGS domain) and the GPCR [71, 72]. This interaction with preferred receptors creates a high degree of specificity in RGS2 function.

- Posttranslational modifications

RGS2 can be phosphorylated and palmitoylated. Depending on the residues involved, these posttranslational modifications can have different effects on the activity of RGS2.

Protein kinase GI-α (PKGI-α) phosphorylates RGS2 on Ser-46 and Ser-64 [73], increasing the ability of RGS2 to associate with membranes and stimulate GTP hydrolysis by Gqα.

Phosphorylation of RGS2 by PKC decreases its capacity to attenuate PLCβ activation and significantly reduces its GAP activity [74].

Cysteine 106, 116 and 199 are multiple putative palmitoylation sites in RGS2. Palmitoylation at sites 106 and 199 elevates GAP activity, and palmitoylation at cysteine 116 impaires its GAP activity *in vitro* [75].

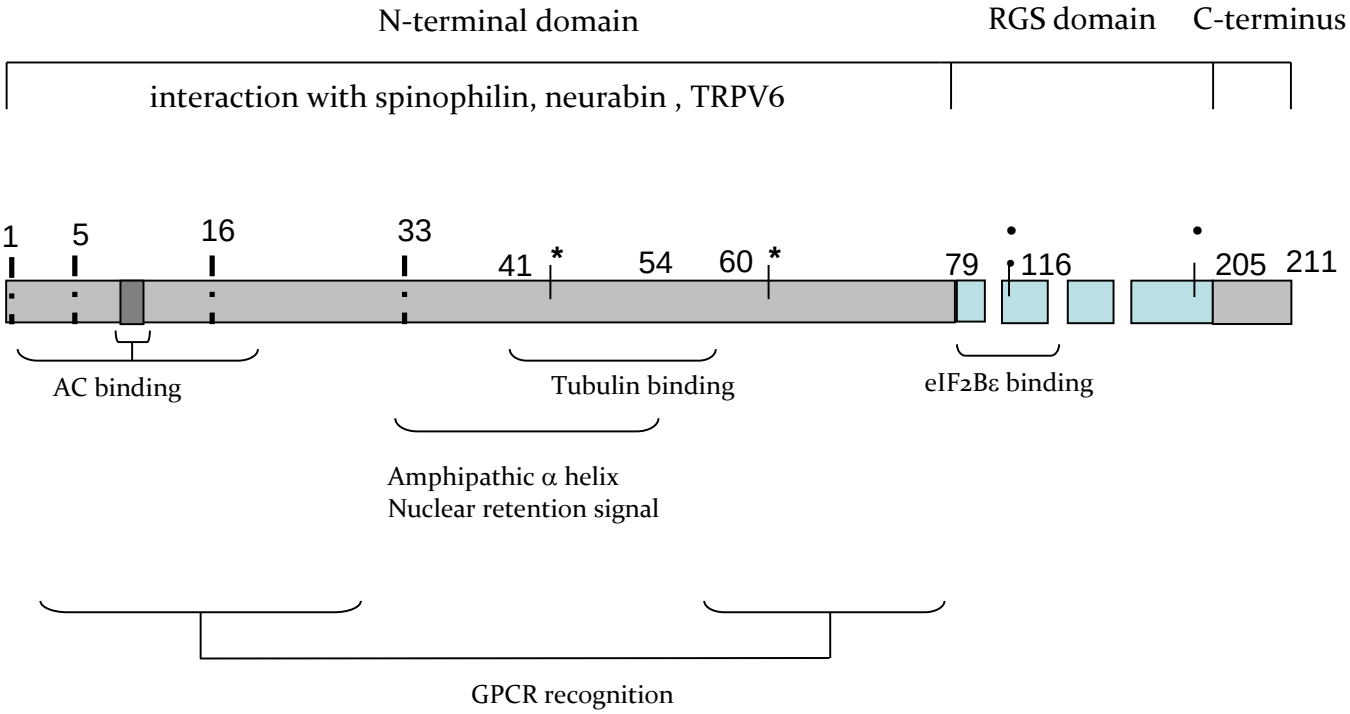

Figure 5: Functional domains of the RGS2 protein.

Four different RGS2 proteins can be translated from the RGS2 mRNA. They differ with regards to their N-terminus, starting at positions 1, 5, 16 and 33 (dotted lines). The N-terminal domain of RGS2 is the site for interaction several proteins: AC (AA 1-19, with the 3 most important residues being AA 9-11), tubulin (AA 41-60), spinophilin, neurabin and TRPV6. The amphipathic α helix and the nuclear retention signal are located between AA 32 to 54. AA 1-32 and 54-79 are involved in GPCR recognition. The RGS domain stretches from AA 79 to 205, and contains a region responsible for binding eIF2Bε. Some residues are targets for posttranslational modifications: AA 46 and 64 can be phosphorylated (*), while AA 106, 116 and 199 are putative palmitoylation sites (•).

2.2.3 Physiological functions of RGS2

Rgs2-deficient mice have been obtained and extensively studied by several groups. They are viable and fertile, but hypertensive, resulting in the development of cardiac hypertrophy [73]. In addition, rgs2-deficient mice are immune compromised. They show a reduced T cell proliferation and IL-2 production,

which translates in an impaired antiviral immunity. They also display increased anxiety responses and decreased male aggression [76]. In conclusion, these studies reveal a role for RGS2 in blood pressure regulation, immunity and the central nervous system. Roles for RGS2 have also been described in adipogenesis and bone formation *in vitro*, cancer and the metabolic syndrome.

2.2.3.1 Role in hypertension

Rgs2-/- as well as rgs2+/- mice show a strong hypertensive phenotype, renovascular abnormalities, persistent constriction of the resistance vasculature and prolonged response of the vasculature to vasoconstrictors in vivo [77]. The hypertensive phenotype in heterozygous mice indicates that there may be a threshold level of RGS2 that is required for normal vascular homeostasis *in vivo* [77]. In humans, RGS2 expression levels have also been associated with hypertension in several studies:

- Patients with Bartter's/Gitelman's syndrome, a hypotensive disorder, have enhanced expression of RGS2, consistent with a role of RGS2 in vascular regulation [78].
- Certain polymorphisms in RGS2 are associated with hypertension in blacks [79], the Japanese population [80] and the Xinjiang Kazakh population [81]. The product of one of these alleles, R44H, is mutated within the N-terminal amphipathic α-helix domain, responsible for plasma membrane targeting. This mutant protein binds to the plasma membrane less efficiently than wild type RGS2 and may lead to altered receptor mediated Gq-inhibition and contribute to the development of hypertension in affected individuals [80]. Another mutation in RGS2, Q2L, a rare N-terminal genetic variant in a Japanese hypertensive cohort, destabilizes the RGS2 protein, making it more susceptible to proteasome degradation, therefore leading to lower RGS2 protein levels [82].
- A study of RGS2 expression in peripheral blood mononuclear cells and skin fibroblasts from hypertensive patients and controls reveals a reduced RGS2

expression and therefore decreased inhibition of Ang II signaling in hypertensive patients [83].

Several mechanisms explain the observed hypertension when RGS2 expression is absent or reduced:

1. Enhanced Gq-mediated vasoconstriction:

RGS2 deficiency leads to prolonged Gq signaling and vasoconstriction in the vasculature. Prolonged activation of Gqα and its effector PLCβ in vascular smooth muscle cells would lead to an enhanced release of intracellular calcium, and consequent activation of myosin light chain kinase to trigger sustained smooth muscle cell contraction. Loss of RGS2 thus increases the duration of contraction by the resistance vasculature, significantly increasing blood pressure. Loss of Gq signaling regulation by RGS2 also exacerbates cardiomyocyte hypertrophy [84].

2. NO-PKGI-α pathway:

RGS2 is activated via the nitric oxide (NO)-cyclic guanosine monophosphate (cGMP) pathway and may influence blood pressure via this pathway. NO and cGMP are largely responsible for vascular smooth muscle relaxation through PKGI-α. PKGI-α phosphorylates RGS2, leading to an enhanced GAP activity. Thus RGS2 mediates the action of the NO-cGMP pathway on blood pressure by promoting the relaxation of the resistance vasculature through its ability to attenuate vasoconstrictor-induced calcium signaling [85].

3. Increased sympathetic activity

Central nervous system mechanisms may also contribute to the increase in blood pressure, given the expression of RGS2 in the brain. In patients with essential hypertension, inappropriately high sympathetic activity is commonly observed [86]. Rgs2 -/- mice show an increased sympathetic nervous system

activity and an inability of the autonomic nervous system to compensate blood pressure changes [87].

2.2.3.2 Role in anxiety

RGS2 is expressed in the cortical and limbic brain regions. The limbic system (including the hippocampus and the amygdala) is involved in emotion, behavior, long-term memory and olfaction. RGS2 gene polymorphisms have been associated with panic disorder, suggesting that RGS2 modulates anxiety not only in mice but also in humans [88, 89]. In addition, RGS2 polymorphisms are associated with suicide and a significantly higher level of RGS2 protein is found in the amygdala of postmortem brain samples of suicide victims compared to controls [90].

2.2.3.3 Role in adipogenesis

The induction of differentiation of mouse 3T3-L1 preadipocytes leads to a rapid increase of RGS2 expression [91]. However, ectopic expression of RGS2 does only induce adipogenesis in the presence of a ligand for peroxisome proliferator-activated receptor γ (PPARγ), a specific transcription factor active during adipogenesis [92]. It seems that overexpression of RGS2 is sufficient for induction of adipocyte differentiation through the PPARγ route.

2.2.3.4 Role in bone formation

cAMP stimulates osteoblast proliferation and differentiation, as do inducers of Gq signaling. Normal cellular levels of RGS2 do not regulate either Gq or Gs signaling in osteoblasts, but at higher expression levels, after induction by either Gs or Gq agonists, RGS2 cross-desensitizes Gs and Gq signals [93].

2.2.3.5 Role in cancer

RGS2 is involved in several types of cancer. Its expression is downregulated in ovarian cancer [94], prostate cancer [95], colorectal cancer [96] and leukemia [55].

Its expression is upregulated in breast cancer [97], fibrolamellar carcinoma [98] and mantle cell lymphoma [99]. This implies an important role for RGS2 in maintaining normal cell growth and differentiation.

2.2.3.6 Role in the metabolic syndrome

The metabolic syndrome is defined as a cluster of cardiovascular risk factors: dyslipidemia, hypertension, glucose intolerance, insulin resistance and central obesity [100]. It is associated with an increased risk for the development of type 2 diabetes mellitus (T2DM) and atherosclerosis. In addition to its role in hypertension and adipocyte differentiation, RGS2 is involved in pancreatic insulin secretion [101] and the gene is located in a region that is linked to the distribution of body fat in men [102] and the metabolic syndrome [103]. In addition, a polymorphism in the *RGS2* promoter region, -395 C/G, is associated with an increased susceptibility to the metabolic syndrome in white European men [104]. The G allele of this polymorphism shows an enhanced promoter activity *in vitro* and it is associated with enhanced RGS2 expression in adipocytes from European men.

III. Platelet signaling

Adapted from: Regulators of platelet cAMP levels: clinical and therapeutic implications. Noé L, Peeters K, Izzi B, Van Geet C, Freson K. Current Medicinal Chemistry, 2010, 17 (26): 2897-2905.

G protein-mediated signaling processes in platelets are crucial to enable them to maintain vascular integrity and prevent bleeding. The major G protein-mediated signaling pathways leading to platelet activation are initiated by the activation of Gqα, G13α (RhoA activation) and Giα. Activation of platelets is highly regulated to control the balance between haemostasis and thrombosis at different levels. The main regulatory factors are calcium, which is critical for platelet activation, and cAMP, which inhibits platelet function.

1 cAMP REGULATION IN PLATELETS

AC activity in platelets is regulated by Giα and Gsα signaling. Platelets express three Giα subfamily members; $Gi_2\alpha$, $Gi_3\alpha$ and Gzα [105] and two Gsα isoforms; Gsα and XLαs [106, 107]. A normal basal cAMP level in platelets reflects ongoing signaling mainly through Gi_2, Gz and Gs. Platelets exhibit ongoing turnover of cAMP formation by AC and breakdown by cAMP phosphodiesterases (PDE), to reach an equilibrium that is still sufficiently high to limit spontaneous platelet activation [108]. The elevation of the platelet basal cAMP levels interferes with basically all known platelet activatory signaling pathways and effectively blocks complex intracellular signaling networks, cytoskeletal rearrangements, fibrinogen receptor activation, degranulation, and expression of pro-inflammatory signaling molecules [109] (Fig. 5). The major target molecule of cAMP in platelets is PKA, which is normally inactive as a tetrameric holoenzyme, consisting of two catalytic and two regulatory units, with the regulatory units blocking the catalytic centers of the catalytic units. cAMP binds to specific locations on the regulatory

units of PKA and causes dissociation between the regulatory and catalytic subunits, thus activating the catalytic units and enabling them to phosphorylate substrate proteins. One of the known substrates of PKA in platelets is the IP_3 receptor that mediates the release of calcium from the dense tubular system, thereby inhibiting its calcium-releasing action [110]. PKA also phosphorylates proteins associated with the platelet cytoskeleton, such as vasodilator-stimulated phosphoprotein (VASP), thereby possibly affecting the platelet shape change [111]. Increased levels of cAMP are also associated with a reduced ability of thrombin to bind its receptor and inhibition of several thrombin-induced responses [112], like the thrombin-induced formation of IP_3 [113].

A major endothelium-derived stimulator of platelet cAMP levels is prostacyclin (PGI_2). PGI_2 acts through the Gs-coupled IP receptor to stimulate AC. IP receptor-deficient mice present with injury-induced vascular proliferation and hyperreactive platelets [114]. Another inhibitor of platelet function by raising cAMP levels is adenosine, released during cell damage. It binds to the Gs-coupled adenosine A_{2a} receptor [115]. On the other hand, platelet activation by decreasing basal cAMP levels is mediated by agonist binding to Gi-coupled receptors. Gi agonists are not able to activate platelets as such, but are able to potentiate the effect of other platelet agonists. Epinephrine acts through the α_{2A}-adrenergic receptor, which preferentially couples to Gz. ADP activates platelets via binding to two different ADP receptors, one of which is coupled to Gi_2 ($P2Y_{12}$) and the other to Gq ($P2Y_1$) [116]. RGS proteins can negatively regulate both Gs and Gi protein-mediated signaling. In human platelets, RGS18 has been described to couple to $Gi_1\alpha$, $Gi_2\alpha$ and $Gi_3\alpha$ [117]. RGS2, which is able to inhibit Gs signaling [67], was detected in rat platelets [118].

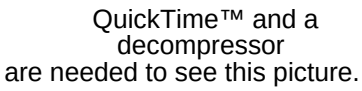

Figure 5: Basal cAMP levels in platelets are the result of the balance between cAMP production by adenylyl cyclase (AC) and cAMP degradation by phosphodiesterase (PDE). cAMP production by AC is stimulated and inhibited by Gsα (Gsα and XLαs) and Giα signaling, respectively. cAMP activates PKA which has several substrates in platelets, one of them being the IP_3 receptor. Phosphorylation of this receptor by PKA inhibits calcium release from the dense tubular system. Increased levels of cAMP also lead to reduced binding of thrombin to its Gq-coupled receptor. Normal Gq signaling involves the activation of phospholipase Cβ (PLCβ) by Gqα. PLCβ hydrolyzes phosphatidylinositol bisphosphate (PIP_2) to diacylglycerol (DAG) and IP_3, which binds the IP_3 receptor leading to a rise in calcium levels. cAMP inhibits the thrombin-induced formation of IP_3.

Defects in the cAMP regulators can lead to functional platelet defects and an imbalance between thrombosis and haemostasis. An increase in Gs function or a defective Gi signaling can be risk factors for bleeding, while a loss of Gs function can result in a prothrombotic state. Defects in Gs- and Gi-coupled receptors, Gsα

and XLαs and their role in regulating platelet cAMP levels will be discussed in relation to human pathology (Table 4).

1.1 Gs-coupled receptor VPAC1

Megakaryocytes and platelets express the Gs-coupled vasoactive intestinal peptide (VIP)/ pituitary adenylate cyclase activating peptide (PACAP) receptor 1 (VPAC1), for which PACAP and VIP are specific agonists [119]. PACAP was first isolated from ovine hypothalamic extracts on the basis of its ability to stimulate cAMP formation in rat anterior pituitary cells [120]. Upon binding to VPAC1, PACAP increases the intracellular cAMP levels via Gsα and as such, platelet function is inhibited [119]. This was elucidated by studying two related patients with a partial monosomy 20p and trisomy 18p, who have three copies of the *PACAP* gene. These patients show elevated PACAP concentrations in the plasma and suffer from multiple neurological (epilepsy, hypotonia, convulsions, mental retardation, tremor, psychotic, hyperactive behavior), gastro-intestinal (diarrhea, vomiting) and endocrinological (hypoplasia of the pituitary gland, hypogonadotropic hypogonadism) problems and have a pronounced bleeding tendency and mild thrombocytopenia [119, 121]. The patients' platelets show a strongly elevated basal cAMP level and, as such, their platelet aggregation is reduced. Moreover, bone marrow examination of the PACAP overexpression patients reveals almost no mature megakaryocytes. Indeed, VPAC1 signaling not only affects platelet function but also megakaryocyte maturation and platelet production [121].

1.2 Gi-coupled receptor $P2Y_{12}$

ADP is stored in platelet dense granules, and secreted upon platelet activation. This agonist causes a full range of activation events, including intraplatelet calcium elevation, thromboxane A_2 (TXA_2) synthesis, protein phosphorylation, shape change, granule secretion and aggregation. All of these events are mediated by

interaction with 2 GPCRs: $P2Y_1$ and $P2Y_{12}$, which couple to Gq and Gi_2 respectively [116]. $P2Y_{12}$ knockout mice show a significantly prolonged bleeding time and are protected from arterial thrombosis [122]. Their platelets show a normal shape change, but an impaired aggregation in response to ADP. $P2Y_{12}$ is the major receptor to amplify and sustain ADP-mediated platelet activation initiated via $P2Y_1$. Several mutations in the gene encoding $P2Y_{12}$ have been described in relation to human pathology. Hollopeter *et al.* describe a patient with a bleeding disorder, who carries a defect in the *$P2Y_{12}$* gene leading to haploinsufficiency [123]. Platelets of this patient show impaired ADP-dependent platelet aggregation and greatly reduced ADP binding activity and lack the ability to inhibit cAMP levels in response to ADP. Cattaneo *et al.* describe a patient with a congenital bleeding disorder with normal shape change, but reduced and reversible aggregation in response to ADP, and failure of ADP to inhibit the rise of cAMP levels after stimulation with a Gs agonist. This patient presents abnormal $P2Y_{12}$-dependent platelet activation despite normal ADP binding to the membrane surface. Analysis of the *$P2Y_{12}$* gene revealed 2 missense mutations, defining a region important for GPCR function [124]. Several other patients with congenital defects in the platelet $P2Y_{12}$ receptor have now been described, characterized by bleeding diathesis, comprised of easy bruising, mucosal bleedings, and excessive post-operative hemorrhage.

1.3 Gi-coupled receptor EP3

The actions of prostaglandins are mediated through binding to specific GPCRs. The receptor for prostaglandin E_2 (PGE_2) consists of four subtypes: EP1, EP2, EP3 and EP4. Signaling of EP1 results in calcium elevation, and EP2 and EP4 stimulation leads to an increase in cAMP levels. The EP3 subtype is coupled to Gi and results in inhibition of AC, leading to a reduction in intracellular cAMP. Via the EP3 receptor, PGE_2 potentiates platelet aggregation induced by TXA_2 and ADP, but it does not induce platelet aggregation by itself. It decreases the threshold at

which agonists activate platelets to aggregate. Mice lacking this receptor show an increased bleeding tendency and a decreased susceptibility to thromboembolism [125, 126]. It has also been demonstrated that PGE_2 produced by atherosclerotic plaques in mice can facilitate arterial thrombosis, acting via EP3 [127]. Studies show that an EP3 antagonist, DG-041, inhibits the pro-aggregatory effect of PGE_2 on platelets and potentiates the protective effect of PGE_2 on platelet aggregation via receptors other than the EP3 receptor [128]. In phase I clinical trials DG-041 prevented EP3-induced platelet aggregation without increasing bleeding times, even when administered at high dose for 7 days [129]. A reduction in thrombosis without an effect on bleeding time would provide an attractive alternative to current antiplatelet therapies. Defects in the EP3 receptor gene are not yet discovered in humans.

1.4 Stimulatory G proteins: Gsα and XLαs

In platelets and megakaryoblasts, Gsα is present in a short (45 kDa) and a long (52 kDa) isoform, the Gsα-S and Gsα-L isoforms, respectively [106]. Platelets also express the XLαs variant [107]. The importance of Gsα function in platelets is demonstrated by the fact that genetic alterations in the *GNAS* cluster have been reported to be associated with both bleeding and thrombotic phenotypes. The platelet Gs activity can be easily studied by using the platelet aggregation-inhibition test, which is based on the inhibition of platelet aggregation upon stimulation with different Gsα agonists such as PGI_2 [130]. With this test, a platelet Gs hyperfunction has been identified in a group of patients having a paternally inherited insertional polymorphism in the *GNASXL* gene that encodes for XLαs [107, 131]. XLαs can mimic Gsα functions being able to bind to βγ subunits and interact with AC [132, 133]. The mutated variant of XLαs is associated with elevated inducible platelet Gs activity and a high level of cAMP formation, and therefore leads to an increased trauma-related bleeding tendency [107, 131]. On the other hand, Gs hypofunction has been shown to be also relevant in platelet function

since a first compound heterozygous Gsα deficient patient has been described to have a thrombotic phenotype due to absence of inhibition of platelet aggregation by Gsα stimulation and extreme platelet hyperreactivity [130]. His platelets show a severely reduced cAMP production after Gs-coupled receptor activation.

Table 4: Regulators of platelet cAMP levels in relation to human pathology.

Gene	OMIM	Disease
VPAC1	192321	Increased stimulation of VPAC1: neurological, gastro-intestinal and endocrinological problems, a pronounced bleeding tendency and mild thrombocytopenia
P2Y12	600515	P2Y12 deficiency: bleeding diathesis, comprised of easy bruising, mucosal bleedings and excessive post-operative hemorrhage
EP3	176806	EP3 deficient mice: increased bleeding tendency
Gsα/Xlαs	139320	Gs hyperfunction: increased trauma-related bleeding tendency; Gs hypofunction: thrombotic phenotype

2 PLATELET SIGNALING IN TYPE 2 DIABETES

2.1 Type 2 diabetes

Diabetes is defined by the World Health Organization as a chronic condition that occurs when the pancreas does not produce enough insulin (type 1 diabetes mellitus) or when the body cannot effectively use the insulin it produces (type 2 diabetes mellitus (T2DM)). Insulin regulates glucose uptake into adipose tissue and muscle, and prevents glucose output from the liver. As blood sugar concentrations rise, insulin is secreted in the blood stream by the pancreatic β cells. Insufficient insulin action leads to decreased glucose uptake and therefore hyperglycemia. If not well treated this leads to serious damage to many of the body's systems, especially the nerves and blood vessels.

A uniform finding in T2DM is insulin resistance. The insulin receptors do not efficiently respond to the produced insulin resulting in an increased demand for insulin, which is inadequately met by insulin secretion. Insulin resistance is a multisystem disorder, associated with multiple metabolic and cellular alterations. Metabolic disturbances that commonly occur in patients with insulin resistance are dyslipidemia, hypertension, glucose intolerance and a prothrombotic state, often in combination with central obesity [134]. This phenotype may precede the development of diabetes by many years and is referred to as the metabolic syndrome [100]. Treatment of T2DM is mainly focused on lifestyle changes, especially dietary and exercise management to obtain weight loss and improve glucose tolerance. In addition, pharmacological therapy is aimed on decreasing insulin resistance and increasing insulin secretion.

2.2 Prothrombotic state

Changes in platelet function have been described in diabetes, leading to a general prothrombotic state. Platelets from diabetic patients have been found to be more adhesive and hypersensitive to a variety of aggregating agents.

Several factors contribute to this increased sensitivity:

- One major reason for platelet hypersensitivity is increased production of arachidonic acid metabolites, like TXA_2, a potent vasoconstrictor and platelet aggregating agent [135].
- A variety of platelet adhesion molecules show an increased expression on the platelet surface [136, 137].
- Insulin has a direct antiplatelet effect. It attenuates thrombin-induced calcium response and platelet aggregation, as well as responses to ADP, collagen, arachidonic acid and platelet activating factor [138]. Insulin has also been described to increase NO production. In diabetic patients, insulin responses are reduced, leading to a reduction of its antiplatelet properties.

- Redox stress plays a major role in the pathogenesis of vascular complications of diabetes. Decreased vascular NO production coupled with the overproduction of reactive oxygen species and oxidants is linked to altered platelet function [139]. Furthermore, diabetes is associated with reduced levels of antioxidants [140].
- Another prominent change in the diabetic platelet is calcium homeostasis [141]. Calcium is increased due to dysregulation of the platelet natrium/calcium exchanger, and due to changes in the activity of calcium ATPases, which are highly sensitive to oxidative damage [142].
- In addition, platelets of diabetic patients have been reported to have diminished sensitivity to PGI_2 [143].

In conclusion, platelets are hypersensitive to aggregants, and hyposensitive to anti-aggregants, and this is thought to contribute to enhanced atherosclerosis via increased platelet activity at sites of vessel injury. The risk of cardiovascular disease is therefore increased in patients with T2DM [144]. Antiplatelet therapy is part of the treatment of T2DM, especially when other risk factors for cardiovascular disease as obesity, hypertension and dyslipidemia are present.

3 REGULATION OF PLATELET cAMP LEVELS AS POTENTIAL THERAPY FOR CARDIOVASCULAR DISEASE

The well-established role of platelets in the pathophysiology of atherosclerosis and atherothrombosis led to the development of many drugs that inhibit platelet function and prevent atherothrombotic events. Current oral antiplatelet therapy consists of aspirin and $P2Y_{12}$ antagonists, mainly targeting the TXA_2 and ADP pathways respectively. $P2Y_{12}$ became an important target for the development of several drugs based upon the functional studies in $P2Y_{12}$ deficient mice and patients. The thienopyridine class of ADP receptor antagonists acts specifically on the $P2Y_{12}$ receptor. Members of this class are ticlopidine and clopidogrel. Ticlopidine was first discovered in 1972, and has been used when aspirin was not

tolerated, or when dual antiplatelet activity was desirable. Now, clopidogrel is more often used since it has an additional methoxycarbonyl group on the benzylic position, which provides an increased pharmacological activity and a better safety and tolerability profile, compared to ticlopidine. In 2002, clopidogrel was approved in addition to standard therapy for the reduction of atherothrombotic events in patients with acute coronary syndromes. Thrombi formed in clopidogrel-treated subjects have a loosely woven structure with few interplatelet contacts [145]. Platelet shape change and intracellular calcium increase after the addition of ADP are not inhibited by clopidogrel. Its active metabolite modifies the $P2Y_{12}$ receptor by the formation of a disulfur bridge between the reactive thiol group of the active metabolite and a cysteine residue of the $P2Y_{12}$ receptor on platelets. This interaction is irreversible for the remainder of the lifespan of the platelets and leads to the inhibition of the downregulation of AC [146]. The active metabolite of clopidogrel is produced in the liver. First clopidogrel is metabolized into 2-oxo-clopidogrel through a CYP450-mediated pathway, which is then hydrolyzed and generates the highly labile active metabolite [147]. The recommended platelet inhibitory treatment for patients with acute coronary syndrome and patients undergoing percutaneous coronary intervention with stent implantation, is a combination of aspirin and clopidogrel. But, 15-40% of patients are poor responders to clopidogrel, and clinical trials show that these patients are at increased risk of stent thrombosis, myocardial infarction and death [148]. This interindividual variability in the response to clopidogrel can be explained by several genetic factors. Allelic variants of genes modulating clopidogrel absorption (ABCB1) and metabolic activation (CYP2C19) are associated with a higher rate of cardiovascular events after an acute myocardial infarction [149]. The genes encoding the CYP enzymes are polymorphic, and certain alleles confer reduced enzymatic function. CYP3A4, CYP3A5 and CYP2C19 are the most abundant hepatic P450 enzymes, and are considered to be the main enzymes involved in thienopyridine metabolism. Carriers of a reduced function CYP2C19 allele have

significantly lower levels of the active metabolite of clopidogrel, diminished platelet inhibition, and a higher rate of major adverse cardiovascular events, than do noncarriers [150]. Because of this variability in response to clopidogrel, other antiplatelet treatments are being developed. Prasugrel is a newer thienopyridine that also irreversibly binds $P2Y_{12}$, but with a more rapid onset of action, a stronger inhibitory effect [151], a lower variability in platelet response, and not susceptible to genetic variation in CYP isoenzymes [152]. Prasugrel first undergoes de-esterification to an intermediate thiolacetone, which is then converted to the active metabolite in a single CYP-dependent step, which is not impacted by reduced function CYP polymorphisms [153]. Recently, other agents that result in reversible inhibition of the $P2Y_{12}$ receptor are being studied, namely cangrelor and ticagrelor. They change the conformation of the $P2Y_{12}$ receptor, resulting in reversible, concentration-dependent inhibition of the receptor. Ticagrelor and cangrelor both directly antagonize ADP binding to the $P2Y_{12}$ receptor without the need for any metabolic activation. Cangrelor reaches steady state concentrations in plasma within 30 min of start of infusion and has a very short half life of less than 9 min [154]. Ticagrelor is rapidly absorbed and undergoes enzymatic degradation after oral administration to at least one active metabolite with similar pharmacokinetics to the parent compound. Maximum plasma concentrations are reached 1 to 3 hours after treatment, and plasma half-life is 6 to 13 hours [155]. Ticagrelor antagonizes ADP-mediated receptor activation in a non-competitive manner, suggesting different binding sites on human $P2Y_{12}$ for ADP and ticagrelor [156]. In patients with acute coronary syndrome, treatment with ticagrelor, as compared with clopidogrel, significantly reduced the rate of death from vascular causes, myocardial infarction, or stroke without an increase in the rate of overall major bleeding but with an increase in the rate of non-procedure-related bleeding. Also, new side effects were seen, as dyspnea, bradyarrhytmia and increased serum levels of uric acid and creatinine [157]. But the availability of 3 agents for

antagonizing platelet ADP receptors may make it possible to individualize antiplatelet therapy.

Chapter II

Aims of the study

The aim of this PhD project was to study the role of RGS2 in physiological processes, based on preliminary results that were obtained in our research group. More specifically we studied RGS2 in platelet production and function on the one hand, and in a number of other physiological processes as type 2 diabetes, adipogenesis and skeletal development on the other hand. To unravel the mechanisms involved we used *ex vivo* and *in vitro* approaches, complemented with *in vivo* studies in the zebrafish model.

1. The role of RGS2 in platelet production and function

We studied the involvement of RGS2 in platelet production and function starting from a patient from UZ Gasthuisberg (Leuven). We identified a heterozygous missense mutation (G23D) in the *RGS2* gene of this patient, her mother and her brother. The carriers of this mutation all have enlarged round platelets, containing abnormal alpha granules, and showing a Gs hypofunction. We characterized the effect of the mutation on RGS2 function and studied the role of RGS2 in megakaryopoiesis and platelet Gs function.

2. Other physiological functions of RGS2

An epidemiological study conducted by our research group identified a functional *RGS2* promoter polymorphism (-395C/G), associated with the metabolic syndrome in white European men [104]. Since the metabolic syndrome is associated with a five-fold increased risk to develop T2DM, we set up an epidemiological study to assess the association of this *RGS2* polymorphism and RGS2 expression levels with T2DM.

Apart from the platelet defects the patient described in part 1 also showed obesity, shortened little fingers and an increased bone alkaline phosphatase. Therefore, we decided to study RGS2 function in adipogenesis and skeletal development in the zebrafish model.

Chapter III

RGS2 in platelet production and function

III.I. RGS2 in platelet production and function: Studies in humans

Adapted from Platelet Gs hypofunction and abnormal morphology resulting from a heterozygous RGS2 mutation. Noé L, Di Michele M, Giets E, Thys C, Wittevrongel C, De Vos R, Overbergh L, Waelkens E, Jaeken J, Van Geet C, Freson K. Journal of Thrombosis and Haemostis, 2010.

Introduction

RGS2 contains an RGS domain (AA 79 to 205) required for the activation of the GTPase activity of G protein α subunits. The RGS domain is flanked by short N- and C-terminal sequences. Via its N-terminal domain, RGS2 is able to interact with several other proteins, and can therefore exert functions independent of its GTPase activating activity. One important function, dependent on sterical inhibition, is the downregulation of Gs-dependent cAMP production by interacting with Gsα and several AC isoforms [67]. Sinnarajah *et al.* showed that, in olfactory neurons, RGS2 attenuates the activation of AC type III [158], which is the predominant AC isoform in platelets [159]. The AC inhibitory domain is located within amino acids 9 to 11 in the N-terminal domain of RGS2.

Here we describe the first human genetic defect in RGS2 and provide evidence that RGS2 plays a role in platelet Gs function and platelet formation. The proposita is a 17-year-old girl with borderline IQ, hirsutism, increased bone alkaline phosphatase and a decreased platelet Gs function. We found a heterozygous mutation in the RGS2 gene of this patient, her mother and her brother, which leads to a reduced production of cAMP after stimulation of the Gs pathway in their platelets. Carriers of this mutation also have enlarged platelets, containing abnormal α granules. This suggests a role for RGS2 in platelet production.

Experimental procedures

Patient studies

Informed consent was obtained from all participants and/or their legal representatives according to the Declaration of Helsinki. This study was approved by the Institutional Review Board.

Platelet electron microscopy

Blood of all family members was anticoagulated with 3.8% (wt/vol) trisodium citrate (9:1). Platelet-rich plasma (PRP) was obtained after centrifugation at 150 g for 15 min. The platelet-rich fractions were immediately fixed overnight in 2.5% glutaraldehyde and 0.1 M phosphate buffer (4°C). After centrifugation at 800 g for 10 min a condensed pellet of platelets was formed. Post-fixation was carried out in 2% osmium tetroxide, 0.1 M phosphate buffer and dehydration in graded series of ethanol. Finally, the pellets were embedded in epoxy resin. Ultrathin sections were cut, stained with uranyl acetate-lead citrate and examined on a Zeiss EM 10 electron microscope (Heidelberg, Germany). Images were recorded digitally with a Jenoptik Progress C14 camera system operated using Image-Pro express software.

Platelet aggregation and ATP secretion

PRP of all family members was obtained as described above, and platelet count was adjusted to 250 x 10^9 platelets/L with autologous platelet-poor plasma. Aggregation was performed on 2 dual-channel Chrono-Log aggregometers (Chrono-log Corp, Havertown, PA, USA). Horm collagen (0.5, 1 and 2 µg/ml; Nycomed Arzneimittel, Munich, Germany), ristocetin (0.5 and 1.2 mg/ml; Kordia Life Sciences, Leiden, The Netherlands), arachidonic acid (1mM; Sigma-Aldrich, St. Louis, MO, USA), the thromboxane A2 analogue U46619 (1.33 µM; Sigma-Aldrich), and ADP (2.5 and 5 µM; Sigma-Aldrich) were used as agonists. ADP was used alone and in combination with a $P2Y_1$ selective inhibitor (MRS-2179; Sigma-Aldrich) or a

$P2Y_{12}$ selective inhibitor (AR-C69931MX; AstraZeneca, Loughborough, UK). To study ATP secretion, platelet aggregation and secretion were recorded in real time at 37°C with stirring after stimulation with Horm collagen (2 μg/ml) and ADP (10 μM). ATP secretion was determined by measuring the release of ATP using luciferin/luciferase reagent (Kordia Life Sciences).

Platelet aggregation-inhibition Gs test and cAMP measurements

Aggregation-inhibition studies involved dose-response curves with the Gs agonist prostaglandin E_1 (Prostin, 0-125 ng/ml; Pharmacia-Upjohn, Peapack, NJ, USA) that was added to adjusted PRP 1 min prior to induction of aggregation by collagen (2 μg/ml). This test is based on cAMP-mediated inhibition of platelet aggregation after Gsα stimulation [160].

Platelet cAMP levels of all family members were measured using the cAMP enzyme immunoassay (GE Healthcare, Uppsala, Sweden) according to the manufacturer's protocol, under unstimulated conditions and after incubating adjusted PRP with prostacyclin (Iloprost, 2 ng/ml; Schering, Kenilworth, NJ, USA), and stopping the reaction at different time points by the addition of 12% trichloroacetic acid (TCA).

Genetic analysis

Genomic DNA was isolated from peripheral blood according to standard procedures.

Total RNA from platelets from all family members and controls was extracted with TRIzol™ total RNA isolation reagent (Invitrogen, Merelbeke, Belgium) according to the manufacturer's protocol. Approximately 1 μg of total RNA, in the presence of RNaseI inhibitor (Invitrogen), was used for oligo(dT)-primed first strand cDNA synthesis using M-MLV reverse transcriptase (Invitrogen). The GNAS cDNA was amplified using primers GSF3 (5'-GCTGCCTCGGGAACAGTAAG-3') and GSR6 (5'-TAATCATGCCCTAGGTGGGTG-3'). The RGS2 gene was amplified using

primers RGS2-F4 (5'-CACTCTTCATTCGAAATCAGG-3') and RGS2-R1 (5'-CCATTTCTGGGC TCCCTTTTAC-3'). In 200 controls, we ruled out the G23D mutation by means of digestion of the fragment generated by primers RGS2-F4 and RGS2-R3 (5'-GTTTGCAGCTTGCAGTGTGGGGC-3') by *Bsu*RI (Fermentas, St. Leon-Rot, Germany). Automated sequencing of GNAS cDNA and all RGS2 exons was performed by BigDye terminator chemistry on an ABI 310 sequencer (Applied Biosystems, Foster City, CA, USA).

Cell culture

HEK293 and MEG-01 cells were grown in Dulbecco's modified Eagle's medium (DMEM) and RPMI-1640 medium (Invitrogen) respectively, supplemented with 10% heat-inactivated FBS and antibiotics (Invitrogen) at 37°C in a humidified atmosphere of 5% CO_2.

cAMP measurements in transfected HEK293 and MEG-01 cells

The coding region of RGS2 wild type (wt) and mutant (G23D) cDNA was amplified using primers RGS2-F8 (5'-ACAGCCGGGGCTCCAGCGG G-3') and RGS2-R1, and cloned into the *Bst*XI cloning site of the pcDNA3.1 vector (Invitrogen). These constructs were transfected in HEK293 and MEG-01 cells using lipofectamine 2000 (Invitrogen) and the Cell Line Nucleofector Kit C (Amaxa AG, Cologne, Germany) respectively, according to the manufacturer's protocol. An equal expression level of both constructs was confirmed by Real-Time PCR (7500 Fast System; Applied Biosystems). Total RNA extracted from transfected cells was converted to cDNA, and RGS2 expression was measured relative to actin expression using TaqMan gene expression assays for both genes (Applied Biosystems). Transfected HEK293 and MEG-01 cells were grown to confluence in a 96 well plate, and incubated with the Gs agonist isoproterenol (1 μM; EMD Chemicals, Gibbstown, NJ, USA) or prostin (200 ng/ml) respectively, in the presence of a phosphodiesterase inhibitor (IBMX, 100 μM; Janssen Chimica,

Beerse, Belgium). cAMP production was stopped at different time points by adding cell lysis buffer supplied by the kit and cAMP levels were measured using the cAMP enzyme immunoassay (GE Healthcare). Data were collected from four wells for each experimental condition. Values were compared by means of the Student's t-test for unpaired data.

In vitro transcription-translation assay

^{35}S-methionine (GE Healthcare) labeled wild type (wt) and mutant (G23D) RGS2 protein were produced in an *in vitro* transcription-translation system (TNT coupled reticulocyte lysate systems, Promega Corporation, Madison, WI, USA) using the pcDNA3.1 constructs. The proteins were mixed with reducing SDS buffer and resolved by means of SDS-PAGE on a 12.5% acrylamide gel. The gel was dried (gel dryer, Bio-Rad Laboratories, Hercules, CA, USA) and the proteins were visualized by means of autoradiography. The experiment was performed in triplicate.

Immunoblot analysis of AC type III

HEK293 cells were lysed in ice-cold PBS containing 1 tablet protease inhibitor cocktail (Roche Diagnostics, Mannheim, Germany), 1% IGEPAL CA-630 (Sigma-Aldrich), 0.015 % DTT and 1 mM EDTA, by means of three freeze-thaw cycles. Lysates were cleared of insoluble debris by centrifugation at 14000g for 20 min at 4°C and protein concentrations were determined using the Bio-Rad Protein Assay (Bio-Rad Laboratories, Hercules, CA, USA).). Protein lysate was mixed with reducing SDS buffer, resolved by SDS-PAGE on 5% acrylamide gels, and transferred to Hybond ECL-nitrocellulose membrane (Amersham Biosciences, GE Healthcare). The blots were blocked for 1h at room temperature in Tris-buffered saline with Tween (TBS-T; 0,1% Tween-20). Blots were revealed with polyclonal anti-AC type III antibody (sc-588; Santa Cruz Biotechnology Inc., Heidelberg, Germany). The secondary antibody was conjugated with HRP (goat anti rabbit;

Dako, Glostrup, Denmark) and staining was performed with the western blotting ECL reagent (Amersham, GE Healthcare).

Immunoprecipitation of RGS2 and AC type III

The coding region of wild type (wt) and mutant (G23D) RGS2 was cloned in the pEGFP-N1 vector (Clontech, Mountain View, CA, USA) at the BamHI and XhoI restriction sites. HEK293 cells were transfected with these GFP fusion constructs using lipofectamine 2000. Transfected cells were selected with and maintained in DMEM supplemented with geneticin (800 µg/ml) (G418, Invitrogen). These cells were lysed as described and protein concentrations were determined using the Bio-Rad Protein Assay (Bio-Rad Laboratories). Protein lysates (250 µg) were added to a mix of 500 µl RIPA binding buffer (10 mM Tris-HCl pH 7.5; 1% sodium deoxycholate, 1% NP40; 150 mM NaCl; 1,5 mM EDTA; 1,5 mM PMSF and 1 tablet protease inhibitor cocktail), 50 µl protein A beads and 5 µl anti-AC type III antibody or anti-dystrophin antibody (sc-15376; Santa Cruz Biotechnology Inc.). After overnight incubation at 4°C with rotary agitation and three wash cycles in RIPA binding buffer, 20 µl of reducing SDS buffer was added to the beads and bound proteins were resolved by SDS-PAGE on 10% acrylamide gels as described. Blots were revealed with polyclonal anti-GFP antibody (Rockland Immunochemicals Inc., Gilbertsville, PA, USA), followed by HRP-conjugated secondary antibody (rabbit anti goat; Dako). The experiment was performed in triplicate. Intensities of the detected proteins were quantified with the ImageJ software (National Institutes of Health, Rockville Pike, MD, USA).

Flow cytometric analysis

PE-conjugated CD62P (AC1.2; BD Biosciences Pharmingen, Heidelberg, Germany) was used to detect P-selectin expression on platelets, before and after stimulation with ADP (20 µM). MEG-01 cells were transfected with the pEGFP-N1 constructs and the pEGFP-N1 vector as negative control. Forward scatter and side

scatter of cells expressing GFP were determined. Values of three measurements were compared by means of the Student's t-test for unpaired data. We used Cell Quest software for 2-color immunofluorescence acquisition on a FACSCalibur flow cytometer (BD Biosciences).

Proteomics of platelet granule protein content

40 mL of blood from patients 1 and 2 and three healthy volunteers was collected into vacutainer ACD-A tubes (BD Biosciences). They had not taken any medication affecting platelets for the previous two weeks. Platelets were obtained from PRP by several centrifugation steps and resuspended in JNL buffer (130 mM NaCl, 10 mM trisodium citrate, 9 mM $NaHCO_3$, 6 mM dextrose, 0.9 mM $MgCl_2$, 0.81 mM KH_2PO_4, 10 mM Tris, pH 7,4) containing 1.8 mM $CaCl_2$. Platelets were stimulated for 5 min with 60 µM A23187 (Calbiochem, La Jolla, CA, USA) and 20 µM TRAP-6 (Sigma-Aldrich) under stirring conditions at 37°C. Immediately after, 1 mM PMSF and 1 tablet of protease inhibitor cocktail were added to the samples to prevent protein degradation. Samples were centrifuged at 1000 g for 10 min and the supernatants, containing released proteins, were further ultracentrifuged at 50 000 g for 1h to remove microvesicle contamination. The released proteins were precipitated at -20°C overnight in 25% TCA in acetone.

Proteins contained in platelet granules and secreted from activated platelets from patients 1 and 2 and three controls were compared by 2D-DIGE, as described previously [161]. In short, platelet releasates (50 µg) were labeled with 400 pmol of Cy3 or Cy5, whereas the pooled internal standard was labeled with Cy2. The labeling reaction was quenched with 10 mM lysine. The first dimensional seperations were carried out on 24 cm, pH 3-11 NL strips on an IPGphor system (GE Healthcare) using the following conditions: 1.5h at 150 V, 1h at 500 V in gradient, 2h at 1000 V in gradient, 3h at 8000 V. IPG strips were first incubated for 20 min in equilibration buffer (6 M urea, 30% glycerol, 2% SDS, 50 mM Tris-HCl pH 8.8) with 1% DTT and then with 4% iodoacetamide. The second dimensional

separation was carried out on a 12% SDS-polyacrylamide gel at 20°C at 12 mA/gel on an Ettan DaltSix system (GE Healthcare). Labeled proteins were visualized using the Typhoon Trio imager (GE Healthcare). The Cy2, Cy3 and Cy5 components of each gel were individually imaged using excitation/emission wavelengths specific for Cy2 (488/520 nm), Cy3 (532/580 nm) and Cy5 (633/670 nm). Gel analysis was performed using DeCyder 2-D Differential Analysis Software v6.5 (GE Healthcare). Fold change was calculated as the ratio of the average standardized abundance between the patients and the controls. Within the BVA (Biological Variation Analysis) module, each comparison was filtered to find the spots having a p-value <0.01 for the paired t-test. After gel visualization with silver staining to pick spots of interest [162], the peptides of interest were tryptic digested, extracted out of the gel plugs, concentrated and desalted using Millipore C18 ZipTips (Millipore, Bedford, MA, USA). The samples were mixed in a 1:1 (v/v) ratio with α-cyano-4-hydroxycinnamic acid matrix (saturated solution in 50% ACN and 2.5% TFA) and spotted onto the target plate. MS/MS analyses were performed on a 4800 MALDI-TOF/TOF instrument (Applied Biosystems, Foster City, CA, USA). Measurements were taken in the positive ion mode between 900 and 3000 m/z. Data interpretation was carried out using the GPC Explorer Software (Version 3.5), and database searching was carried out using the Mascot program (Version 2.0.00). MS/MS searches were conducted with the following settings: NCBI and MSDB (taxonomy set on humans) as database, MS/MS tolerance for precursor and fragment ions of 1 Da, carbamidomethylation of cysteine and methionine oxidation as fixed and variable modification, respectively. A maximum of one tryptic missed cleavage was allowed. Using these parameters the probability-based MOWSE (Molecular Weight Search) scores greater than the given cutoff value for MS/MS fragmentation data were taken as significant ($p<0.05$).

Results

Patients description

The proposita (patient 1) was born from consanguineous parents. She showed a delay in walking without support at 20 months but had no other problems until the age of 9 years, when she started to develop neurological regression, a bizarre behavior and hallucinations, as well as anorexia. At the age of 11.5 years, clinical examination showed a slowly acting girl with weight of 43.9 kg (between the 75th and 97th centiles), height of 141.5 cm (25th centile), head circumference of 52 cm (25th centile), and shortened little fingers. She presented ptosis of the eyelids, internal strabism and myopia. On the Wechsler Intelligence Scale for Children (WISC-R) she obtained a global score of 75 with equal scores for total intelligence quotient (TIQ), vocal intelligence quotient (VIQ) and practical intelligence quotient (PIQ). Neurotechnical investigations including electromyography and nerve conduction velocity, ophthalmologic investigation and brain magnetic resonance imaging were normal. Results from extensive laboratory investigations including calcium, inorganic phosphorus and thyroid-stimulating hormone levels, were normal, except for an increased serum IgA (4.11 g/L; normal: 0.6-2.7) and a repeated increase of serum alkaline phosphatase (1030 and 1192 U/L; normal: < 720) due to an increased bone isozyme. At the age of 14, she also presented with hirsutism. Now, at the age of 17, the neurological problems and hallucinations diminished, and serum alkaline phosphatase values normalized (327 U/L; normal: < 936). The mother (patient 2), brother (patient 3) and father do not show any obvious clinical abnormalities.

The shortened fingers and low IQ of patient 1 are also seen in patients with Albright Hereditary Osteodystrophy (AHO), which is associated with loss of Gs function, caused by heterozygous inactivating mutations in the coding region of the Gsalpha gene (GNAS) [35]. AHO is further characterized by short stature,

obesity, round face and subcutaneous ossifications, but the severity of these symptoms can vary largely between different patients.

Functional platelet studies

We studied platelet Gs activity in all family members by means of an aggregation-inhibition test, as described previously [163]. Collagen-induced platelet aggregation was dose-dependently inhibited with a specific agonist for Gs-coupled receptors, namely prostaglandin E_1 (Prostin). Platelets from patients 1, 2 and 3 were less sensitive to Gs stimulation compared to platelets from the father, which showed a normal response (Fig. 1A). Basal cAMP levels were comparable in patients 1 and 2, the father and three controls (Fig. 1B). These results suggest a reduced cAMP production after stimulation of the Gs signaling pathway in the platelets from the patients. This was confirmed by measurements of platelet cAMP levels in patients 1 and 2, before and after stimulation of the Gs pathway with a stable prostacyclin analogue (Iloprost; 2 ng/ml) at different time points (Fig. 1C).

A

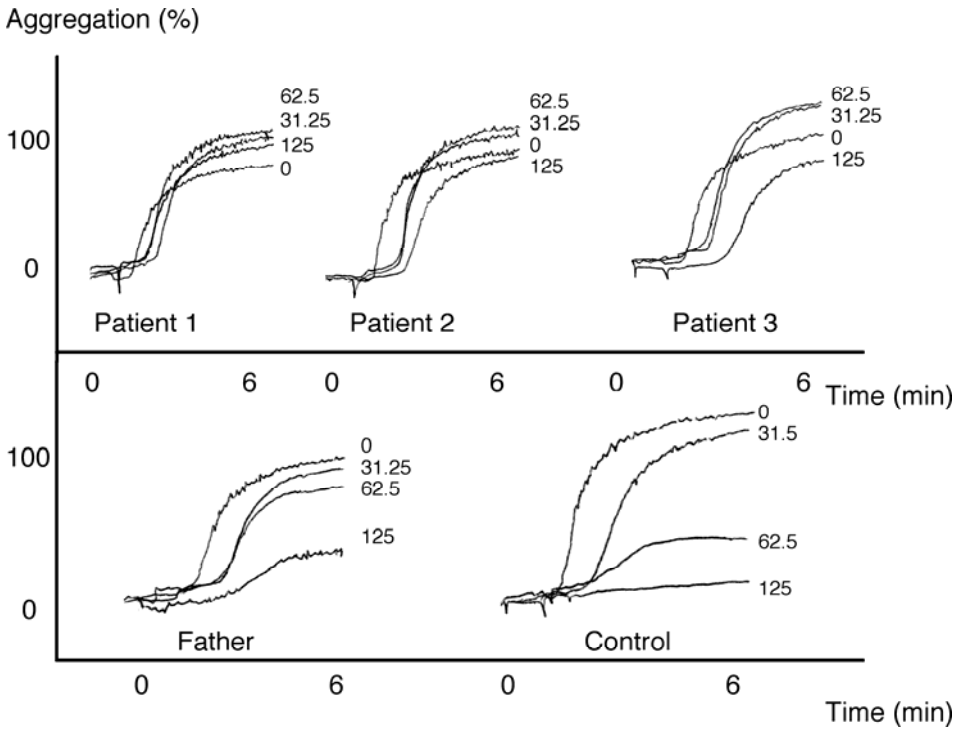

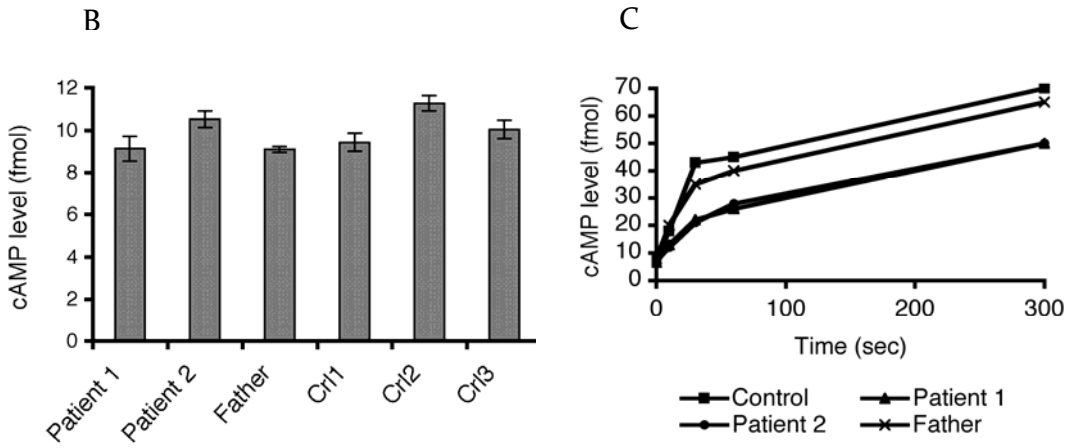

Figure 1: Platelet Gs signaling in patients and controls.

A. Induction of platelet aggregation with collagen (2 µg/ml) is inhibited with different concentrations of prostaglandin E1 (Prostin; ng/ml). Higher concentrations of Gs agonist are necessary to inhibit platelet aggregation in patients 1, 2 and 3 compared to the father and a control.

B. cAMP measurements in unstimulated platelets from patients 1 and 2, the father and three controls (crl 1-3). Basal platelet cAMP levels are comparable in patients and controls.

C. cAMP measurements before and after stimulation with prostacyclin (Iloprost; 2 ng/ml). cAMP levels were measured in platelets from a control, patients 1 and 2, and the father at different time points. Lower levels of cAMP are produced in platelets from patients 1 and 2 compared to the father and the control.

Routine platelet aggregations in response to ADP, ristocetin, arachidonic acid and U46619 were normal in all patients. When $P2Y_1$ and $P2Y_{12}$ specific inhibitors were used in combination with ADP, platelet aggregation in patients 1 and 2 was comparable to platelet aggregation in unrelated age-matched normal controls, suggesting a normal Gi and Gq signaling (Fig. 2A). Platelet aggregation in response

to Horm collagen was normal in patients 1 and 2, but the patients showed no shape change (Fig. 2B).

A

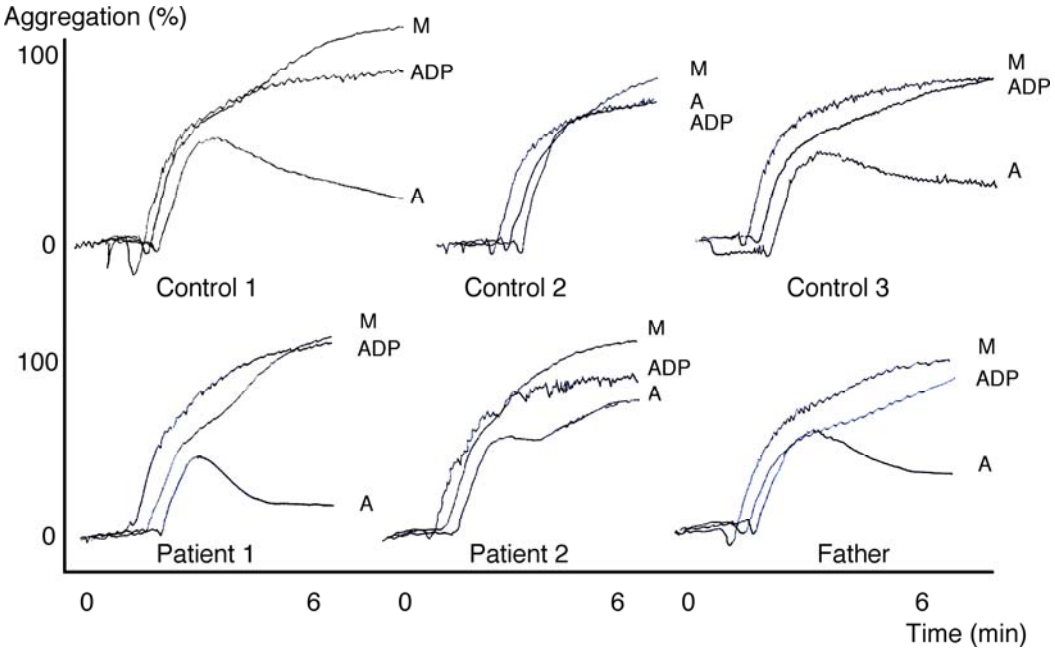

B

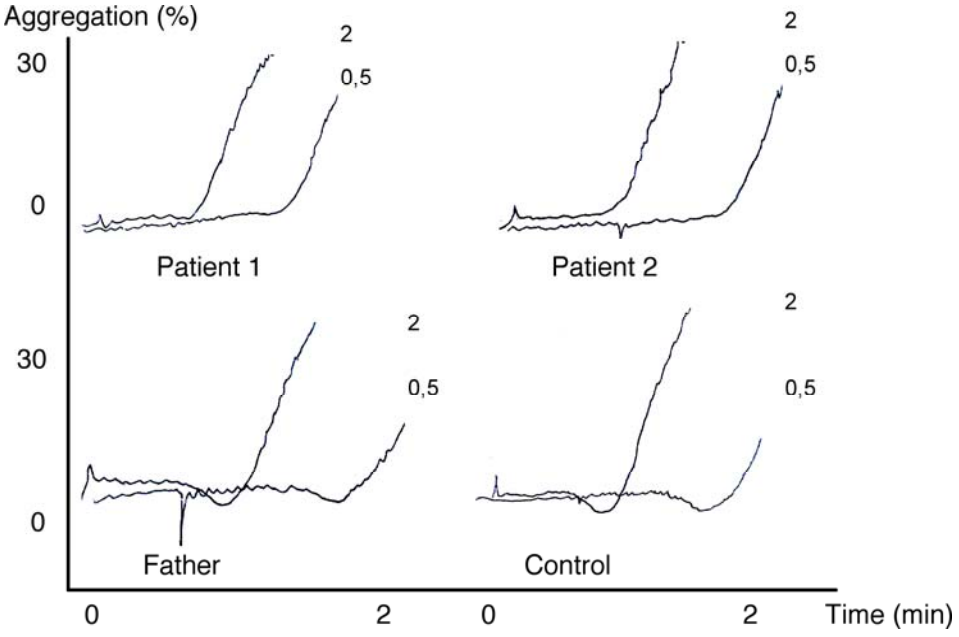

Figure 2: Platelet Gi and Gq signaling and shape change in patients and controls.

A. Platelet aggregation in response to ADP (10 μM) alone (ADP) and in combination with a selective inhibitor for the Gq-coupled ADP-receptor $P2Y_1$ (M) or the Gi-coupled ADP-receptor $P2Y_{12}$ (A), is comparable in patients and controls. Control 1 is age-matched for patient 1, control 2 for patient 2 and control 3 for the father.
B. Platelet aggregation in response to collagen (0.5 and 2 μg/ml) shows the absence of shape change in patients 1 and 2. Shape change is normal in the father, as compared to control platelets.

Genetic screening

The observed loss of Gs function in the platelets from the patients led us to screen the GNAS gene, but we found no mutations. As RGS2 is known to downregulate Gs signaling, we screened the RGS2 gene in all family members, and found a heterozygous G to A substitution in exon 1 at nucleotide position 68 in patients 1, 2 and 3 (Fig. 3A). This was confirmed by restriction digestion analysis with *Bsu*RI, recognizing only the normal sequence (Fig. 3B). The mutation was not found in 200 unrelated normal controls. It results in a Gly to Asp substitution at amino acid position 23 (G23D). This residue is well conserved in different species, suggesting that it is important for normal RGS2 function (Fig. 3C). Since this substitution was found in all family members with a Gs hypofunction in their platelets, we hypothesized that it is responsible for the reduced cAMP production.

A

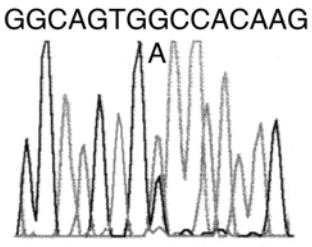

B

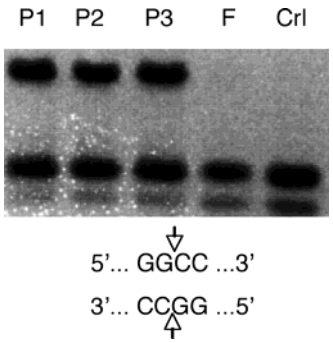

C

Homo sapiens:	QHDCRPMDKSAGS**G**HKSEE
Macaca mulatta:	QHDCRPMDTSAGS**G**HKSEE
Rattus Norvegicus:	QHDCVPMDKSAGN**G**PKVEE
Equus caballus:	QHDCGPMDKSAGS**G**PKSEE
Xenopus tropicalis:	QHNCGQVERSSPG**G**CQKNE
Mus musculus:	QHDCVPMDKSAGN**G**PKVEE
Cavia porcellus:	QHDCVPMDKSAGS**G**SKSEE

Figure 3: Mutation in exon 1 of RGS2

A. At nucleotide position 68 a heterozygous G to A substitution was found.
B. *Bsu*RI digestion of a PCR-fragment containing the mutation shows that patients 1, 2 and 3 (P 1-3) are heterozygous carriers of this mutation (F: father, Crl: control).
C. Evolutionary conservation of the affected RGS2 amino acid 23 in different species. In patients 1, 2 and 3 glycine is substituted by aspartic acid at this position.

Functional characterization of the RGS2 mutation

The functional relevance of the mutation was further studied *in vitro* in HEK293 cells and the megakaryocytic cell line MEG-01 overexpressing wild type (wt) or mutant (G23D) RGS2. Equal expression of wt and G23D RGS2 was confirmed by real-time PCR (Fig. 4). cAMP levels were measured at different time points after incubation of the transfected cells with Gs agonists in the presence of IBMX (100 µM). This showed a significantly reduced production of cAMP in cells overexpressing mutant RGS2, compared to wild type after 2 and 3 minutes of isoproterenol stimulation in HEK293 cells (Fig. 4A) and after 1 and 2 minutes of prostin stimulation in MEG-01 cells (Fig. 4B). This indicates that the reduced cAMP levels in the platelets from the affected members are a functional consequence of the mutation.

A

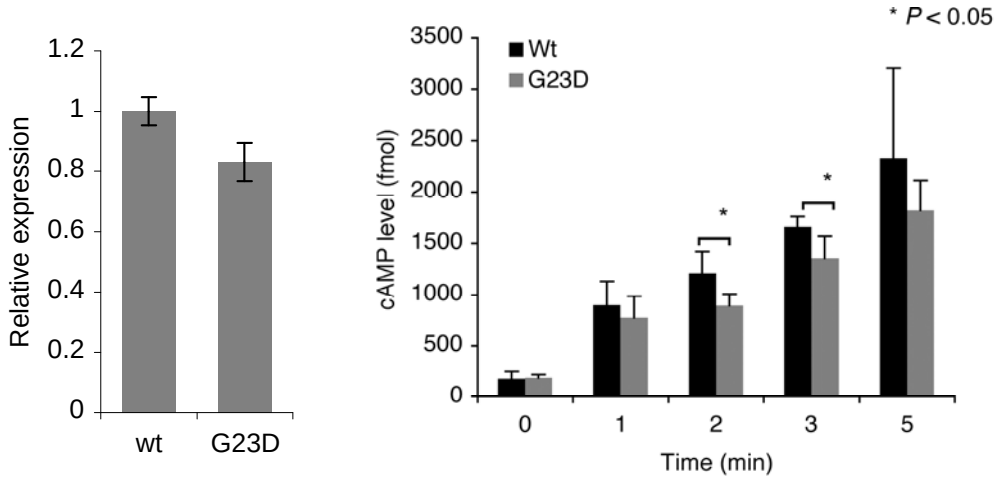

B

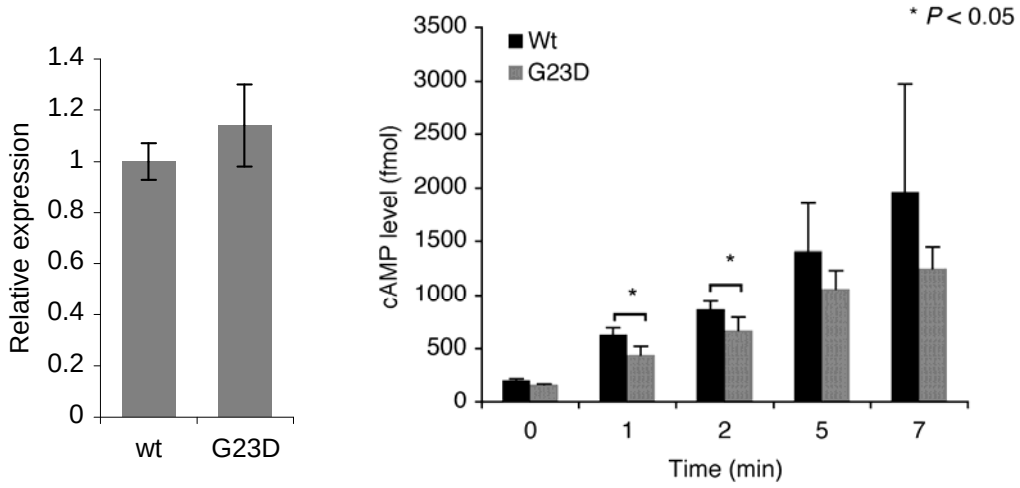

Figure 4: cAMP measurements in cells transfected with wild type and mutant RGS2.

A. HEK293 cells:

Left: Expression level of wild type and mutant RGS2 in transfected cells relative to actin expression, using wild type RGS2 expression as a calibrator.

Right: cAMP production is significantly reduced after 2 and 3 minutes of incubation with isoproterenol (1 µM) in cells transfected with mutant RGS2 (gray) compared to those transfected with wild type RGS2 (black).

B. MEG-01 cells:

Left: Expression level of wild type and mutant RGS2 in transfected cells relative to actin expression, using wild type RGS2 expression as a calibrator.

Right: cAMP production is significantly reduced after 1 and 2 minutes of incubation with prostin (200 ng/ml) in cells transfected with mutant RGS2 (gray) compared to those transfected with wild type RGS2 (black).

Bars represent means + SD, * P<0.05. Data were collected from 4 wells for each condition.

To understand why this mutation leads to an altered function of RGS2, we also studied the effect of the mutation at the protein level. Since RGS2 mRNA gives rise to four different RGS2 proteins (Fig. 5A), we performed an *in vitro* transcription-translation assay to study the effect of the mutation on the use of the multiple translation initiation sites. We observed an increased expression of the largest RGS2 isoforms for the mutant RGS2 compared to the most abundant wild type protein starting from methionine 16 (Fig. 5B). The G23D mutation is located in the proximity of translation initiation sites at positions 16 and 33 and therefore, we postulate that its presence interferes with the use of these initiation sites that are also generating the RGS2 isoforms known to lack the AC inhibitory domain [56].

A

B

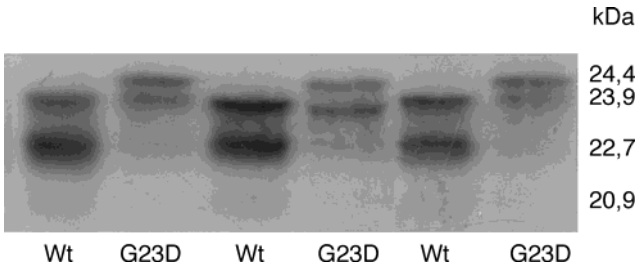

Figure 5: *In vitro* transcription-translation of wild type and mutant RGS2.

A. RGS2 mRNA gives rise to four different proteins, starting at amino acid positions 1, 5, 16 and 33, with different molecular weights (kDa). The AC binding domain is located within amino acids 9 to 11 (white box). The G23D mutation is indiciated.
B. Wild type (wt) and mutant (G23D) RGS2 proteins were generated *in vitro* by means of a reticulocyte system and detected by autoradiography. This was performed in triplicate. A different protein expression profile is observed when the mutation is present. The molecular mass of the different proteins is indicated (kDa).

Since we hypothesized that the RGS2 G23D mutation interferes with RGS2 translation and subsequently with AC binding, the binding of AC type III with wild type and mutant RGS2 protein was examined. The interaction of RGS2 and AC type III was studied in HEK293 cells transfected with GFP-coupled wild type and mutant RGS2 constructs via an immunoprecipitation assay. We could show that wild type as well as G23D RGS2 are able to bind AC type III, but the binding was stronger for G23D RGS2 (Fig. 6).

A B

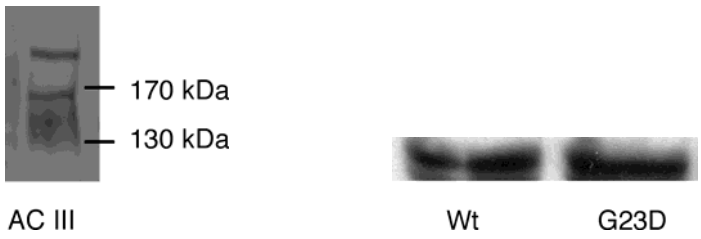

C

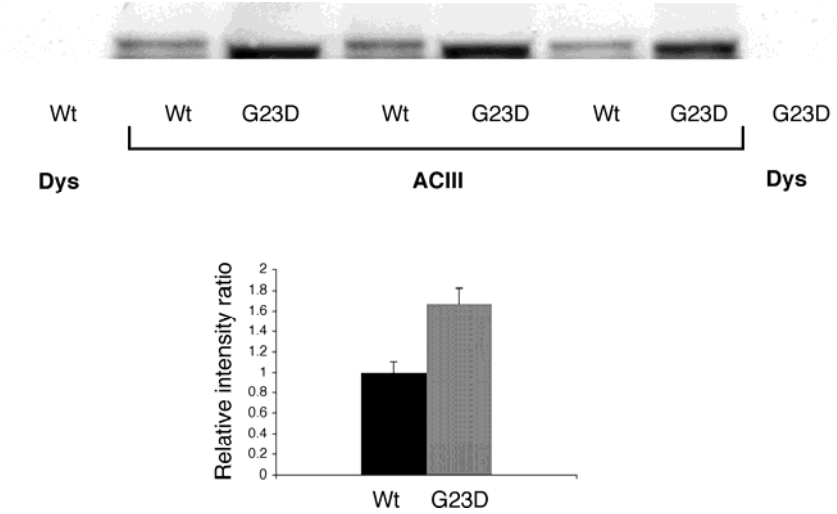

Figure 6: Immunoprecipitation of RGS2 and AC type III.

A. Immunoblot analysis with an anti-ACIII antibody shows the presence of AC type III in HEK293 cells.
B. Immunoblot analysis of lysates from HEK293 cells transfected with GFP-coupled wild type (wt) or mutant (G23D) RGS2. The amount loaded represents 10% of the input of the immunoprecipitation assay. Equal amounts of GFP-coupled wt and G23D RGS2 proteins are detected with an anti-GFP antibody.
C. GFP-coupled RGS2 can be immunoprecipitated from transfected HEK293 cells with an anti-ACIII antibody (ACIII), but not with an anti-dystrophin antibody (negative control; Dys). The assay was performed in triplicate. Quantification of the band intensity of the mutant protein was performed relative to the band intensity of the wild type protein. Mutant (G23D) RGS2 binds AC type III 1.7 times stronger than does wild type (wt) RGS2. Bars represent means + SD.

Platelet morphology and granule content

Blood analysis of patients 1, 2 and 3 showed normal platelet counts (211, 238 and 135 * 10^9 platelets/L, respectively; normal range of 140–440 * 10^9 platelets/L), but with an increased mean platelet volume (12.1 fL; 12.8 fL and 13.8 fL respectively, normal range of 8.0-12.0 fL). This was confirmed by electron microscopy, which showed that patients 1, 2 and 3 have some enlarged round platelets (Fig. 7A). The father has normal sized platelets. Furthermore, platelets from patient 1, 2 and 3 contain abnormal alpha granules, characterized by a dense core surrounded by a lighter content (Fig. 7B). We transfected MEG-01 cells with GFP and GFP-coupled wt and G23D RGS2 to study the effect of the mutation on megakaryocytic morphology by flow cytometry. Cells transfected with GFP-coupled wt and G23D RGS2 have a significantly higher forward scatter, which is a measure of size, compared to cells transfected with GFP alone ($p<0.01$). Furthermore, cells transfected with G23D RGS2 show a significant ($p<0.01$) increase in forward scatter and side scatter (measure for granularity) compared to cells transfected with wt RGS2 (Fig. 7C). These results show an effect of RGS2 expression on MEG-01 cell morphology, which is emphasized by the presence of the mutation. Also, granularity of the cells seems to be affected by the mutation.

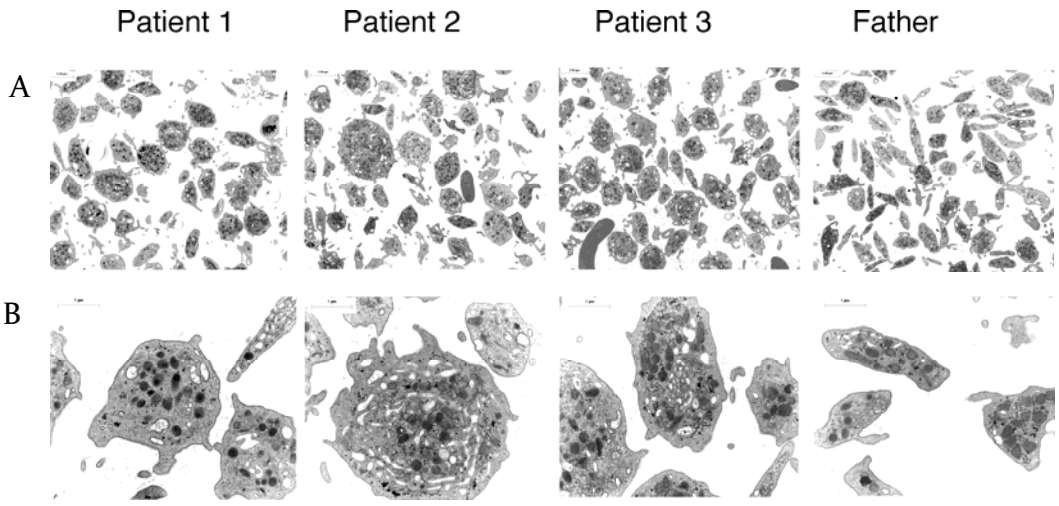

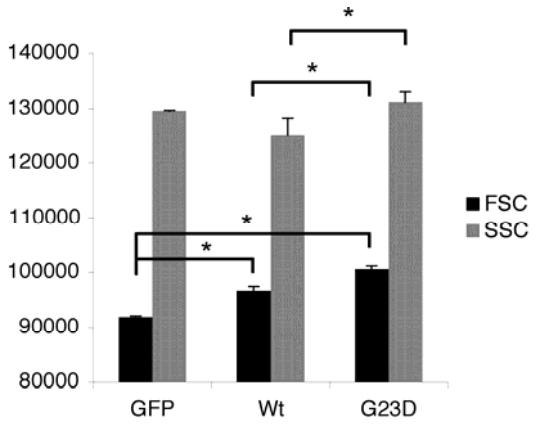

Figure 7: Morphology of platelets and MEG-01 cells transfected with wild type and mutant RGS2.

A. Enlarged, round platelets are present in patients 1, 2 and 3. The father has normal sized platelets.
B. More detailed images show abnormal α granules in platelets from patients 1, 2 and 3.
C. Flow cytometric analysis of MEG-01 cells transfected with GFP (GFP), GFP-coupled wild type RGS2 (wt) and GFP-coupled mutant RGS2 (G23D). Forward scatter (FSC; black) is significantly increased when cells are transfected with wild type or mutant RGS2, compared to cells transfected with GFP. FSC and side scatter (SSC; gray) is significantly increased when cells are transfected with mutant RGS2 compared to wild type RGS2. Bars represent means + SD, * $P<0.01$. Data were collected from 3 measurements.

We further studied the granules in platelets of the patients. The platelet dense granule ATP secretion was normal for all patients and flow cytometry showed a normal P-selectin expression after stimulation of platelets from patient 1 compared to a control (Fig. 8).

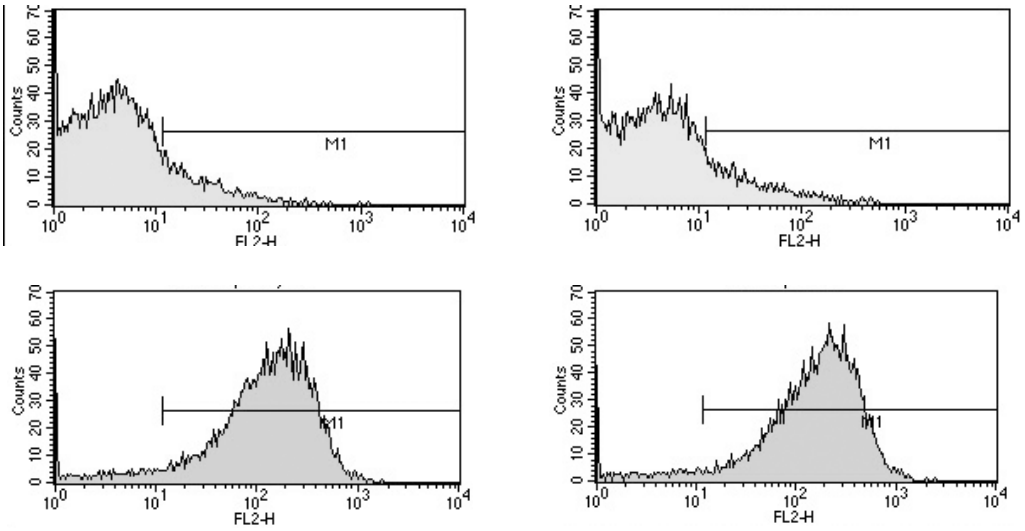

Figure 8: Flow cytometric determination of P-selectin expression.
P-selectin expression on platelets from patient 1 is comparable to the expression on control platelets in basal conditions (upper panel; M1= 95.17% and 96.12% respectively) and upon activation with ADP (20 µM) (lower panel; M1= 13.02% and 14.33% respectively).

We used a proteomic approach to further analyze the platelet granule proteins released upon activation of platelets from patient 1, patient 2 and three unrelated normal controls. DIGE coupled to MS was used to identify differentially expressed proteins. From the comparison of proteomic maps, 13 protein spots showed a change in expression in a statistically significant way ($p<0.01$) and were successfully identified by MS (Table 1). In some instances, more than 1 protein spot was found to correspond to the same protein, consistent with the presence of different posttranslational modified forms of the same protein. Most differentially expressed proteins are not granule content proteins but are actually cytoskeletal (-binding) proteins, which could be related to the reduced platelet shape change in patients after collagen activation (Figure 2).

Table 1: Differentially expressed proteins in platelet releasates (p<0.01).

Identification [a]	Biological function	SwissProt Code	Mascot Score [b]	Ratio [c]
Serum albumin precursor	Transport	P02768	867	2.6
Vinculin	Cytoskeletal related proteins	P18206	524	1.5
Fibrinogen beta chain precursor	Platelet activation	P02675	539	1.3
Fibrinogen gamma-A chain precursor	Platelet activation	P02679	400	-1.2
Apolipoprotein A-I	Transport/Cytoskeletal related proteins	P02647	388	-1.3
Glutathione S-transferase omega-1	Metabolism	P78417	117	-1.3
Elastase inhibitor	Protease inhibitor	P30740	123	-1.3
Gelsolin	Cytoskeletal related proteins	P06396	154	-1.5
Phosphoglycerate kinase	Metabolism/Cytoskeletal related proteins	P00558	96	-1.5
Glyceraldehyde 3-phosphate dehydrogenase	Metabolism/Cytoskeletal related proteins	Q2TSD0	213	-1.6
Annexin V	Platelet activation	P08758	110	-1.6
Glyceraldehyde 3-phosphate dehydrogenase	Metabolism/Cytoskeletal related proteins	Q2TSD0	397	-1.7
Thrombospondin 1 precursor	Cell adhesion/Cytoskeletal related proteins	P07996	84	-2.0

[a] Protein identifications performed by DIGE and MALDI-TOF/TOF

[b] Score is -10*log(P), where P is the probability that the observed match is a random event; based on the NCBI nr database using the MASCOT searching program.

[c] Fold change of protein expression between patients (1 and 2) and controls (three healthy volunteers). + for upregulated protein expression, - for downregulated protein expression.

III.II. RGS2 in platelet production and function: Studies in zebrafish

Introduction

1 ZEBRAFISH AS A MODEL OF HUMAN PHYSIOLOGY

Most of the research to unravel human physiological processes at the molecular level is performed in animal models. They enable us to create genetic models to mimic monogenic diseases and to study the development of the disease and the effects of possible therapies. The mouse model has been the primary model to study human pathologies, because of the homology between the murine and human genome, physiology and anatomy. However, the surprising degree of conservation in basic cell-biological processes between mammals and invertebrates has made it possible to model the disruption of these processes at a genetic level in worms and flies. There are some disadvantages of these models, like the lack of several structures and organ systems involved in human disease pathogenesis. The zebrafish model has now gained interest as a genetically tractable vertebrate model system. Zebrafish can be used to perform forward genetic studies, as is also possible in the invertebrate models, but with additional relevance to vertebrate development. One important advantage of the zebrafish model is the transparency of the embryos during development.

2 DEVELOPMENTAL STAGES OF ZEBRAFISH EMBRYOS

Kimmel *et al.* described 7 developmental stages during the first 3 days after fertilization: zygote, cleavage, blastula, gastrula, segmentation, pharyngula and hatching [164].

At the time of fertilization the zygote is about 0,7 mm in diameter. During the first 10 minutes, the blastodisc migrates towards the animal pole and segregates from the yolk cytoplasm. The first cleavage occurs approximately 40 min after fertilization. After the first cleavage, the cells divide every ± 15 minutes. Until the 16-cell stage cells are incompletely cleaved from each other, leaving them

interconnected by cytoplasmic bridges. During the 16-cell stage the 4 most central blastomeres are completely cleaved. After $2^{1/4}$ hours, the embryo reaches the 128-cell stage, the beginning of the blastula period. 3 hours later the morphogenetic cell movements of involution, convergence and extension occur, giving rise to the primary germ layers and the embryonic axis. This is called the gastrula period. This is followed by the segmentation period, during which the organs become visible and the embryo, especially the tail, elongates. The pharyngula stage at 24 hpf is the time of development at which morphologies of embryos of diverse vertebrates are very comparable. Pigmentation starts, the circulatory system forms and blood begins to circulate. Finally, there is behavioral development, as the appearance of tactile sensitivity and swimming movements. After 2 days the embryos start to hatch. During hatching the embryos continue to grow. Morphogenesis of the organs is rather completed and slows down considerably, except for the dietary tract.

3 THROMBOCYTE PRODUCTION IN ZEBRAFISH

The zebrafish thrombocyte is the haemostatic homologue of the mammalian platelet [165]. Thrombocyte production differs from platelet generation as the nucleus is retained and each cell remains diploid during differentiation [165], so they do not appear to derive from megakaryocytes [166]. Thrombocytes are born in the kidney via prothrombocytic intermediates that then circulate through the peripheral blood and spleen. In transgenic zebrafish with GFP-expressing thrombocytes (CD41-GFP zebrafish [166]), GFP^+ cells are observed by 48 hpf, between the dorsal aorta and the caudal vein. Cells are occasionally seen in the cardiac sinus region at that time. At 3 dpf, there is an increase in the number of GFP^+ cells in the caudal region, and they begin to circulate [166].

Zebrafish thrombocytes are functionally similar to human platelets. They can form aggregates and contain a canalicular system. In addition, similar glycoprotein

complexes are present on their membranes. Also, thrombocyte functions as adhesion, aggregation and secretion are conserved [165].

4 GENE FUNCTION STUDIES IN ZEBRAFISH

4.1 Overexpression studies

One powerful approach for gene function studies is to microinject *in vitro* transcribed capped RNA in zebrafish embryos. Capped RNA behaves similarly to eukaryotic mRNAs found *in vivo* due to the presence of the CAP analog.

4.2 Knockdown studies

To investigate loss-of-function, RNA encoding dominant negative forms of the gene of interest can be injected, but most commonly morpholino phosphorodiamidate oligonucleotides are used. These are antisense oligomers of which the ribose sugar has been replaced with a morpholine moiety and the phosphodiester linkage between nucleotides by a phosphorodiamidate linkage, leading to a neutral charge of the molecule. They are stable within biological systems because they are resistant to a wide range of nucleases and proteases [167]. When designed upstream or immediately downstream of the initiation codon, morpholino oligonucleotides block the 40S ribosomal subunit scanning process, thereby inhibiting initiation of translation of the targeted mRNA (ATG morpholino) [168]. A different strategy is to design the morpholino against splice-acceptor or splice-donor sites, thereby modifying splicing of the pre-mRNA (splice morpholino) [169].

In this part we wanted to assess the effect of rgs2 overexpression and knockdown on platelet production in zebrafish.

Experimental procedures

Zebrafish housing and maintenance of embryos

CD41-GFP zebrafish [166] were maintained under standard laboratory conditions. After zygote injections, embryos were maintained at 28.5°C in E3 medium (5 mM NaCl, 0.17 mM KCl, 0.33 mM $CaCl_2$, 0.33 mM $MgSO_2$ and 0.1% methylene blue).

Zebrafish rgs2 RNA production

RNA was extracted with TRIzol™ (Invitrogen) from 25 sonicated zebrafish according to the manufacturer's protocol. . Approximately 1 µg of total RNA, in the presence of RNaseI inhibitor (Invitrogen), was used for oligo(dT)-primed first strand cDNA synthesis using M-MLV reverse transcriptase (Invitrogen). rgs2 cDNA was amplified with primers rgs2-ZF-F () and rgs2-ZF-R (). This was cloned in the pGEM®-T Easy vector (Promega Corporation, Madison, WI, USA). Capped rgs2 RNA was obtained by *in vitro* transcription from the T7 promoter after linearization with *Sal*I with the mMessage mMachine® kit according to the manufacturer's protocol (Applied Biosystems/Ambion, Austin, TX, USA). The sample was purified with the RNeasy Mini kit (Qiagen, Inc.) and the concentration was measured (Nanodrop).

Zebrafish rgs2 morpholino sequence

The rgs2 morpholino antisense oligo sequence was designed against the region containing the ATG start codon (5'-TGGTCAATCTGTCCATTGCTATCAA-3'; Gene Tools, Philomath, OR, USA).

Injection of zebrafish embryos

Micropipettes are made by heating and pulling borosilicate glass capillary tubes in a micropipette puller device (). The micropipette was placed in a pressure-

pulsed micro injector apparatus (). A drop of mineral oil was brought on a micrometer slide (), and the injection volume was adjusted to a drop diameter of 0.1 mm or 2 nL in volume.

Injection of RNA (630 ng/µl) or morpholino (800 µM) in zebrafish embryos was performed ideally before the first cleavage of the zygote (40 min after fertilization), but was possible up to the 4-cell stage. The chorion and the yolk were penetrated with the micropipette in order to inject into the embryo. Over the next several hours and days of embryo development, the embryos were observed for phenotypes of interest. The expression of GFP was monitored in the developing embryos by *in vivo* whole-embryo fluorescence microscopy ().

Immunoblot analysis

GFP-expression in morpholino-, RNA- and buffer-injected zebrafish was analyzed and compared by immunoblot analysis. Zebrafish were lysed in ice-cold PBS containing 1 tablet protease inhibitor cocktail, 1% IGEPAL CA-630, 0.015 % DTT and 1 mM EDTA, by means of sonication. Lysates were cleared of insoluble debris by centrifugation at 14000g for 20 min at 4°C. 15 µL of protein lysate was mixed with reducing SDS buffer, resolved by SDS-PAGE on 10% acrylamide gels, and transferred to Hybond ECL-nitrocellulose membrane. The blots were blocked for 1h at room temperature in TBS-T. Blots were revealed with polyclonal anti-GFP antibody (Rockland Immunochemicals Inc.), followed by HRP-conjugated secondary antibody (rabbit anti goat; Dako). The experiment was performed in triplicate. Intensities of the detected proteins were quantified with the ImageJ software (National Institutes of Health).

Flow cytometric analysis

Whole CD41-GFP zebrafish were lysed with 0.05% trypsine at 28°C for 15 min. After addition of FCS, the lysed fish were filtered and centrifuged during 5 min at 1000 rpm. The pellet was resuspended in 500 µl of 2% FCS in PBS. Forward scatter

and side scatter of cells expressing GFP were determined. We used Cell Quest software for immunofluorescence acquisition on a FACSCalibur flow cytometer (BD Biosciences).

cAMP measurements

cAMP measurements were performed with the cAMP enzyme immunoassay (GE Healthcare) according to the manufacturer's protocol. Buffer-, RNA- and morpholino-injected zebrafish were deyolked and lysed in the presence of IBMX (100 μM). Data were collected from five wells, each well containing lysate from 5 zebrafish. Values were compared by means of the Student's t-test for unpaired data.

Results

Effect of rgs2 expression levels on platelet production in zebrafish

CD41-GFP zebrafish zygotes were injected with rgs2 RNA, a morpholino against the ATG initiation site of rgs2 (rgs2 morpholino) or buffer (control). We wanted to study the effect of rgs2 overexpression or knockdown on platelet production in these zebrafish. Since the platelets are GFP labeled, changes in the number of platelets would affect GFP protein levels. Immunoblotting for the GFP protein showed an increased GFP expression level in fish injected with rgs2 RNA and rgs2 morpholino compared to buffer-injected fish (Fig. 1).

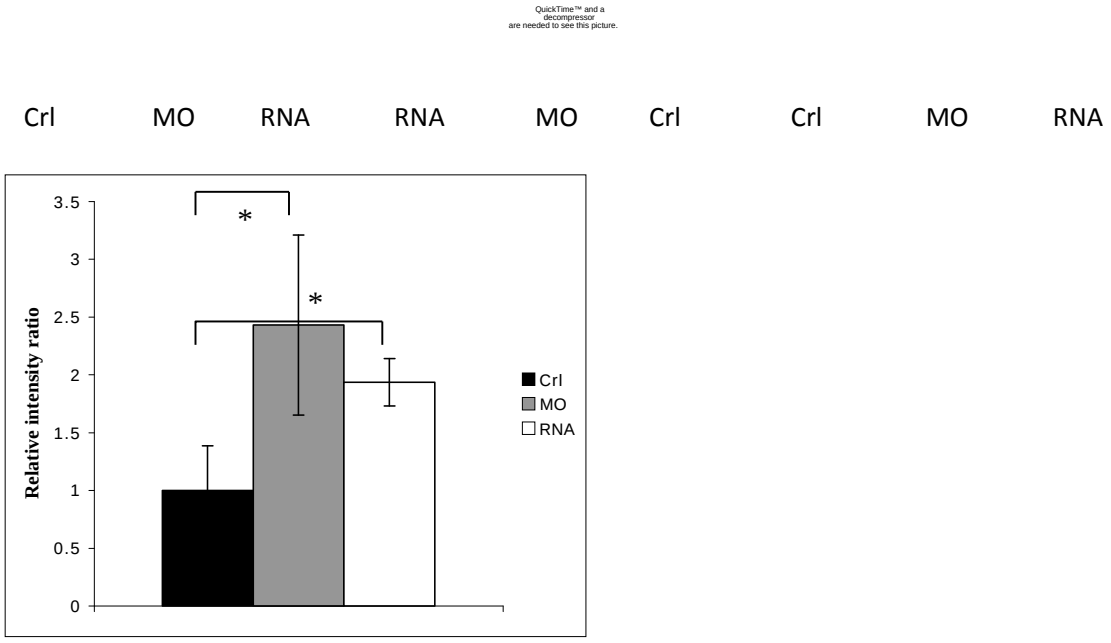

Figure 1: GFP expression in a pool of 10 zebrafish injected with buffer (Crl), rgs2 morpholino (MO) and rgs2 RNA (RNA). Band intensity ratios are calculated relative to the band intensity of the GFP protein of Crl zebrafish. Bars represent means +/- SD, * $P<0.05$.

To quantify and visualize the GFP expressing cells in morpholino- and RNA-injected fish, flow cytometric analysis was performed at 3 dpf (Fig.2). This showed that the increased GFP expression in morpholino-injected fish can mainly be explained by a population with higher side scatter, compared to buffer- and RNA-injected fish.

Buffer

QuickTime™ and a
decompressor
are needed to see this picture.

QuickTime™ and a
decompressor
are needed to see this picture.

MO

QuickTime™ and a
decompressor
are needed to see this picture.

QuickTime™ and a
decompressor
are needed to see this picture.

RNA

QuickTime™ and a
decompressor
are needed to see this picture.

QuickTime™ and a
decompressor
are needed to see this picture.

Figure 2: Flow cytometric analysis of whole zebrafish injected with buffer, morpholino (MO) or RNA. The ratio of GFP^+ to GFP^- cells is 0.149, 0.251 and 0.230, in buffer-, morpholino- and RNA-injected zebrafish respectively.

CD41-GFP zebrafish show a GFP^{high} subset, which corresponds to thrombocytes, a GFP^{low} subset that corresponds to thrombocyte precursors and a group of non-mobile GFP^+ cells, which are most likely early hematopoietic stem cells [166]. By fluorescent microscopy at 3 dpf, it was obvious that in RNA-injected zebrafish the increase in GFP protein levels could be attributed to an increased number of circulating platelets (Fig. 3). In morpholino-injected zebrafish this difference could not be observed.

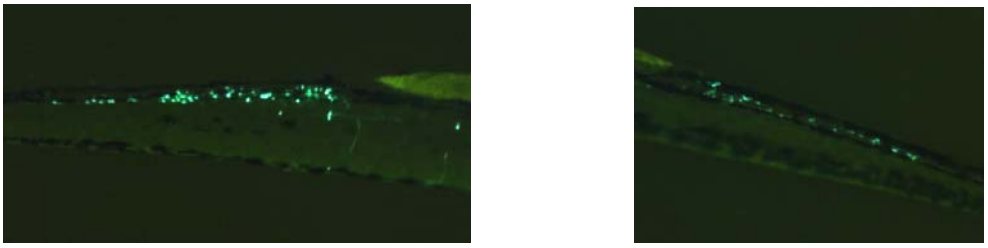

Figure 3: GFP-labeled platelets in zebrafish injected with rgs2 RNA (left) versus control RNA (right) (3 dpf).

Effect of rgs2 expression levels on Gs signaling in zebrafish

To show that rgs2 regulates Gs signaling and cAMP production in zebrafish, we measured cAMP levels in buffer-, morpholino- and RNA-injected zebrafish at 3 dpf (Fig.4).

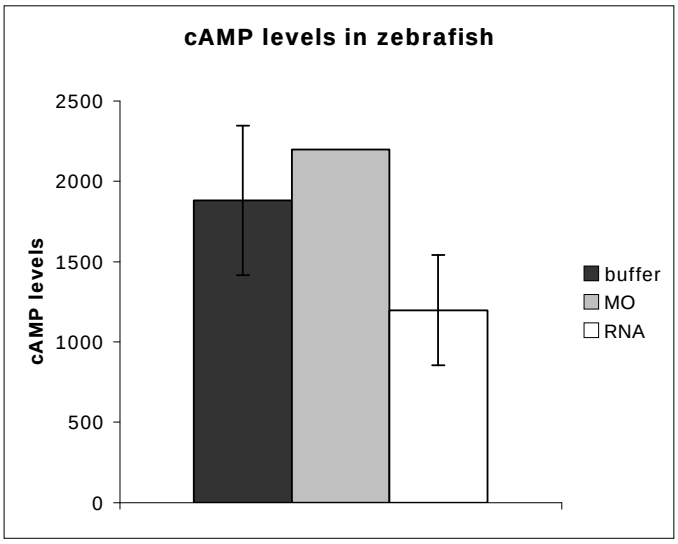

Figure 4: cAMP levels in zebrafish injected with buffer, morpholino (MO) and rgs2 RNA.

These results confirm the negative regulatory effect of rgs2 on Gs signaling, and could present an explanation for the increased number of GFP^+ cells in morpholino-injected zebrafish. This population could represent hematopoietic stem cells since enhanced Gs signaling, which is expected after knockdown of rgs2 expression, is known to inhibit stem cell apoptosis [170] and enhance stem cell proliferation [171].

III.III. Conclusions from human and animal studies

We describe a girl (patient 1) with borderline IQ, hirsutism, increased bone alkaline phosphatase and shortened little fingers. These characteristics are also seen in patients with AHO, which is associated with a loss of Gs function due to heterozygous inactivating mutations in the GNAS gene. The Gs functional test and cAMP measurements in the platelets from patient 1 indeed showed a loss of Gs function. This Gs hypofunction was also seen in platelets from her mother (patient 2) and her brother (patient 3). We screened the GNAS gene, but found no abnormalities for our patient.

Since RGS2 acts as a negative regulator of Gs protein-mediated signaling [67, 158, 172] dysfunction of this protein could possibly lead to an AHO-like phenotype by interfering with cAMP production. We indeed found a heterozygous mutation in the RGS2 gene of patients 1, 2 and 3 resulting in a G23D RGS2 protein. We could further show that this mutant RGS2 protein has an increased inhibitory effect on cAMP production. RGS2 is described to inhibit cAMP via direct interaction with Gsα and/or AC [67, 158, 172]. We questioned whether the mutation alters the inhibitory capacity of RGS2 on cAMP production at the level of the interaction with AC or Gsα. Gu *et al.* found four different translation initiation sites in the RGS2 mRNA at amino acid positions 1, 5, 16 and 33 which give rise to a set of four functionally distinct RGS2 proteins with regards to their ability to inhibit AC [56]. The RGS2 isoforms initiated at positions 16 and 33 lack the domain necessary for the interaction with AC and therefore are not able to inhibit AC, resulting in higher cAMP levels after Gs stimulation. The G23D mutation is located near the translation initiation sites at positions 16 and 33 and causes a relative preference for the use of the translation initiation sites at positions 1 and 5, compared to the wild type sequence. We showed that both wild type and mutant RGS2 interact with AC type III, the predominant AC isoform in platelets. It seems that this interaction is enhanced when the mutation is present, which can be explained by the altered RGS2 isoform expression pattern. The RGS domain (residues 79 to 205), which interacts with Gsα, is not affected by the mutation.

The carriers of the mutation also have enlarged rounder platelets with abnormal α granules. This leads to the hypothesis that RGS2 could play a role in megakaryopoiesis and platelet formation. This is further supported by an increase in forward and side scatter of MEG-01 cells transfected with mutant RGS2 compared to wild type RGS2. We studied platelet production in CD41-GFP zebrafish with rgs2 overexpression and knockdown, and found that GFP levels were increased in both cases. Since in CD41-GFP zebrafish not only thrombocytes, but also hematopoietic stem cells are GFP-labeled, the increased GFP expression levels in zebrafish injected with rgs2 morpholino could be explained by enhanced Gs signaling, and thereby increased proliferation and decreased apoptosis of stem cells [170, 171]. In RNA-injected zebrafish however, the number of thrombocytes is visibly increased, further supporting a role for RGS2 in platelet production.

Since processes such as cellular differentiation, vesicle release and cell division involve the interface between G proteins and the microtubule cytoskeleton, RGS2 can affect these processes via a combination of its G protein regulatory properties and the ability to interact with cytoskeleton-associated proteins. For example, RGS2 directly interacts with tubulin via a short region at the N-terminus (amino acids 41-60), thereby enhancing microtubule polymerization *in vitro* and enhancing neurite outgrowth in PC12 cells [65]. Tubulin was also shown to specifically and tightly bind to Gsα, Gqα and $Gi\alpha_1$ [173]. We hypothesize that the mutant RGS2 protein interferes with the platelets' AC activity but could also be responsible for changes in the organization of the cytoskeleton. The proteomic analysis of the platelet granules might provide a good starting point for further studies on the role of RGS2 in megakaryopoiesis, platelet formation and platelet Gs function. All detected proteins have also been identified in other platelet releasate studies after TRAP activation [174]. Several of the differentially expressed proteins are described to play a role in cytoskeleton-associated processes [175-180]. Changes in the structural organization of the platelet cytoskeletal actin-binding proteins of the patients could result in changes in the platelet shape change as we observed

after stimulation with Horm collagen for all patients. Further studies are however needed to define the role of RGS2 in the cytoskeleton of megakaryocytes and platelets.

In conclusion, we here describe the first human defect in RGS2, and its effect on Gs signaling in platelets by altering the use of the different translation initiation sites in the RGS2 mRNA. Furthermore, a role for RGS2 in platelet production has been suggested, which is further supported by studies in the zebrafish model.

Chapter IV

Other physiological functions of RGS2

IV.I. Other physiological functions of RGS2: Studies in humans

Introduction

The metabolic syndrome refers to the clustering of cardiovascular risk factors that include insulin resistance, obesity, dyslipidemia and hypertension. Insulin resistance and visceral obesity have been recognized as the most important pathogenic factors of the syndrome. The exact description of the metabolic syndrome has been a matter of debate, and 3 main definitions have been proposed by the World Health Organization (WHO), the National Cholesterol Education Program – Adult Treatment Panel III (NCEP-ATPIII) and the International Diabetes Federation (IDF) (Table 1) [181].

Table 1: Definitions of the metabolic syndrome

	Visceral obesity	Dyslipidemia	Hypertension	IGT	Other
WHO (≥ 2 criteria)	WHR: > 0.9 (m) > 0.85 (w)	TG ≥ 150 mg/dl or HDL < 35 mg/dl (m) and < 39 mg/dl (w)	Blood pressure ≥ 190/40 mmHg	IFG, IGT or insulin resistance	Urinary albumin excretion rate > 20 mcg/min
NCEP-ATPIII (≥ 3 criteria)	WC: > 102 cm (m) > 88 cm (w)	TG ≥ 150 mg/dl or HDL < 40 mg/dl (m) and < 50 mg/dl (w)	Blood pressure ≥ 130/85 mmHg	Serum glucose ≥ 110 mg/dl	
IDF (≥ 2 criteria)	WC: > 94 cm (m) > 80 cm (w)	TG ≥ 150 mg/dl or HDL < 40 mg/dl (m) and < 50 mg/dl (w)	Blood pressure ≥ 130/85 mmHg	Serum glucose ≥ 110 mg/dl	

WHR: waist-to-hip ratio; WC: waist circumference; TG: triglycerides; IFG: impaired fasting glucose; IGT: impaired glucose tolerance

RGS2 is involved in all different aspects of the metabolic syndrome. It plays a role in hypertension [77, 79], adipocyte differentiation [91, 92], pancreatic insulin secretion [101] and the *RGS2* gene is located in a region that is linked to the distribution of body fat in men [102] and the metabolic syndrome [103]. In addition, a polymorphism in the *RGS2* promoter region, -395 C/G, is associated

with an increased susceptibility to the metabolic syndrome in white European men [104]. The G allele of this polymorphism shows an enhanced promoter activity *in vitro* and it is associated with enhanced RGS2 expression in adipocytes from European men. The polymorphism results in loss of a recognition site for transcription factor Sp1. This transcription factor is essential for the transcriptional regulation of RGS2 during 3T3-L1 mice preadipocyte differentiation by binding a recognition site in the first 78 bp of the *Rgs2* promoter [182].

Since people with the metabolic syndrome experience a five-fold increased risk to develop T2DM, we wanted to study the association of this RGS2 promoter polymorphism with T2DM. In addition, since diabetic platelets are hypersensitive to agonists, we wanted to study the Gs signaling pathway in platelets from type 2 diabetic patients.

Experimental procedures

Patient studies

Informed consent was obtained from all participants according to the declaration of Helsinki. This study was approved by the Institutional Review Board.

Aggregation-inhibition Gs test

Blood of 210 patients with T2DM was anticoagulated with 3.8% (wt/vol) trisodium citrate (9:1). PRP was obtained and platelet count was adjusted to 250 x 10^9 platelets/L. The Gs pathway in their platelets was functionally analyzed by means of the aggregation-inhibition test. Prostacyclin (iloprost, 0-2.5 ng/ml) was added to PRP that was pre-incubated (5 min) with aspirin (Aspégic, 500 µM; Sanofi-Aventis, Brussels, Belgium) to correct for the intake of aspirin by most of the patients. After 1 min, collagen (5 µg/ml) was added to induce platelet aggregation.

cAMP measurements

Platelet basal cAMP levels and levels after stimulation of the Gs pathway with iloprost during 2 and 5 min (2 ng/ml), in the presence of IBMX, were measured using the cAMP enzyme immunoassay (GE Healthcare) according to the manufacturer's protocol. The reaction was stopped by the addition of 12% TCA.

Screening the -395 C/G promoter polymorphism

The -395C/G *RGS2* promoter polymorphism was screened in 198 type 2 diabetic patients and controls. The *RGS2* promoter region was amplified with primers 5'-CTCTTCATTCGAAATCAGGC-3' and 5'-CATTATCGTTCTCCCGCT G-3', and the -395C/G polymorphism was detected by restriction digestion of the PCR fragment with *Eco*52I.

Platelet RGS2 mRNA levels

RGS2 mRNA levels in platelets from the patients were determined by Real Time-PCR (7500 Fast System; Applied Biosystems). Total RNA was extracted from platelets with TRIzol™ total RNA isolation reagent (Invitrogen) according to the manufacturer's protocol. Approximately 1 μg of total RNA was converted to cDNA, and *RGS2* expression was measured relative to actin expression using TaqMan gene expression assays for both genes (Applied Biosystems).

Results

Gs signaling in platelets from patients with T2DM

We performed the aggregation-inhibition test on platelets from 210 patients. Based on this test we could identify 3 groups in our patient population: patients with a normal Gs signaling (77%), patients with an increased Gs function (15%) and patients with an overall reduction of platelet aggregation (8%) (Fig.1).

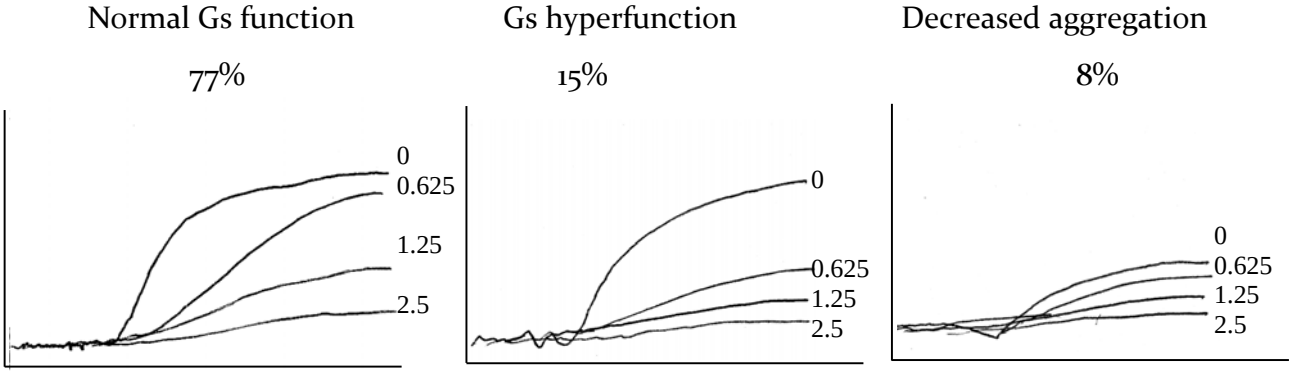

Figure 1: Aggregation-inhibition test. Platelet aggregation was induced by collagen (5 µg/ml), and inhibited by addition of different concentrations of Gs agonist (iloprost; ng/ml).

RGS2 promoter polymorphism and platelet cAMP levels

We studied the presence of the -395 C/G polymorphism in the promoter region of *RGS2* and the expression levels of *RGS2* mRNA in the platelets from these patients. We made comparisons between our entire patient population and a control population. In addition, we compared the 3 groups in our patient population to evaluate the effect of the *RGS2* polymorphism and *RGS2* expression levels on platelet function in patients with T2DM.

The G-allele was found to be associated with the metabolic syndrome in white European men [104]. However, we could not find a significant difference in the

prevalence of the G-allele in the type 2 diabetic patient population (or women and men separately) compared to the European control population described in [104] (Table 1).

Table 1. Frequency of the -395 promoter polymorphism genotypes.

	GG	CG	CC
198 patients	61%	35%	4%
109 Women	65%	28%	7%
89 Men	55%	43%	2%
3080 controls (European) [104]	54,1%	39,5%	6,4%

Although the -395 C/G polymorphism was found to affect the *RGS2* promoter activity (the G-allele is associated with a higher expression level [104]), no association of a specific genotype with altered platelet Gs function could be found. This was confirmed by measurements of basal cAMP levels and cAMP levels after stimulation with a Gs agonist in platelets from patients with the CG genotype versus patients with the GG genotype (Fig.2). Also, we measured platelet *RGS2* mRNA levels and found a large variation of *RGS2* expression, independent from the patients' *RGS2* promoter genotypes, suggesting that the effect of the polymorphism on *RGS2* promoter activity does not result in altered RGS2 expression levels in their platelets.

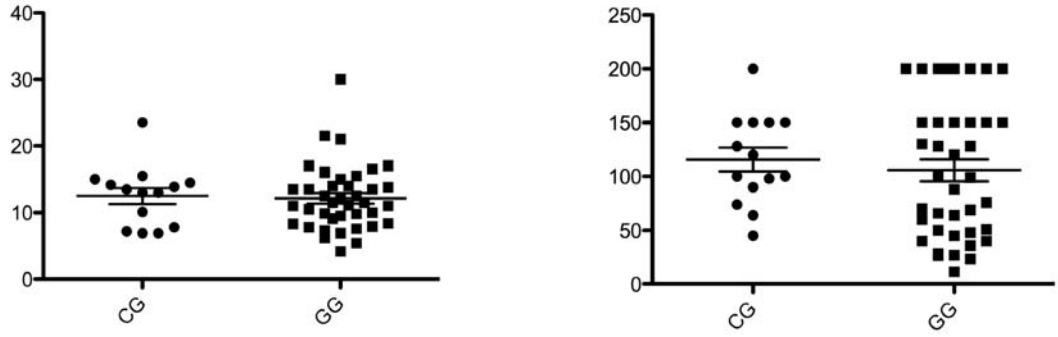

Figure 2: cAMP levels in platelets from patients with the CG and GG genotypes at position -395 in the *RGS2* promoter, before (left) and after stimulation with a Gs agonist (iloprost; right).

IV.II. Other physiological functions of RGS2: Studies in zebrafish

Introduction

The G23D RGS2 mutation described earlier (Chapter III) was associated with enhanced RGS2 function and AHO in patient 1, characterized by obesity and bone abnormalities. In addition, a role for RGS2 has already been shown in adipogenesis *in vitro* [91, 92]. Therefore we chose to study the effect of RGS2 overexpression on adipogenesis and bone development in the zebrafish model.

1 ADIPOGENESIS IN ZEBRAFISH

The cellular anatomy of zebrafish adipocytes is similar to that of mammalian white adipocytes [183]. This homology establishes the zebrafish as a new model for adipocyte research. An exogenous nutrient supply is required for adipocyte development and in zebrafish feeding commences at approximately 5 dpf. At that time, the yolk mass is the major depot of neutral lipid, together with the swim bladder. After yolk absorption at 7 dpf, the first neutral lipid droplets appear in the right visceral cavity, in close proximity to the pancreas. Larvae enter metamorphosis at 14 dpf, resulting in an adult body plan by 28 dpf. Upon completion of metamorphosis at 28 dpf the visceral cavity represents the largest neutral lipid depot, with smaller depots appearing in the pectoral fin plate, jaw, spinal column and at subcutaneous, pericardial and periorbital positions. Adult zebrafish fat depots are mobilized in reponse to starvation and deposited in response to refeeding. Differentiated adipocytes express pparγ, the zebrafish ortholog of mammalian PPARγ as early as 15 dpf.

2 EARLY SKELETAL DEVELOPMENT IN ZEBRAFISH

During zebrafish development, skeletal structures appear in a progressive fashion from head to tail. The early skeletal elements are mostly made of cartilage, and are located not far beneath the surface, where they can be easily visualized. In

the jaw primordia, cartilage development can be studied. Two arches, the mandibular and hyoid arches, constitute the jaw and the associated supportive apparatus. After 2 days it is possible, yet difficult, to visualize early precartilage condensations in the mandibular and hyoid arches [164]. Calcified structures of the jaw develop first at 5 dpf and are followed by the axial skeleton in the trunk (7 dpf) [184].

Experimental procedures

Visualization of zebrafish adipocytes

rgs2 RNA and buffer-injected larvae were placed in E3 medium containing a 1/10 dilution of heavy whipping cream at 5 dpf, as described by Schlegel *et al.* [185]. Nile Red () was added to the E3 medium at a final concentration 10 ng/mL, as described by Jones *et al.* [186]. Zebrafish larvae were imaged using whole-embryo fluorescence microscopy ().

Zebrafish skeletal staining

A two color acid-free cartilage and bone stain was performed with alcian blue (0.4% alcian blue in 70% ethanol) and alizarin red (0.5% in water). Zebrafish at 5dpf, injected with rgs2 RNA or buffer, were fixated with 4% paraformaldehyde (PFA). After washing with 50% ethanol, staining solution is added (1 ml of alcian blue solution + 10 µl of alizarin red solution) overnight. Stained fish are bleached for 1h with 3.5% H_2O_2 in 1% KOH. Clearance is obtained by sequential incubation with 20% glycerol + 0.25% KOH and 50% glycerol + 0.25% KOH for 30 min and 2h respectively. The stained skeletal structures were analyzed with light microscopy ().

Results

Effect of rgs2 overexpression on zebrafish adipogenesis

In order to study the effect of rgs2 overexpression on adipocyte development, zebrafish injected with rgs2 RNA or buffer (control) were put in a high-fat environment. After 3 hours they were stained with Nile Red to visualize lipid storage (Fig. 1).

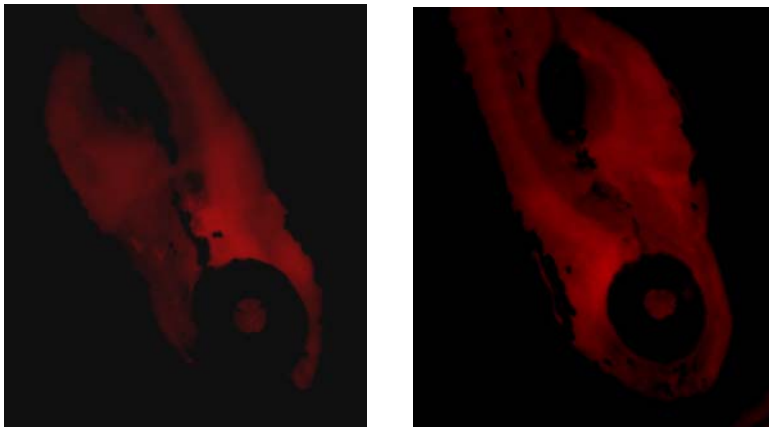

Crl RNA

Figure 1: Nile Red staining of high-fat treated buffer (Crl)- and RNA-injected zebrafish at 5 dpf.

No differences could be observed between buffer-injected zebrafish and zebrafish overexpressing rgs2.

Effect of rgs2 overexpression on skeletal development in zebrafish

To study the effect of rgs2 overexpression on skeletal development, we primarily observed jaw morphogenesis during zebrafish development. At 5 dpf buffer- and RNA-injected zebrafish were stained with alcian blue and alizarin red to specifically stain calcified structures (Fig. 2).

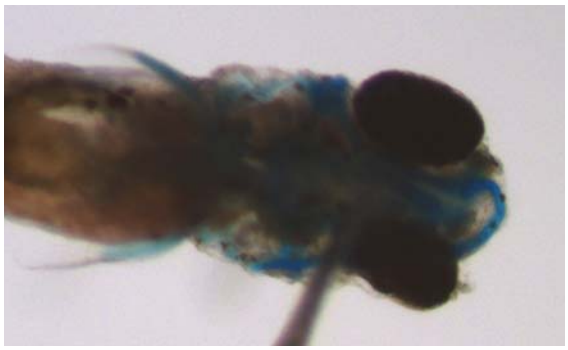

Crl RNA

Figure 2: Alcian blue- alizarin red staining of buffer (Crl)- and rgs2 RNA-injected zebrafish at 5 dpf.

No differences could be observed between buffer-injected zebrafish and zebrafish overexpressing rgs2.

IV.III. Conclusions from human and animal studies

In this chapter we studied the role of RGS2 in processes other than platelet production and function, namely T2DM, adipogenesis and skeletal development.

Since a RGS2 promoter polymorphism, associated with increased RGS2 expression levels, was shown to be associated with the metabolic syndrome in white European men, and the metabolic syndrome leads to an increased risk at the development of T2DM, we wanted to study the association between the same promoter polymorphism, namely -395 C/G, and T2DM. However, we could not find a significant association between this polymorphism and T2DM. Also, no difference in *RGS2* expression or Gs function was found in combination with the different genotypes of this polymorphism in the platelets from these patients.

A role for RGS2 in adipocyte differentiation has already been described in literature [91, 92]. In addition, patient 1 described in chapter III, and carrier of a mutation in RGS2 leading to an enhanced RGS2 function, is prone to obesity. Therefore, we studied the effect of rgs2 overexpression on adipogenesis in zebrafish. We could not show a difference in adipocyte staining between rgs2 RNA- and buffer-injected zebrafish at 5 dpf. Patient 1 also has some additional AHO-like characteristics as shortened fingers. We have studied the effect of rgs2 overexpression on skeletal development in zebrafish but because RNA-injection only leads to a transient rgs2 overexpression, we could only study early skeletal development of the jaws. However, rgs2 expression seemed not to influence jaw development.

It would be worthwhile to further study the effect of rgs2 overexpression on adipogenesis and skeletal development at later stages of the zebrafish development, but unfortunately this is not feasible by RNA-injection. It would be usefull to repeat these studies in zebrafish stably overexpressing rgs2.

Chapter V

General discussion and future perspectives

Summary

Samenvatting

Publications

Platelet Gs hypofunction and abnormal morphology resulting from a heterozygous RGS2 mutation.
Noé L, Di Michele M, Giets E, Thys C, Wittevrongel C, De Vos R, Overbergh L, Waelkens E, Jaeken J, Van Geet C, Freson K. Journal of Thrombosis and Haemostis, 2010, 8 (7): 1594-1603.

Regulators of platelet cAMP levels: clinical and therapeutic implications.
Noé L, Peeters K, Izzi B, Van Geet C, Freson K. Current Medicinal Chemistry, 2010, 17 (26): 2897-2905.

References

[1] Lee, R. E.; Young, R. H.; Castleman, B. James Homer Wright: a biography of the enigmatic creator of the Wright stain on the occasion of its centennial. *Am J Surg Pathol,* **2002,** *26*, 88-96.

[2] Drachman, J. G. Inherited thrombocytopenia: when a low platelet count does not mean ITP. *Blood*, **2004,** *103*, 390-8.

[3] Shivdasani, R. A.; Orkin, S. H. The transcriptional control of hematopoiesis. *Blood*, **1996,** *87*, 4025-39.

[4] Long, M. W. Megakaryocyte differentiation events. *Semin Hematol,* **1998,** *35*, 192-9.

[5] Drouin, A., Cramer, E.M., Production of platelets. In *Platelets in thrombotic and non-thrombotic disorders: pathophysiology, pharmacology and therapeutics*, Gresele, P., Page, C., Fuster, V., Vermylen, J., Ed. Cambridge University Press: Cambridge, UK, 2002; pp 25-40.

[6] Hoffman, R.; Straneva, J.; Yang, H. H.; Bruno, E.; Brandt, J. New insights into the regulation of human megakaryocytopoiesis. *Blood Cells*, **1987,** *13*, 75-86.

[7] Briddell, R. A.; Brandt, J. E.; Straneva, J. E.; Srour, E. F.; Hoffman, R. Characterization of the human burst-forming unit-megakaryocyte. *Blood,* **1989,** *74*, 145-51.

[8] Vitrat, N.; Cohen-Solal, K.; Pique, C.; Le Couedic, J. P.; Norol, F.; Larsen, A. K.; Katz, A.; Vainchenker, W.; Debili, N. Endomitosis of human megakaryocytes are due to abortive mitosis. *Blood,* **1998,** *91*, 3711-23.

[9] Jackson, C. W.; Steward, S. A.; Hutson, N. K.; McDonald, T. P. Genetic and physiological variations in megakaryocyte DNA content distributions. *Int J Cell Cloning,* **1990,** *8*, 260-6.

[10] Radley, J. M.; Haller, C. J. The demarcation membrane system of the megakaryocyte: a misnomer? *Blood*, **1982,** *60*, 213-9.

[11] Radley, J. M.; Scurfield, G. The mechanism of platelet release. *Blood,* **1980,** *56*, 996-9.

[12] Italiano, J. E., Jr.; Lecine, P.; Shivdasani, R. A.; Hartwig, J. H. Blood platelets are assembled principally at the ends of proplatelet processes produced by differentiated megakaryocytes. *J Cell Biol*, **1999,** *147*, 1299-312.

[13] Stenberg, P. E.; Levin, J. Mechanisms of platelet production. *Blood Cells,* **1989,** *15*, 23-47.

[14] Lichtman, M. A.; Chamberlain, J. K.; Simon, W.; Santillo, P. A. Parasinusoidal location of megakaryocytes in marrow: a determinant of platelet release. *Am J Hematol,* **1978,** *4*, 303-12.

[15] Behnke, O. An electron microscope study of the rat megacaryocyte. II. Some aspects of platelet release and microtubules. *J Ultrastruct Res,* **1969,** *26*, 111-29.

[16] Handagama, P. J.; Feldman, B. F.; Jain, N. C.; Farver, T. B.; Kono, C. S. Circulating proplatelets: isolation and quantitation in healthy rats and in rats with induced acute blood loss. *Am J Vet Res,* **1987,** *48*, 962-5.

[17] Zucker-Franklin, D.; Philipp, C. S. Platelet production in the pulmonary capillary bed: new ultrastructural evidence for an old concept. *Am J Pathol,* **2000,** *157*, 69-74.

[18] Richardson, J. L.; Shivdasani, R. A.; Boers, C.; Hartwig, J. H.; Italiano, J. E., Jr. Mechanisms of organelle transport and capture along proplatelets during platelet production. *Blood,* **2005,** *106*, 4066-75.
[19] Rendu, F., Brohard-Bohn, B., Platelet organelles. In *Platelets in thrombotic and non-thrombotic disorders: pathophysiology, pharmacology and therapeutics*, Gresele, P., Page, C., Fuster, V., Vermylen, J., Ed. Cambridge University Press: Cambridge, UK, 2002; pp 104-12.
[20] McNicol, A.; Israels, S. J. Platelets and anti-platelet therapy. *J Pharmacol Sci,* **2003,** *93*, 381-96.
[21] Gerrard, J. M.; White, J. G.; Peterson, D. A. The platelet dense tubular system: its relationship to prostaglandin synthesis and calcium flux. *Thromb Haemost,* **1978,** *40*, 224-31.
[22] Rendu, F.; Brohard-Bohn, B. The platelet release reaction: granules' constituents, secretion and functions. *Platelets,* **2001,** *12*, 261-73.
[23] Fox, J. E. The platelet cytoskeleton. *Thromb Haemost,* **1993,** *70*, 884-93.
[24] Spiegel, A. M. Inborn errors of signal transduction: mutations in G proteins and G protein-coupled receptors as a cause of disease. *J Inherit Metab Dis,* **1997,** *20*, 113-21.
[25] Tesmer, J. J. The quest to understand heterotrimeric G protein signaling. *Nat Struct Mol Biol, 17*, 650-2.
[26] Peters, J.; Wroe, S. F.; Wells, C. A.; Miller, H. J.; Bodle, D.; Beechey, C. V.; Williamson, C. M.; Kelsey, G. A cluster of oppositely imprinted transcripts at the Gnas locus in the distal imprinting region of mouse chromosome 2. *Proc. Natl. Acad. Sci. U.S.A.*, **1999,** *96*, 3830-5.
[27] Liu, J.; Yu, S.; Litman, D.; Chen, W.; Weinstein, L. S. Identification of a methylation imprint mark within the mouse Gnas locus. *Mol. Cell. Biol.,* **2000,** *20*, 5808-17.
[28] Coombes, C.; Arnaud, P.; Gordon, E.; Dean, W.; Coar, E. A.; Williamson, C. M.; Feil, R.; Peters, J.; Kelsey, G. Epigenetic properties and identification of an imprint mark in the Nesp-Gnasxl domain of the mouse Gnas imprinted locus. *Mol. Cell. Biol.,* **2003,** *23*, 5475-88.
[29] Plagge, A.; Kelsey, G.; Germain-Lee, E. L. Physiological functions of the imprinted Gnas locus and its protein variants Galpha(s) and XLalpha(s) in human and mouse. *J. Endocrinol.,* **2008,** *196*, 193-214.
[30] Kelsey, G.; Bodle, D.; Miller, H. J.; Beechey, C. V.; Coombes, C.; Peters, J.; Williamson, C. M. Identification of imprinted loci by methylation-sensitive representational difference analysis: application to mouse distal chromosome 2. *Genomics,* **1999,** *62*, 129-38.
[31] Yu, S.; Yu, D.; Lee, E.; Eckhaus, M.; Lee, R.; Corria, Z.; Accili, D.; Westphal, H.; Weinstein, L. S. Variable and tissue-specific hormone resistance in heterotrimeric Gs protein alpha-subunit (Gsalpha) knockout mice is due to tissue-specific imprinting of the gsalpha gene. *Proc Natl Acad Sci U S A,* **1998,** *95*, 8715-20.
[32] Mantovani, G.; Ballare, E.; Giammona, E.; Beck-Peccoz, P.; Spada, A. The gsalpha gene: predominant maternal origin of transcription in human thyroid gland and gonads. *J Clin Endocrinol Metab,* **2002,** *87*, 4736-40.

[33] Chen, M.; Wang, J.; Dickerson, K. E.; Kelleher, J.; Xie, T.; Gupta, D.; Lai, E. W.; Pacak, K.; Gavrilova, O.; Weinstein, L. S. Central nervous system imprinting of the G protein G(s)alpha and its role in metabolic regulation. *Cell Metab*, **2009,** *9*, 548-55.
[34] Miric, A.; Vechio, J. D.; Levine, M. A. Heterogeneous mutations in the gene encoding the alpha-subunit of the stimulatory G protein of adenylyl cyclase in Albright hereditary osteodystrophy. *J Clin Endocrinol Metab*, **1993,** *76*, 1560-8.
[35] Weinstein, L. S.; Liu, J.; Sakamoto, A.; Xie, T.; Chen, M. Minireview: GNAS: normal and abnormal functions. *Endocrinology*, **2004,** *145*, 5459-64.
[36] Carel, J. C.; Le Stunff, C.; Condamine, L.; Mallet, E.; Chaussain, J. L.; Adnot, P.; Garabedian, M.; Bougneres, P. Resistance to the lipolytic action of epinephrine: a new feature of protein Gs deficiency. *J Clin Endocrinol Metab*, **1999,** *84*, 4127-31.
[37] Landis, C. A.; Harsh, G.; Lyons, J.; Davis, R. L.; McCormick, F.; Bourne, H. R. Clinical characteristics of acromegalic patients whose pituitary tumors contain mutant Gs protein. *J Clin Endocrinol Metab*, **1990,** *71*, 1416-20.
[38] O'Sullivan, C.; Barton, C. M.; Staddon, S. L.; Brown, C. L.; Lemoine, N. R. Activating point mutations of the gsp oncogene in human thyroid adenomas. *Mol Carcinog*, **1991,** *4*, 345-9.
[39] Weinstein, L. S.; Shenker, A.; Gejman, P. V.; Merino, M. J.; Friedman, E.; Spiegel, A. M. Activating mutations of the stimulatory G protein in the McCune-Albright syndrome. *N Engl J Med*, **1991,** *325*, 1688-95.
[40] Chen, M.; Gavrilova, O.; Liu, J.; Xie, T.; Deng, C.; Nguyen, A. T.; Nackers, L. M.; Lorenzo, J.; Shen, L.; Weinstein, L. S. Alternative Gnas gene products have opposite effects on glucose and lipid metabolism. *Proc Natl Acad Sci U S A*, **2005,** *102*, 7386-91.
[41] Xie, T.; Chen, M.; Zhang, Q. H.; Ma, Z.; Weinstein, L. S. Beta cell-specific deficiency of the stimulatory G protein alpha-subunit Gsalpha leads to reduced beta cell mass and insulin-deficient diabetes. *Proc Natl Acad Sci U S A*, **2007,** *104*, 19601-6.
[42] Chen, M.; Feng, H. Z.; Gupta, D.; Kelleher, J.; Dickerson, K. E.; Wang, J.; Hunt, D.; Jou, W.; Gavrilova, O.; Jin, J. P.; Weinstein, L. S. G(s)alpha deficiency in skeletal muscle leads to reduced muscle mass, fiber-type switching, and glucose intolerance without insulin resistance or deficiency. *Am J Physiol Cell Physiol*, **2009,** *296*, C930-40.
[43] Watson, N.; Linder, M. E.; Druey, K. M.; Kehrl, J. H.; Blumer, K. J. RGS family members: GTPase-activating proteins for heterotrimeric G-protein alpha-subunits. *Nature*, **1996,** *383*, 172-5.
[44] Hepler, J. R.; Berman, D. M.; Gilman, A. G.; Kozasa, T. RGS4 and GAIP are GTPase-activating proteins for Gq alpha and block activation of phospholipase C beta by gamma-thio-GTP-Gq alpha. *Proc Natl Acad Sci U S A*, **1997,** *94*, 428-32.
[45] Zheng, B.; De Vries, L.; Gist Farquhar, M. Divergence of RGS proteins: evidence for the existence of six mammalian RGS subfamilies. *Trends Biochem Sci*, **1999,** *24*, 411-4.
[46] Ross, E. M.; Wilkie, T. M. GTPase-activating proteins for heterotrimeric G proteins: regulators of G protein signaling (RGS) and RGS-like proteins. *Annu Rev Biochem*, **2000,** *69*, 795-827.
[47] Jean-Baptiste, G.; Yang, Z.; Greenwood, M. T. Regulatory mechanisms involved in modulating RGS function. *Cell Mol Life Sci*, **2006,** *63*, 1969-85.
[48] De Vries, L.; Zheng, B.; Fischer, T.; Elenko, E.; Farquhar, M. G. The regulator of G protein signaling family. *Annu Rev Pharmacol Toxicol*, **2000,** *40*, 235-71.

[49] Popov, S.; Yu, K.; Kozasa, T.; Wilkie, T. M. The regulators of G protein signaling (RGS) domains of RGS4, RGS10, and GAIP retain GTPase activating protein activity in vitro. *Proc Natl Acad Sci U S A*, **1997,** *94*, 7216-20.
[50] Tesmer, J. J.; Berman, D. M.; Gilman, A. G.; Sprang, S. R. Structure of RGS4 bound to AlF4--activated G(i alpha1): stabilization of the transition state for GTP hydrolysis. *Cell*, **1997,** *89*, 251-61.
[51] Sprang, S. R. G protein mechanisms: insights from structural analysis. *Annu Rev Biochem*, **1997,** *66*, 639-78.
[52] Abramow-Newerly, M.; Roy, A. A.; Nunn, C.; Chidiac, P. RGS proteins have a signalling complex: interactions between RGS proteins and GPCRs, effectors, and auxiliary proteins. *Cell Signal*, **2006,** *18*, 579-91.
[53] Berman, D. M.; Wilkie, T. M.; Gilman, A. G. GAIP and RGS4 are GTPase-activating proteins for the Gi subfamily of G protein alpha subunits. *Cell*, **1996,** *86*, 445-52.
[54] Siderovski, D. P.; Heximer, S. P.; Forsdyke, D. R. A human gene encoding a putative basic helix-loop-helix phosphoprotein whose mRNA increases rapidly in cycloheximide-treated blood mononuclear cells. *DNA Cell Biol*, **1994,** *13*, 125-47.
[55] Wu, H. K.; Heng, H. H.; Shi, X. M.; Forsdyke, D. R.; Tsui, L. C.; Mak, T. W.; Minden, M. D.; Siderovski, D. P. Differential expression of a basic helix-loop-helix phosphoprotein gene, G0S8, in acute leukemia and localization to human chromosome 1q31. *Leukemia*, **1995,** *9*, 1291-8.
[56] Gu, S.; Anton, A.; Salim, S.; Blumer, K. J.; Dessauer, C. W.; Heximer, S. P. Alternative translation initiation of human regulators of G-protein signaling-2 yields a set of functionally distinct proteins. *Mol Pharmacol*, **2008,** *73*, 1-11.
[57] Kehrl, J. H.; Sinnarajah, S. RGS2: a multifunctional regulator of G-protein signaling. *Int J Biochem Cell Biol*, **2002,** *34*, 432-8.
[58] Grant, S. L.; Lassegue, B.; Griendling, K. K.; Ushio-Fukai, M.; Lyons, P. R.; Alexander, R. W. Specific regulation of RGS2 messenger RNA by angiotensin II in cultured vascular smooth muscle cells. *Mol Pharmacol*, **2000,** *57*, 460-7.
[59] Xie, Z.; Gong, M. C.; Su, W.; Turk, J.; Guo, Z. Group VIA phospholipase A2 (iPLA2beta) participates in angiotensin II-induced transcriptional up-regulation of regulator of g-protein signaling-2 in vascular smooth muscle cells. *J Biol Chem*, **2007,** *282*, 25278-89.
[60] Zmijewski, J. W.; Song, L.; Harkins, L.; Cobbs, C. S.; Jope, R. S. Second messengers regulate RGS2 expression which is targeted to the nucleus. *Biochim Biophys Acta*, **2001,** *1541*, 201-11.
[61] Tikhonova, I. G.; Boulegue, C.; Langer, I.; Fourmy, D. Modeled structure of the whole regulator G-protein signaling-2. *Biochem Biophys Res Commun*, **2006,** *341*, 715-20.
[62] Nguyen, C. H.; Ming, H.; Zhao, P.; Hugendubler, L.; Gros, R.; Kimball, S. R.; Chidiac, P. Translational control by RGS2. *J Cell Biol*, **2009,** *186*, 755-65.
[63] Wang, X.; Zeng, W.; Soyombo, A. A.; Tang, W.; Ross, E. M.; Barnes, A. P.; Milgram, S. L.; Penninger, J. M.; Allen, P. B.; Greengard, P.; Muallem, S. Spinophilin regulates Ca2+ signalling by binding the N-terminal domain of RGS2 and the third intracellular loop of G-protein-coupled receptors. *Nat Cell Biol*, **2005,** *7*, 405-11.

[64] Wang, X.; Zeng, W.; Kim, M. S.; Allen, P. B.; Greengard, P.; Muallem, S. Spinophilin/neurabin reciprocally regulate signaling intensity by G protein-coupled receptors. *Embo J,* **2007,** *26*, 2768-76.
[65] Heo, K.; Ha, S. H.; Chae, Y. C.; Lee, S.; Oh, Y. S.; Kim, Y. H.; Kim, S. H.; Kim, J. H.; Mizoguchi, A.; Itoh, T. J.; Kwon, H. M.; Ryu, S. H.; Suh, P. G. RGS2 promotes formation of neurites by stimulating microtubule polymerization. *Cell Signal,* **2006,** *18*, 2182-92.
[66] Schoeber, J. P.; Topala, C. N.; Wang, X.; Diepens, R. J.; Lambers, T. T.; Hoenderop, J. G.; Bindels, R. J. RGS2 inhibits the epithelial Ca2+ channel TRPV6. *J Biol Chem,* **2006,** *281*, 29669-74.
[67] Roy, A. A.; Baragli, A.; Bernstein, L. S.; Hepler, J. R.; Hebert, T. E.; Chidiac, P. RGS2 interacts with Gs and adenylyl cyclase in living cells. *Cell Signal,* **2006,** *18*, 336-48.
[68] Salim, S.; Sinnarajah, S.; Kehrl, J. H.; Dessauer, C. W. Identification of RGS2 and type V adenylyl cyclase interaction sites. *J Biol Chem,* **2003,** *278*, 15842-9.
[69] Anger, T.; Zhang, W.; Mende, U. Differential contribution of GTPase activation and effector antagonism to the inhibitory effect of RGS proteins on Gq-mediated signaling in vivo. *J Biol Chem,* **2004,** *279*, 3906-15.
[70] Chatterjee, T. K.; Fisher, R. A. Cytoplasmic, nuclear, and golgi localization of RGS proteins. Evidence for N-terminal and RGS domain sequences as intracellular targeting motifs. *J Biol Chem,* **2000,** *275*, 24013-21.
[71] Bernstein, L. S.; Ramineni, S.; Hague, C.; Cladman, W.; Chidiac, P.; Levey, A. I.; Hepler, J. R. RGS2 binds directly and selectively to the M1 muscarinic acetylcholine receptor third intracellular loop to modulate Gq/11alpha signaling. *J Biol Chem,* **2004,** *279*, 21248-56.
[72] Hague, C.; Bernstein, L. S.; Ramineni, S.; Chen, Z.; Minneman, K. P.; Hepler, J. R. Selective inhibition of alpha1A-adrenergic receptor signaling by RGS2 association with the receptor third intracellular loop. *J Biol Chem,* **2005,** *280*, 27289-95.
[73] Tang, K. M.; Wang, G. R.; Lu, P.; Karas, R. H.; Aronovitz, M.; Heximer, S. P.; Kaltenbronn, K. M.; Blumer, K. J.; Siderovski, D. P.; Zhu, Y.; Mendelsohn, M. E. Regulator of G-protein signaling-2 mediates vascular smooth muscle relaxation and blood pressure. *Nat Med,* **2003,** *9*, 1506-12.
[74] Cunningham, M. L.; Waldo, G. L.; Hollinger, S.; Hepler, J. R.; Harden, T. K. Protein kinase C phosphorylates RGS2 and modulates its capacity for negative regulation of Galpha 11 signaling. *J Biol Chem,* **2001,** *276*, 5438-44.
[75] Ni, J.; Qu, L.; Yang, H.; Wang, M.; Huang, Y. Palmitoylation and its effect on the GTPase-activating activity and conformation of RGS2. *Int J Biochem Cell Biol,* **2006,** *38*, 2209-18.
[76] Oliveira-Dos-Santos, A. J.; Matsumoto, G.; Snow, B. E.; Bai, D.; Houston, F. P.; Whishaw, I. Q.; Mariathasan, S.; Sasaki, T.; Wakeham, A.; Ohashi, P. S.; Roder, J. C.; Barnes, C. A.; Siderovski, D. P.; Penninger, J. M. Regulation of T cell activation, anxiety, and male aggression by RGS2. *Proc Natl Acad Sci U S A,* **2000,** *97*, 12272-7.
[77] Heximer, S. P.; Knutsen, R. H.; Sun, X.; Kaltenbronn, K. M.; Rhee, M. H.; Peng, N.; Oliveira-dos-Santos, A.; Penninger, J. M.; Muslin, A. J.; Steinberg, T. H.; Wyss, J. M.; Mecham, R. P.; Blumer, K. J. Hypertension and prolonged vasoconstrictor signaling in RGS2-deficient mice. *J Clin Invest,* **2003,** *111*, 1259.

[78] Calo, L. A.; Pagnin, E.; Davis, P. A.; Sartori, M.; Ceolotto, G.; Pessina, A. C.; Semplicini, A. Increased expression of regulator of G protein signaling-2 (RGS-2) in Bartter's/Gitelman's syndrome. A role in the control of vascular tone and implication for hypertension. *J Clin Endocrinol Metab,* **2004,** *89*, 4153-7.
[79] Riddle, E. L.; Rana, B. K.; Murthy, K. K.; Rao, F.; Eskin, E.; O'Connor, D. T.; Insel, P. A. Polymorphisms and haplotypes of the regulator of G protein signaling-2 gene in normotensives and hypertensives. *Hypertension,* **2006,** *47*, 415-20.
[80] Gu, S.; Tirgari, S.; Heximer, S. P. The RGS2 gene product from a candidate hypertension allele shows decreased plasma membrane association and inhibition of Gq. *Mol Pharmacol,* **2008,** *73*, 1037-43.
[81] Li, N. F.; Zhang, J. H.; Yang, J.; Zhou, L.; Luo, W. L.; Guo, Y. Y.; Yao, X. G.; Wang, H. M.; Chang, J. H. Association of genetic variations of regulator of G-protein signaling 2 with hypertension in the general Xinjiang Kazakh population. *Clin Exp Hypertens, 32*, 256-61.
[82] Clark, M. A.; Sethi, P. R.; Lambert, N. A. Active Galpha(q) subunits and M3 acetylcholine receptors promote distinct modes of association of RGS2 with the plasma membrane. *FEBS Lett,* **2007,** *581*, 764-70.
[83] Semplicini, A.; Lenzini, L.; Sartori, M.; Papparella, I.; Calo, L. A.; Pagnin, E.; Strapazzon, G.; Benna, C.; Costa, R.; Avogaro, A.; Ceolotto, G.; Pessina, A. C. Reduced expression of regulator of G-protein signaling 2 (RGS2) in hypertensive patients increases calcium mobilization and ERK1/2 phosphorylation induced by angiotensin II. *J Hypertens*, **2006,** *24*, 1115-24.
[84] Zhang, W.; Anger, T.; Su, J.; Hao, J.; Xu, X.; Zhu, M.; Gach, A.; Cui, L.; Liao, R.; Mende, U. Selective loss of fine tuning of Gq/11 signaling by RGS2 protein exacerbates cardiomyocyte hypertrophy. *J Biol Chem,* **2006,** *281*, 5811-20.
[85] Sun, X.; Kaltenbronn, K. M.; Steinberg, T. H.; Blumer, K. J. RGS2 is a mediator of nitric oxide action on blood pressure and vasoconstrictor signaling. *Mol Pharmacol,* **2005,** *67*, 631-9.
[86] Esler, M.; Rumantir, M.; Kaye, D.; Jennings, G.; Hastings, J.; Socratous, F.; Lambert, G. Sympathetic nerve biology in essential hypertension. *Clin Exp Pharmacol Physiol,* **2001,** *28*, 986-9.
[87] Gross, V.; Tank, J.; Obst, M.; Plehm, R.; Blumer, K. J.; Diedrich, A.; Jordan, J.; Luft, F. C. Autonomic nervous system and blood pressure regulation in RGS2-deficient mice. *Am J Physiol Regul Integr Comp Physiol,* **2005,** *288*, R1134-42.
[88] Leygraf, A.; Hohoff, C.; Freitag, C.; Willis-Owen, S. A.; Krakowitzky, P.; Fritze, J.; Franke, P.; Bandelow, B.; Fimmers, R.; Flint, J.; Deckert, J. Rgs 2 gene polymorphisms as modulators of anxiety in humans? *J Neural Transm,* **2006,** *113*, 1921-5.
[89] Smoller, J. W.; Paulus, M. P.; Fagerness, J. A.; Purcell, S.; Yamaki, L. H.; Hirshfeld-Becker, D.; Biederman, J.; Rosenbaum, J. F.; Gelernter, J.; Stein, M. B. Influence of RGS2 on anxiety-related temperament, personality, and brain function. *Arch Gen Psychiatry,* **2008,** *65*, 298-308.
[90] Cui, H.; Nishiguchi, N.; Ivleva, E.; Yanagi, M.; Fukutake, M.; Nushida, H.; Ueno, Y.; Kitamura, N.; Maeda, K.; Shirakawa, O. Association of RGS2 gene polymorphisms with suicide and increased RGS2 immunoreactivity in the postmortem brain of suicide victims. *Neuropsychopharmacology,* **2008,** *33*, 1537-44.

[91] Imagawa, M.; Tsuchiya, T.; Nishihara, T. Identification of inducible genes at the early stage of adipocyte differentiation of 3T3-L1 cells. *Biochem Biophys Res Commun,* **1999,** *254*, 299-305.
[92] Nishizuka, M.; Honda, K.; Tsuchiya, T.; Nishihara, T.; Imagawa, M. RGS2 promotes adipocyte differentiation in the presence of ligand for peroxisome proliferator-activated receptor gamma. *J Biol Chem,* **2001,** *276*, 29625-7.
[93] Roy, A. A.; Nunn, C.; Ming, H.; Zou, M. X.; Penninger, J.; Kirshenbaum, L. A.; Dixon, S. J.; Chidiac, P. Up-regulation of endogenous RGS2 mediates cross-desensitization between Gs and Gq signaling in osteoblasts. *J Biol Chem,* **2006,** *281*, 32684-93.
[94] Hurst, J. H.; Mendpara, N.; Hooks, S. B. Regulator of G-protein signalling expression and function in ovarian cancer cell lines. *Cell Mol Biol Lett,* **2009,** *14*, 153-74.
[95] Cao, X.; Qin, J.; Xie, Y.; Khan, O.; Dowd, F.; Scofield, M.; Lin, M. F.; Tu, Y. Regulator of G-protein signaling 2 (RGS2) inhibits androgen-independent activation of androgen receptor in prostate cancer cells. *Oncogene,* **2006,** *25*, 3719-34.
[96] Jiang, Z.; Wang, Z.; Xu, Y.; Wang, B.; Huang, W.; Cai, S. Analysis of RGS2 expression and prognostic significance in stage II and III colorectal cancer. *Biosci Rep,* **2009**.
[97] Smalley, M. J.; Iravani, M.; Leao, M.; Grigoriadis, A.; Kendrick, H.; Dexter, T.; Fenwick, K.; Regan, J. L.; Britt, K.; McDonald, S.; Lord, C. J.; Mackay, A.; Ashworth, A. Regulator of G-protein signalling 2 mRNA is differentially expressed in mammary epithelial subpopulations and over-expressed in the majority of breast cancers. *Breast Cancer Res,* **2007,** *9*, R85.
[98] Kannangai, R.; Vivekanandan, P.; Martinez-Murillo, F.; Choti, M.; Torbenson, M. Fibrolamellar carcinomas show overexpression of genes in the RAS, MAPK, PIK3, and xenobiotic degradation pathways. *Hum Pathol,* **2007,** *38*, 639-44.
[99] Zhu, Y.; Hollmen, J.; Raty, R.; Aalto, Y.; Nagy, B.; Elonen, E.; Kere, J.; Mannila, H.; Franssila, K.; Knuutila, S. Investigatory and analytical approaches to differential gene expression profiling in mantle cell lymphoma. *Br J Haematol,* **2002,** *119*, 905-15.
[100] Sorrentino, M. J. Implications of the metabolic syndrome: the new epidemic. *Am J Cardiol,* **2005,** *96*, 3E-7E.
[101] Tseng, C. C.; Zhang, X. Y. Role of regulator of G protein signaling in desensitization of the glucose-dependent insulinotropic peptide receptor. *Endocrinology,* **1998,** *139*, 4470-5.
[102] Hegele, R. A.; Brunt, J. H.; Connelly, P. W. Genetic variation on chromosome 1 associated with variation in body fat distribution in men. *Circulation,* **1995,** *92*, 1089-93.
[103] Langefeld, C. D.; Wagenknecht, L. E.; Rotter, J. I.; Williams, A. H.; Hokanson, J. E.; Saad, M. F.; Bowden, D. W.; Haffner, S.; Norris, J. M.; Rich, S. S.; Mitchell, B. D. Linkage of the metabolic syndrome to 1q23-q31 in Hispanic families: the Insulin Resistance Atherosclerosis Study Family Study. *Diabetes,* **2004,** *53*, 1170-4.
[104] Freson, K.; Stolarz, K.; Aerts, R.; Brand, E.; Brand-Herrmann, S. M.; Kawecka-Jaszcz, K.; Kuznetsova, T.; Tikhonoff, V.; Thijs, L.; Vermylen, J.; Staessen, J. A.; Van Geet, C. -391 C to G substitution in the regulator of G-protein signalling-2 promoter increases susceptibility to the metabolic syndrome in white European men: consistency between molecular and epidemiological studies. *J Hypertens,* **2007,** *25*, 117-25.

[105] Yang, J.; Wu, J.; Jiang, H.; Mortensen, R.; Austin, S.; Manning, D. R.; Woulfe, D.; Brass, L. F. Signaling through Gi family members in platelets. Redundancy and specificity in the regulation of adenylyl cyclase and other effectors. *J. Biol. Chem.,* **2002,** *277*, 46035-42.
[106] van Willigen, G.; Donath, J.; Lapetina, E. G.; Akkerman, J. W. Identification of alpha-subunits of trimeric GTP-binding proteins in human platelets by RT-PCR. *Biochem. Biophys. Res. Commun.,* **1995,** *214*, 254-62.
[107] Freson, K.; Jaeken, J.; Van Helvoirt, M.; de Zegher, F.; Wittevrongel, C.; Thys, C.; Hoylaerts, M. F.; Vermylen, J.; Van Geet, C. Functional polymorphisms in the paternally expressed XLalphas and its cofactor ALEX decrease their mutual interaction and enhance receptor-mediated cAMP formation. *Hum. Mol. Genet.,* **2003,** *12*, 1121-30.
[108] Feijge, M. A.; Ansink, K.; Vanschoonbeek, K.; Heemskerk, J. W. Control of platelet activation by cyclic AMP turnover and cyclic nucleotide phosphodiesterase type-3. *Biochem. Pharmacol.,* **2004,** *67*, 1559-67.
[109] Schwarz, U. R.; Walter, U.; Eigenthaler, M. Taming platelets with cyclic nucleotides. *Biochem. Pharmacol.,* **2001,** *62*, 1153-61.
[110] Cavallini, L.; Coassin, M.; Borean, A.; Alexandre, A. Prostacyclin and sodium nitroprusside inhibit the activity of the platelet inositol 1,4,5-trisphosphate receptor and promote its phosphorylation. *J. Biol. Chem.,* **1996,** *271*, 5545-51.
[111] Butt, E.; Abel, K.; Krieger, M.; Palm, D.; Hoppe, V.; Hoppe, J.; Walter, U. cAMP- and cGMP-dependent protein kinase phosphorylation sites of the focal adhesion vasodilator-stimulated phosphoprotein (VASP) in vitro and in intact human platelets. *J. Biol. Chem.,* **1994,** *269*, 14509-17.
[112] Lerea, K. M.; Glomset, J. A. Agents that elevate the concentration of cAMP in platelets inhibit the formation of a NaDodSO4-resistant complex between thrombin and a 40-kDa protein. *Proc. Natl. Acad. Sci. U.S.A.,* **1987,** *84*, 5620-4.
[113] Watson, S. P.; McConnell, R. T.; Lapetina, E. G. The rapid formation of inositol phosphates in human platelets by thrombin is inhibited by prostacyclin. *J. Biol. Chem.,* **1984,** *259*, 13199-203.
[114] Cheng, Y.; Austin, S. C.; Rocca, B.; Koller, B. H.; Coffman, T. M.; Grosser, T.; Lawson, J. A.; FitzGerald, G. A. Role of prostacyclin in the cardiovascular response to thromboxane A2. *Science,* **2002,** *296*, 539-41.
[115] Ledent, C.; Vaugeois, J. M.; Schiffmann, S. N.; Pedrazzini, T.; El Yacoubi, M.; Vanderhaeghen, J. J.; Costentin, J.; Heath, J. K.; Vassart, G.; Parmentier, M. Aggressiveness, hypoalgesia and high blood pressure in mice lacking the adenosine A2a receptor. *Nature,* **1997,** *388*, 674-8.
[116] Murugappa, S.; Kunapuli, S. P. The role of ADP receptors in platelet function. *Front. Biosci.,* **2006,** *11*, 1977-86.
[117] Gagnon, A. W.; Murray, D. L.; Leadley, R. J. Cloning and characterization of a novel regulator of G protein signalling in human platelets. *Cell. Signal.,* **2002,** *14*, 595-606.
[118] Kim, S. D.; Sung, H. J.; Park, S. K.; Kim, T. W.; Park, S. C.; Kim, S. K.; Cho, J. Y.; Rhee, M. H. The expression patterns of RGS transcripts in platelets. *Platelets,* **2006,** *17*, 493-7.
[119] Freson, K.; Hashimoto, H.; Thys, C.; Wittevrongel, C.; Danloy, S.; Morita, Y.; Shintani, N.; Tomiyama, Y.; Vermylen, J.; Hoylaerts, M. F.; Baba, A.; Van Geet, C. The

pituitary adenylate cyclase-activating polypeptide is a physiological inhibitor of platelet activation. *J. Clin. Invest.,* **2004,** *113*, 905-12.
[120] Miyata, A.; Arimura, A.; Dahl, R. R.; Minamino, N.; Uehara, A.; Jiang, L.; Culler, M. D.; Coy, D. H. Isolation of a novel 38 residue-hypothalamic polypeptide which stimulates adenylate cyclase in pituitary cells. *Biochem. Biophys. Res. Commun.,* **1989,** *164*, 567-74.
[121] Freson, K.; Peeters, K.; De Vos, R.; Wittevrongel, C.; Thys, C.; Hoylaerts, M. F.; Vermylen, J.; Van Geet, C. PACAP and its receptor VPAC1 regulate megakaryocyte maturation: therapeutic implications. *Blood,* **2008,** *111*, 1885-93.
[122] Andre, P.; Delaney, S. M.; LaRocca, T.; Vincent, D.; DeGuzman, F.; Jurek, M.; Koller, B.; Phillips, D. R.; Conley, P. B. P2Y12 regulates platelet adhesion/activation, thrombus growth, and thrombus stability in injured arteries. *J. Clin. Invest.,* **2003,** *112*, 398-406.
[123] Hollopeter, G.; Jantzen, H. M.; Vincent, D.; Li, G.; England, L.; Ramakrishnan, V.; Yang, R. B.; Nurden, P.; Nurden, A.; Julius, D.; Conley, P. B. Identification of the platelet ADP receptor targeted by antithrombotic drugs. *Nature,* **2001,** *409*, 202-7.
[124] Cattaneo, M.; Zighetti, M. L.; Lombardi, R.; Martinez, C.; Lecchi, A.; Conley, P. B.; Ware, J.; Ruggeri, Z. M. Molecular bases of defective signal transduction in the platelet P2Y12 receptor of a patient with congenital bleeding. *Proc. Natl. Acad. Sci. U.S.A.,* **2003,** *100*, 1978-83.
[125] Fabre, J. E.; Nguyen, M.; Athirakul, K.; Coggins, K.; McNeish, J. D.; Austin, S.; Parise, L. K.; FitzGerald, G. A.; Coffman, T. M.; Koller, B. H. Activation of the murine EP3 receptor for PGE2 inhibits cAMP production and promotes platelet aggregation. *J. Clin. Invest.,* **2001,** *107*, 603-10.
[126] Ma, H.; Hara, A.; Xiao, C. Y.; Okada, Y.; Takahata, O.; Nakaya, K.; Sugimoto, Y.; Ichikawa, A.; Narumiya, S.; Ushikubi, F. Increased bleeding tendency and decreased susceptibility to thromboembolism in mice lacking the prostaglandin E receptor subtype EP(3). *Circulation,* **2001,** *104*, 1176-80.
[127] Gross, S.; Tilly, P.; Hentsch, D.; Vonesch, J. L.; Fabre, J. E. Vascular wall-produced prostaglandin E2 exacerbates arterial thrombosis and atherothrombosis through platelet EP3 receptors. *J. Exp. Med.,* **2007,** *204*, 311-20.
[128] Heptinstall, S.; Espinosa, D. I.; Manolopoulos, P.; Glenn, J. R.; White, A. E.; Johnson, A.; Dovlatova, N.; Fox, S. C.; May, J. A.; Hermann, D.; Magnusson, O.; Stefansson, K.; Hartman, D.; Gurney, M. DG-041 inhibits the EP3 prostanoid receptor--a new target for inhibition of platelet function in atherothrombotic disease. *Platelets,* **2008,** *19*, 605-13.
[129] Singh, J.; Zeller, W.; Zhou, N.; Hategen, G.; Mishra, R.; Polozov, A.; Yu, P.; Onua, E.; Zhang, J.; Zembower, D.; Kiselyov, A.; Ramirez, J. L.; Sigthorsson, G.; Bjornsson, J. M.; Thorsteinsdottir, M.; Andresson, T.; Bjarnadottir, M.; Magnusson, O.; Fabre, J. E.; Stefansson, K.; Gurney, M. E. Antagonists of the EP(3) Receptor for Prostaglandin E(2) Are Novel Antiplatelet Agents That Do Not Prolong Bleeding. *ACS Chem. Biol.,* **2009**.
[130] Freson, K.; Izzi, B.; Labarque, V.; Van Helvoirt, M.; Thys, C.; Wittevrongel, C.; Bex, M.; Bouillon, R.; Godefroid, N.; Proesmans, W.; de Zegher, F.; Jaeken, J.; Van Geet, C. GNAS defects identified by stimulatory G protein alpha-subunit signalling studies in platelets. *J. Clin. Endocrinol. Metab.,* **2008,** *93*, 4851-9.

[131] Freson, K.; Hoylaerts, M. F.; Jaeken, J.; Eyssen, M.; Arnout, J.; Vermylen, J.; Van Geet, C. Genetic variation of the extra-large stimulatory G protein alpha-subunit leads to Gs hyperfunction in platelets and is a risk factor for bleeding. *Thromb. Haemost.*, **2001,** *86*, 733-8.
[132] Pasolli, H. A.; Klemke, M.; Kehlenbach, R. H.; Wang, Y.; Huttner, W. B. Characterization of the extra-large G protein alpha-subunit XLalphas. I. Tissue distribution and subcellular localization. *J. Biol. Chem.*, **2000,** *275*, 33622-32.
[133] Klemke, M.; Pasolli, H. A.; Kehlenbach, R. H.; Offermanns, S.; Schultz, G.; Huttner, W. B. Characterization of the extra-large G protein alpha-subunit XLalphas. II. Signal transduction properties. *J. Biol. Chem.*, **2000,** *275*, 33633-40.
[134] Reaven, G. M. Banting lecture 1988. Role of insulin resistance in human disease. *Diabetes*, **1988,** *37*, 1595-607.
[135] Davi, G.; Catalano, I.; Averna, M.; Notarbartolo, A.; Strano, A.; Ciabattoni, G.; Patrono, C. Thromboxane biosynthesis and platelet function in type II diabetes mellitus. *N Engl J Med*, **1990,** *322*, 1769-74.
[136] Eibl, N.; Krugluger, W.; Streit, G.; Schrattbauer, K.; Hopmeier, P.; Schernthaner, G. Improved metabolic control decreases platelet activation markers in patients with type-2 diabetes. *Eur J Clin Invest*, **2004,** *34*, 205-9.
[137] Tschoepe, D.; Roesen, P.; Kaufmann, L.; Schauseil, S.; Kehrel, B.; Ostermann, H.; Gries, F. A. Evidence for abnormal platelet glycoprotein expression in diabetes mellitus. *Eur J Clin Invest*, **1990,** *20*, 166-70.
[138] Trovati, M.; Anfossi, G.; Cavalot, F.; Massucco, P.; Mularoni, E.; Emanuelli, G. Insulin directly reduces platelet sensitivity to aggregating agents. Studies in vitro and in vivo. *Diabetes*, **1988,** *37*, 780-6.
[139] Trovati, M.; Anfossi, G. Influence of insulin and of insulin resistance on platelet and vascular smooth muscle cell function. *J Diabetes Complications*, **2002,** *16*, 35-40.
[140] Seghieri, G.; Di Simplicio, P.; Anichini, R.; Alviggi, L.; De Bellis, A.; Bennardini, F.; Franconi, F. Platelet antioxidant enzymes in insulin-dependent diabetes mellitus. *Clin Chim Acta*, **2001,** *309*, 19-23.
[141] Yamaguchi, T.; Kadono, K.; Tetsutani, T.; Yasunaga, K. Platelet free Ca2+ concentration in non-insulin-dependent diabetes mellitus. *Diabetes Res*, **1991,** *18*, 89-94.
[142] Vangheluwe, P.; Raeymaekers, L.; Dode, L.; Wuytack, F. Modulating sarco(endo)plasmic reticulum Ca2+ ATPase 2 (SERCA2) activity: cell biological implications. *Cell Calcium*, **2005,** *38*, 291-302.
[143] Akai, T.; Naka, K.; Okuda, K.; Takemura, T.; Fujii, S. Decreased sensitivity of platelets to prostacyclin in patients with diabetes mellitus. *Horm Metab Res*, **1983,** *15*, 523-6.
[144] Stamler, J.; Vaccaro, O.; Neaton, J. D.; Wentworth, D. Diabetes, other risk factors, and 12-yr cardiovascular mortality for men screened in the Multiple Risk Factor Intervention Trial. *Diabetes Care*, **1993,** *16*, 434-44.
[145] Humbert, M.; Nurden, P.; Bihour, C.; Pasquet, J. M.; Winckler, J.; Heilmann, E.; Savi, P.; Herbert, J. M.; Kunicki, T. J.; Nurden, A. T. Ultrastructural studies of platelet aggregates from human subjects receiving clopidogrel and from a patient with an inherited defect of an ADP-dependent pathway of platelet activation. *Arterioscler. Thromb. Vasc. Biol.*, **1996,** *16*, 1532-43.

[146] Savi, P.; Herbert, J. M. Clopidogrel and ticlopidine: P2Y12 adenosine diphosphate-receptor antagonists for the prevention of atherothrombosis. *Semin. Thromb. Hemost.*, **2005,** *31*, 174-83.
[147] Savi, P.; Herbert, J. M.; Pflieger, A. M.; Dol, F.; Delebassee, D.; Combalbert, J.; Defreyn, G.; Maffrand, J. P. Importance of hepatic metabolism in the antiaggregating activity of the thienopyridine clopidogrel. *Biochem. Pharmacol.*, **1992,** *44*, 527-32.
[148] Gurbel, P. A.; Bliden, K. P.; Hiatt, B. L.; O'Connor, C. M. Clopidogrel for coronary stenting: response variability, drug resistance, and the effect of pretreatment platelet reactivity. *Circulation*, **2003,** *107*, 2908-13.
[149] Simon, T.; Verstuyft, C.; Mary-Krause, M.; Quteineh, L.; Drouet, E.; Meneveau, N.; Steg, P. G.; Ferrieres, J.; Danchin, N.; Becquemont, L. Genetic determinants of response to clopidogrel and cardiovascular events. *N. Engl. J. Med.*, **2009,** *360*, 363-75.
[150] Mega, J. L.; Close, S. L.; Wiviott, S. D.; Shen, L.; Hockett, R. D.; Brandt, J. T.; Walker, J. R.; Antman, E. M.; Macias, W.; Braunwald, E.; Sabatine, M. S. Cytochrome p-450 polymorphisms and response to clopidogrel. *N. Engl. J. Med.*, **2009,** *360*, 354-62.
[151] Wallentin, L.; Varenhorst, C.; James, S.; Erlinge, D.; Braun, O. O.; Jakubowski, J. A.; Sugidachi, A.; Winters, K. J.; Siegbahn, A. Prasugrel achieves greater and faster P2Y12receptor-mediated platelet inhibition than clopidogrel due to more efficient generation of its active metabolite in aspirin-treated patients with coronary artery disease. *Eur. Heart J.*, **2008,** *29*, 21-30.
[152] Jernberg, T.; Payne, C. D.; Winters, K. J.; Darstein, C.; Brandt, J. T.; Jakubowski, J. A.; Naganuma, H.; Siegbahn, A.; Wallentin, L. Prasugrel achieves greater inhibition of platelet aggregation and a lower rate of non-responders compared with clopidogrel in aspirin-treated patients with stable coronary artery disease. *Eur. Heart J.*, **2006,** *27*, 1166-73.
[153] Brandt, J. T.; Close, S. L.; Iturria, S. J.; Payne, C. D.; Farid, N. A.; Ernest, C. S., 2nd; Lachno, D. R.; Salazar, D.; Winters, K. J. Common polymorphisms of CYP2C19 and CYP2C9 affect the pharmacokinetic and pharmacodynamic response to clopidogrel but not prasugrel. *J. Thromb. Haemost.*, **2007,** *5*, 2429-36.
[154] Storey, R. F.; Oldroyd, K. G.; Wilcox, R. G. Open multicentre study of the P2T receptor antagonist AR-C69931MX assessing safety, tolerability and activity in patients with acute coronary syndromes. *Thromb. Haemost.*, **2001,** *85*, 401-7.
[155] Husted, S.; Emanuelsson, H.; Heptinstall, S.; Sandset, P. M.; Wickens, M.; Peters, G. Pharmacodynamics, pharmacokinetics, and safety of the oral reversible P2Y12 antagonist AZD6140 with aspirin in patients with atherosclerosis: a double-blind comparison to clopidogrel with aspirin. *Eur. Heart. J.*, **2006,** *27*, 1038-47.
[156] JJ, V. A. N. G.; Nilsson, L.; Berntsson, P.; Wissing, B. M.; Giordanetto, F.; Tomlinson, W.; Greasley, P. J. Ticagrelor binds to human P2Y(12) independently from ADP but antagonizes ADP-induced receptor signaling and platelet aggregation. *J Thromb Haemost*, **2009,** *7*, 1556-65.
[157] Wallentin, L.; Becker, R. C.; Budaj, A.; Cannon, C. P.; Emanuelsson, H.; Held, C.; Horrow, J.; Husted, S.; James, S.; Katus, H.; Mahaffey, K. W.; Scirica, B. M.; Skene, A.; Steg, P. G.; Storey, R. F.; Harrington, R. A.; Freij, A.; Thorsen, M. Ticagrelor versus clopidogrel in patients with acute coronary syndromes. *N. Engl. J. Med.*, **2009,** *361*, 1045-57.

[158] Sinnarajah, S.; Dessauer, C. W.; Srikumar, D.; Chen, J.; Yuen, J.; Yilma, S.; Dennis, J. C.; Morrison, E. E.; Vodyanoy, V.; Kehrl, J. H. RGS2 regulates signal transduction in olfactory neurons by attenuating activation of adenylyl cyclase III. *Nature,* **2001,** *409*, 1051-5.
[159] Katsel, P. L.; Tagliente, T. M.; Schwarz, T. E.; Craddock-Royal, B. D.; Patel, N. D.; Maayani, S. Molecular and biochemical evidence for the presence of type III adenylyl cyclase in human platelets. *Platelets,* **2003,** *14*, 21-33.
[160] Freson, K.; Izzi, B.; Labarque, V.; Van Helvoirt, M.; Thys, C.; Wittevrongel, C.; Bex, M.; Bouillon, R.; Godefroid, N.; Proesmans, W.; de Zegher, F.; Jaeken, J.; Van Geet, C. GNAS defects identified by stimulatory G protein alpha-subunit signalling studies in platelets. *J Clin Endocrinol Metab,* **2008,** *93*, 4851-9.
[161] Di Michele, M.; Della Corte, A.; Cicchillitti, L.; Del Boccio, P.; Urbani, A.; Ferlini, C.; Scambia, G.; Donati, M. B.; Rotilio, D. A proteomic approach to paclitaxel chemoresistance in ovarian cancer cell lines. *Biochim Biophys Acta,* **2009,** *1794*, 225-36.
[162] Shevchenko, A.; Wilm, M.; Vorm, O.; Mann, M. Mass spectrometric sequencing of proteins silver-stained polyacrylamide gels. *Anal Chem,* **1996,** *68*, 850-8.
[163] Freson, K.; Hoylaerts, M. F.; Jaeken, J.; Eyssen, M.; Arnout, J.; Vermylen, J.; Van Geet, C. Genetic variation of the extra-large stimulatory G protein alpha-subunit leads to Gs hyperfunction in platelets and is a risk factor for bleeding. *Thromb Haemost,* **2001,** *86*, 733-8.
[164] Kimmel, C. B.; Ballard, W. W.; Kimmel, S. R.; Ullmann, B.; Schilling, T. F. Stages of embryonic development of the zebrafish. *Dev Dyn,* **1995,** *203*, 253-310.
[165] Jagadeeswaran, P.; Sheehan, J. P.; Craig, F. E.; Troyer, D. Identification and characterization of zebrafish thrombocytes. *Br J Haematol,* **1999,** *107*, 731-8.
[166] Lin, H. F.; Traver, D.; Zhu, H.; Dooley, K.; Paw, B. H.; Zon, L. I.; Handin, R. I. Analysis of thrombocyte development in CD41-GFP transgenic zebrafish. *Blood,* **2005,** *106*, 3803-10.
[167] Hudziak, R. M.; Barofsky, E.; Barofsky, D. F.; Weller, D. L.; Huang, S. B.; Weller, D. D. Resistance of morpholino phosphorodiamidate oligomers to enzymatic degradation. *Antisense Nucleic Acid Drug Dev,* **1996,** *6*, 267-72.
[168] Sumanas, S.; Larson, J. D. Morpholino phosphorodiamidate oligonucleotides in zebrafish: a recipe for functional genomics? *Brief Funct Genomic Proteomic,* **2002,** *1*, 239-56.
[169] Kole, R.; Sazani, P. Antisense effects in the cell nucleus: modification of splicing. *Curr Opin Mol Ther,* **2001,** *3*, 229-34.
[170] Negrotto, S.; Pacienza, N.; D'Atri, L. P.; Pozner, R. G.; Malaver, E.; Torres, O.; Lazzari, M. A.; Gomez, R. M.; Schattner, M. Activation of cyclic AMP pathway prevents CD34(+) cell apoptosis. *Exp Hematol,* **2006,** *34*, 1420-8.
[171] Hoggatt, J.; Singh, P.; Sampath, J.; Pelus, L. M. Prostaglandin E2 enhances hematopoietic stem cell homing, survival, and proliferation. *Blood,* **2009,** *113*, 5444-55.
[172] Ko, J. K.; Choi, K. H.; Kim, I. S.; Jung, E. K.; Park, D. H. Inducible RGS2 is a cross-talk regulator for parathyroid hormone signaling in rat osteoblast-like UMR106 cells. *Biochem Biophys Res Commun,* **2001,** *287*, 1025-33.
[173] Wang, N.; Yan, K.; Rasenick, M. M. Tubulin binds specifically to the signal-transducing proteins, Gs alpha and Gi alpha 1. *J Biol Chem,* **1990,** *265*, 1239-42.

[174] Piersma, S. R.; Broxterman, H. J.; Kapci, M.; de Haas, R. R.; Hoekman, K.; Verheul, H. M.; Jimenez, C. R. Proteomics of the TRAP-induced platelet releasate. *J Proteomics*, **2009,** *72*, 91-109.
[175] Asijee, G. M.; Sturk, A.; Bruin, T.; Wilkinson, J. M.; Ten Cate, J. W. Vinculin is a permanent component of the membrane skeleton and is incorporated into the (re)organising cytoskeleton upon platelet activation. *Eur J Biochem*, **1990,** *189*, 131-6.
[176] Ito, J.; Kheirollah, A.; Nagayasu, Y.; Lu, R.; Kato, K.; Yokoyama, S. Apolipoprotein A-I increases association of cytosolic cholesterol and caveolin-1 with microtubule cytoskeletons in rat astrocytes. *J Neurochem*, **2006,** *97*, 1034-43.
[177] Lind, S. E.; Yin, H. L.; Stossel, T. P. Human platelets contain gelsolin. A regulator of actin filament length. *J Clin Invest*, **1982,** *69*, 1384-7.
[178] Walsh, J. L.; Keith, T. J.; Knull, H. R. Glycolytic enzyme interactions with tubulin and microtubules. *Biochim Biophys Acta*, **1989,** *999*, 64-70.
[179] Tisdale, E. J.; Azizi, F.; Artalejo, C. R. Rab2 utilizes glyceraldehyde-3-phosphate dehydrogenase and protein kinase C{iota} to associate with microtubules and to recruit dynein. *J Biol Chem*, **2009,** *284*, 5876-84.
[180] Saumet, A.; de Jesus, N.; Legrand, C.; Dubernard, V. Association of thrombospondin-1 with the actin cytoskeleton of human thrombin-activated platelets through an alphaIIbbeta3- or CD36-independent mechanism. *Biochem J*, **2002,** *363*, 473-82.
[181] Duvnjak, L.; Duvnjak, M. The metabolic syndrome - an ongoing story. *J Physiol Pharmacol*, **2009,** *60 Suppl 7*, 19-24.
[182] Cheng, Y. S.; Lee, T. S.; Hsu, H. C.; Kou, Y. R.; Wu, Y. L. Characterization of the transcriptional regulation of the regulator of G protein signaling 2 (RGS2) gene during 3T3-L1 preadipocyte differentiation. *J Cell Biochem*, **2008,** *105*, 922-30.
[183] Flynn, E. J., 3rd; Trent, C. M.; Rawls, J. F. Ontogeny and nutritional control of adipogenesis in zebrafish (Danio rerio). *J Lipid Res*, **2009,** *50*, 1641-52.
[184] Du, S. J.; Frenkel, V.; Kindschi, G.; Zohar, Y. Visualizing normal and defective bone development in zebrafish embryos using the fluorescent chromophore calcein. *Dev Biol*, **2001,** *238*, 239-46.
[185] Schlegel, A.; Stainier, D. Y. Microsomal triglyceride transfer protein is required for yolk lipid utilization and absorption of dietary lipids in zebrafish larvae. *Biochemistry*, **2006,** *45*, 15179-87.
[186] Jones, K. S.; Alimov, A. P.; Rilo, H. L.; Jandacek, R. J.; Woollett, L. A.; Penberthy, W. T. A high throughput live transparent animal bioassay to identify non-toxic small molecules or genes that regulate vertebrate fat metabolism for obesity drug development. *Nutr Metab (Lond)*, **2008,** *5*, 23.

Curriculum vitae

PERSONAL INFORMATION

FULL NAME	Laura Noé
HOME ADDRESS	Meerstraat 8, 3320 Hoegaarden
E-MAIL (PERSONAL)	laura_noe@yahoo.com
DATE OF BIRTH	August 30, 1982
PLACE OF BIRTH	Leuven, Belgium

EDUCATION

2005-2010: Katholieke Universiteit Leuven (KUL)– Faculty of Medicine
Ph.D. training program Biomedical Sciences; FWO aspirant
Doctoral school 'Molecular and Developmental Genetics'
Title: The role of Regulator of G protein Signaling 2 (RGS2) in megakaryopoiesis, platelet function and the metabolic syndrome.

2009-2010: KUL- Faculty of Medicine
Multidisciplinary Forensic Science
Thesis: De mogelijkheden en beperkingen van forensisch DNA-onderzoek

2002-2005: Master in Bio-engineering – KUL – Faculty of Bio-engineering
Magna cum Laude

- Major: Cell- and Gene-biotechnology
- Minor: Food and Health
- Thesis: De (patho)fysiologische karakterisatie van transcriptie-factoren en TPO-signalisatie gedurende megakaryopoïese en bloedplaatjesvorming.

2000-2002: Bachelor in Bio-engineering – KUL – Faculty of Bio-engineering
Cum Laude

1994-2000: Secondary school

- 1998-2000: Sciences – Mathematics (8h)
  O.L.V.-College (VIA), Tienen
- 1994-1998: Latin – Mathematics
  Sint-Janscollege, Meldert (Hoegaarden)

ORAL COMMUNICATIONS

Loss of Gs activity in platelets from carriers with a heterozygous missense mutation in the regulator of G protein signaling 2 (RGS2).

- Belgian Society on Thrombosis and Haemostasis, annual meeting. Affligem, Belgium. 15-16 november 2007.
- 50th Annual meeting of The American Society of Hematology. San Francisco, California, USA. 6-9 december 2008.